

**Part 1: Introduction to the Relative
Motion of Spacecraft About the
Sun-Earth L_2 Point**

Contents

Part 1: Introduction to the Relative Motion of Spacecraft About the Sun-Earth L_2 Point	1
Part 2: Linear and Quadratic Modelling and Solution of the Relative Motion	43
Part 3: Modelling the Perturbations — Elliptical Earth Orbit, Lunar Gravity, Solar Radiation Pressure, Thrusters	97

PREFACE

This Memorandum Report consists of a compilation of three individual reports, of increasing complexity, describing investigations of formation flight of spacecraft in the vicinity of the L_2 Sun-Earth libration point. The individual reports form the following parts of this compilation:

- Introduction to the relative motion of spacecraft about the Sun-Earth L_2 Point
- Linear and quadratic modelling and solution of the relative motion
- Modelling the Perturbations — Elliptical Earth Orbit, Lunar Gravity, Solar Radiation Pressure, Thrusters

The three parts are self-contained, with somewhat varying notation and terminology.

This work was funded by the Distributed Spacecraft Technology Program at NASA's Goddard Space Flight Center. The sponsor was Dr. Jesse Leitner of the Mission Engineering and Systems Analysis Division.

After fairly significant literature searches, this new work (of Parts 2 and 3) is deemed to be unique because it describes the primary perturbations to the description of relative motion between nearby spacecraft. The effect of the elliptical motion of the Earth about the Sun was verified to be the dominant perturbation to the circular restricted three body problem. Contributions due to lunar gravity and solar radiation pressure are seen to have much smaller effect.

Contents

1	Introduction	5
2	Problem Definition	5
3	Full Nonlinear Equations for Circular Restricted Three-Body Problem (relative to barycenter)	8
4	Full Nonlinear Equations for Circular Restricted Three-Body Problem (relative to a libration point)	10
5	Linear Equations for Circular Restricted Three-Body Problem	12
6	Quadratic Equations for Circular Restricted Three-Body Problem	14
7	Linear Relative Motion Equations for Circular Restricted Three-Body Problem	15
7.1	Relative Motion of Two Objects on Same Trajectory	16
7.2	Relative Motion With Insertion Position or Time Error	18
8	Some Examples	20
	Appendices	24
A	Derivation of the Full NonLinear Equations of Motion for the Circular Restricted Three-Body Problem (relative to barycenter)	24
B	Derivation of the Full Nonlinear Equations of Motion for the Circular Restricted Three-Body Problem Near L_2	27
C	Derivation of the Linear Equations of Motion for the Circular Restricted Three-Body Problem Near L_2	29
D	Derivation of Quadratic Differential Equations for Circular Restricted Motion Near L_2	35

1 Introduction

The long-term goals of our sponsor are to develop high-fidelity equations of motion representing orbiting spacecraft near the Sun-Earth L_2 point and equations of relative motion between orbiting spacecraft near the L_2 point. These equations will be used to develop orbit control schemes for a constellation of spacecraft near this L_2 point.

This report provides a starting point to the future development of high-fidelity equations by first developing equations of motion for the circular restricted three-body problem. Additionally, equations are derived for analytical expressions for the relative motion between spacecraft orbiting near the L_2 point.

We follow the terminology of Hamilton's thesis [1] as we present four sets of equations of motion: three nonlinear sets and a linearized set. Their derivations are in separate appendices. These equations were developed to examine relative errors of the linearized and quadratic effect models with respect to the baseline set full nonlinear equations.

The four types of models for the circular restricted three-body problem:

- full nonlinear model of spacecraft motion with respect to the system barycenter
- full nonlinear model of spacecraft motion with respect to the L_2 point
- linearized model of spacecraft motion with respect to the L_2 point
- quadratic (nonlinear) model spacecraft motion with respect to the L_2 point.

We formed a Taylor series expansion of the nonlinear equations about the libration point. Our linearized and quadratic models are respectively the first- and second-order Taylor series.

The analytical expressions of relative motion are based on the solutions to the linearized equations.

2 Problem Definition

The restricted three-body problem is a simplification to the general three-body problem. The general three-body problem is the description of orbital

motion of three bodies, of arbitrary mass, in arbitrary orbits. The general three-body problem has not been solved in closed form. "Work has focused on simplifying the general problem. One special analytical solution--the restricted three-body problem--has been known since the time of Euler and Lagrange." [2]

"We define our problem as follows: Two bodies revolve around their center of mass in circular orbits under the influence of their mutual gravitational attraction and a third body (attracted by the previous two but not influencing their motion) moves in the plane defined by the two revolving bodies. *The restricted problem of three bodies is to describe the motion of this third body.*" [3]

The two revolving bodies are called the primaries. The masses m_1 and m_2 of these bodies are arbitrary and are considered as point masses. The mass of the third body, m_3 , is infinitesimal and does not influence the motion of masses m_1 and m_2 . In our problem, consider the m_3 mass to be a spacecraft. Also consider the sum of the mass of the Earth and its Moon to be m_2 . Assume the Earth and Moon are in circular orbit about their common barycenter (system's center of mass). In turn, this barycenter is in circular orbit about the Sun, which is mass m_1 . These four masses compose our system; however, there are two large bodies. The larger of the large bodies is the Sun and the smaller of the large bodies located at the Earth-Moon barycenter ($m_1 > m_2$).

We copy portions of Hamilton's thesis Section 2.1 to define terminology and coordinate systems.

For this preliminary analysis, the orbits of the Moon around the Earth and the Earth around the Sun are assumed to be circular, have a constant angular speed, and be in the same orbital plane. (Spacecraft motions are not restricted to the plane.) When these assumptions are made, the restricted three-body problem becomes the more specific circular restricted three-body problem.

The rotating coordinate frame shown in Figure 1 is used for the development of the equations of motion. The origin is the system barycenter of m_1 and m_2 . The first basis vector, \hat{a}_1 , points toward the smaller body. The third basis vector, \hat{a}_3 , is parallel to the orbit normal with origin at the system barycenter. The second basis vector, \hat{a}_2 , is defined by the cross product of \hat{a}_3 and \hat{a}_1 ($\hat{a}_2 = \hat{a}_3 \times \hat{a}_1$). These vectors form an orthogonal coordinate frame.

The position vector of the spacecraft in this rotating frame is

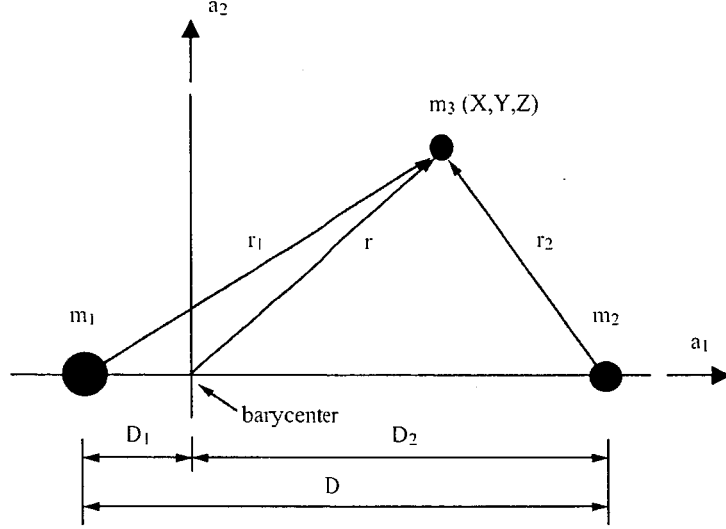


Figure 1: The Three-Body Problem's Rotating Coordinate System.

$$\bar{r} = X\hat{a}_1 + Y\hat{a}_2 + Z\hat{a}_3.$$

Writing vectors from the large bodies to spacecraft in the rotating frame gives

$$\bar{r}_1 = (X + D_1)\hat{a}_1 + Y\hat{a}_2 + Z\hat{a}_3$$

and

$$\bar{r}_2 = (X - D_2)\hat{a}_1 + Y\hat{a}_2 - Z\hat{a}_3,$$

where D_1 is the distance from the barycenter to m_1 and D_2 is the distance from the barycenter to m_2 . Note that

$$D = D_1 + D_2.$$

Use the equation for the definition of center of mass: $m_1 D_1 = m_2 D_2$ to calculate the magnitudes of D_1 and D_2 given D :

$$D_1 = \frac{D}{1 + \frac{m_1}{m_2}}$$

$$D_2 = \frac{D}{1 + \frac{m_2}{m_1}}.$$

Define the constant angular speed of the frame about \hat{a}_3 as

$$\omega = \sqrt{\frac{G(m_1 + m_2)}{D^3}} = \sqrt{\frac{G(m_{Sun} + m_{Earth} + m_{Moon})}{D^3}},$$

where G is the gravitational constant. As shown in Appendix A, we define the constant angular speed of the frame about \hat{a}_3 as the two-body mean motion $\hat{\omega} = \omega \hat{a}_3$

Also define

$$\mu_1 = Gm_1 = Gm_{Sun}$$

and

$$\mu_2 = Gm_2 = G(m_{Earth} + m_{Moon}).$$

With these definitions, we state four sets of equations that describe the motion of the spacecraft. The derivation of these equations is shown in respective appendices.

3 Full Nonlinear Equations for Circular Restricted Three-Body Problem (relative to barycenter)

These equations describe the spacecraft's motion relative to the system's barycenter in a rotating coordinate frame. The frame rotates with a constant angular speed.

$$\ddot{X} - 2\omega\dot{Y} - \omega^2 X = -\frac{\mu_1(X + D_1)}{|r_1|^3} - \frac{\mu_2(X - D_2)}{|r_2|^3} \quad (1)$$

$$\ddot{Y} + 2\omega\dot{X} - \omega^2 Y = -\frac{\mu_1 Y}{|r_1|^3} - \frac{\mu_2 Y}{|r_2|^3} \quad (2)$$

$$\ddot{Z} = -\frac{\mu_1 Z}{|r_1|^3} - \frac{\mu_2 Z}{|r_2|^3} \quad (3)$$

where $|r_1|$ and $|r_2|$ are the magnitudes of the vectors \bar{r}_1 and \bar{r}_2 , respectively.

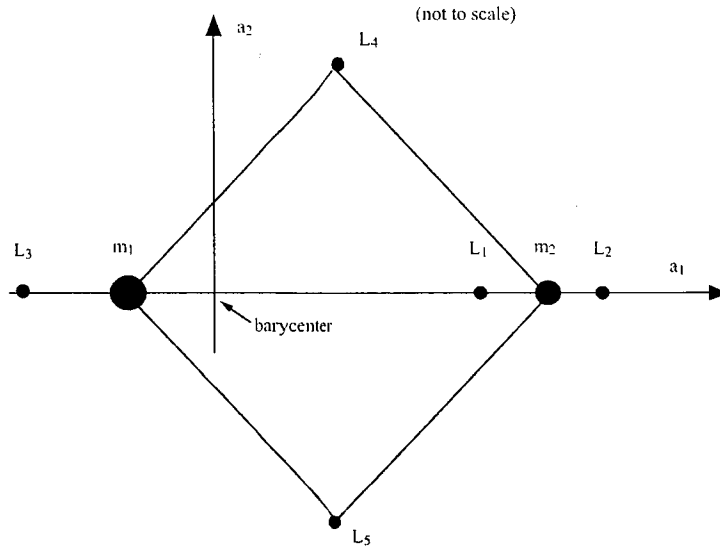


Figure 2: Libration Point Locations.

The initial conditions to be specified are

$$\begin{array}{ll} X(0) & \dot{X}(0) \\ Y(0) & \dot{Y}(0) \\ Z(0) & \dot{Z}(0). \end{array}$$

These equations are derived in Appendix A.

By setting all time derivatives in these equations of motion to zero, five libration points can be calculated. The location of these points depend on the masses and distances of the bodies: however, three points, shown in Figure 2, are always collinear with the two large bodies (L_1 , L_2 , L_3), and the other two points form equilateral triangles with the two large bodies (L_4 and L_5).

The motion near the collinear libration points is always unstable due to the existence of a positive real root of the characteristic equation for any value of μ . An unperturbed object in an orbit around a collinear libration point will move away from that point.

The four initial conditions corresponding to the in-plane motions (X-Y plane) cannot be arbitrarily selected. This will be further explained in Section 5. Szebehely discusses that the selection of initial conditions at the collinear libration points show considerable inherent instability. Even when

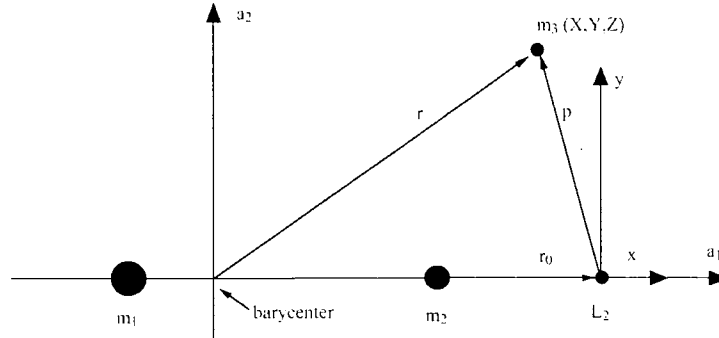


Figure 3: Relative Position with respect to L_2 .

initial conditions are chosen according to the linearized requirements, the spacecraft orbits maybe once or twice around L_2 before moving away. Fortunately, periodic orbits may be obtained by slight modification of the initial conditions which follow from the linearized solution. The point is that the orbits are very sensitive to changes in the initial conditions.

4 Full Nonlinear Equations for Circular Restricted Three-Body Problem (relative to a libration point)

We continue from Hamilton.

Motion around a collinear libration point is more easily expressed in a local coordinate frame, shown in Figure 3, with the origin located at the libration point of interest.

Note the vector addition

$$\bar{r} = \bar{r}_0 + \bar{p}$$

where \bar{r}_0 has components (X_0, Y_0, Z_0) to define the location of the libration point relative to the system barycenter. The "0" subscript refers to any one of the libration points. (Y_0 and Z_0 are both zero for collinear libration points.) Vector \bar{p} has components (X, Y, Z) to specify the location of m_3 relative to the libration point. Using

$$X = X_0 + x \tag{4}$$

$$Y = Y_0 + y \quad (5)$$

$$Z = Z_0 + z, \quad (6)$$

be reminded that (X, Y, Z) is the spacecraft position relative to the system barycenter. The radial direction, x , is collinear with \hat{a}_1 , going from the Sun (or largest body) through the libration point. The cross-track direction, z , is parallel and in the same direction as \hat{a}_3 , the orbit normal. The component y is in the direction of \hat{a}_2 . When circular motion is assumed, the y direction is the tangential velocity direction of the libration point around the system barycenter. These axes form an orthogonal coordinate system. Motion in the x - y plane is referred to as in-plane and any motion in the z direction will be referred to as out-of-plane.

The equations below describe the spacecraft's motion in a local coordinate frame relative to the libration point (origin) chosen by selection of (X_0, Y_0, Z_0) . Unique distances corresponding to each of the five libration points exist for each set of (X_0, Y_0, Z_0) .

The equations below are the full, coupled, nonlinear equations of motion for the circular restricted three-body problem. The coordinate frame rotates with a constant angular speed.

Equations (1) – (3) yield by simple substitution of Equations (4) – (6):

$$\begin{aligned} \ddot{x} - 2\omega\dot{y} - \omega^2(X_0 + x) &= -\frac{\mu_1(X_0 + x + D_1)}{r_1^3} - \frac{\mu_2(X_0 + x - D_2)}{r_2^3} \\ \ddot{y} + 2\omega\dot{x} - \omega^2(Y_0 + y) &= -\frac{\mu_1(Y_0 + y)}{r_1^3} - \frac{\mu_2(Y_0 + y)}{r_2^3} \\ \ddot{z} &= -\frac{\mu_1(Z_0 + z)}{r_1^3} - \frac{\mu_2(Z_0 + z)}{r_2^3}. \end{aligned}$$

where r_1 and r_2 are now defined below as

$$\begin{aligned} r_1 &= \sqrt{(X_0 + x + D_1)^2 + (Y_0 + y)^2 + (Z_0 + z)^2} \\ r_2 &= \sqrt{(X_0 + x - D_2)^2 + (Y_0 + y)^2 + (Z_0 + z)^2}. \end{aligned}$$

The initial conditions to be specified are

$$\begin{aligned} x(0) & \quad \dot{x}(0) \\ y(0) & \quad \dot{y}(0) \\ z(0) & \quad \dot{z}(0). \end{aligned}$$

These equations are derived in Appendix B.

For the L_2 point, where only $X_0 \neq 0$, the equations further simplify.

5 Linear Equations for Circular Restricted Three-Body Problem

At a chosen equilibrium point, the nonlinear, full, equations of motion can be linearized in order to exploit standard solutions to linear equations. The linear equations of motion about the local coordinate frame (origin at collinear libration point L_2) are given here:

$$\begin{aligned}\ddot{x} - 2\omega\dot{y} - U_{XX}x &= 0 \\ \ddot{y} + 2\omega\dot{x} - U_{YY}y &= 0 \\ \ddot{z} - U_{ZZ}z &= 0,\end{aligned}$$

where, evaluated at the L_2 collinear libration point, where $X = X_0$, $Y = 0$, $Z = 0$

$$\begin{aligned}U_{XX}|_{L_2} &= \omega^2 + \frac{2\mu_1}{(X_0 + D_1)^3} + \frac{2\mu_2}{(X_0 - D_2)^3} \\ U_{YY}|_{L_2} &= \omega^2 - \frac{\mu_1}{(X_0 + D_1)^3} - \frac{\mu_2}{(X_0 - D_2)^3} \\ U_{ZZ}|_{L_2} &= -\frac{\mu_1}{(X_0 + D_1)^3} - \frac{\mu_2}{(X_0 - D_2)^3}.\end{aligned}$$

The initial conditions to be specified are

$$\begin{aligned}x(0) & \quad \dot{x}(0) \\ y(0) & \quad \dot{y}(0) \\ z(0) & \quad \dot{z}(0).\end{aligned}$$

These equations are derived in Appendix C.

When evaluated at L_2 U_{XX} , U_{YY} , and U_{ZZ} , which were formed from U , are constant. The pseudopotential U is the centrifugal plus gravitational force potential defined as

$$U = \frac{1}{2}\omega^2(X^2 + Y^2) + \frac{\mu_1}{r_1} + \frac{\mu_2}{r_2}$$

and

$$r_1 = \sqrt{(X + D_1)^2 + Y^2 + Z^2}$$

$$r_2 = \sqrt{(X - D_2)^2 + Y^2 + Z^2}.$$

The respective double-lettered subscript indicates the second derivative of U with respect to that lettered-variable.

The selection of initial conditions for the first-order linear model summarizes the discussions of Szebehely [3], Farquhar [5], and Wie [4]. The in-plane characteristic equation of the linearized equations of motion about the collinear equilibrium points is of fourth degree. Solution yields two real roots (equal in magnitude, but opposite in sign) and two imaginary roots. The in-plane position has a convergent mode (due to the negative real root), a divergent mode (due to the positive real root), and an oscillatory mode. All three collinear libration points are unstable.

The out-of-plane characteristic equation of the linearized equations of motion about the collinear equilibrium points is of second degree. The two eigenvalues are imaginary. Thus, out-of-plane motion is simply oscillatory.

For the linearized equations of motion, these authors show that a solution to the equations can be made to contain only the oscillatory modes with proper choice of initial conditions:

Choose

$$\dot{x}(0) = \left(\frac{\omega_{xy}}{k}\right) y(0) \quad (7)$$

$$\dot{y}(0) = -k\omega_{xy}x(0) \quad (8)$$

where $k = \frac{\omega_{xy}^2 + U_{XX}}{2\omega_{xy}\omega}$ and ω_{xy} is the nondimensional frequency of the in-plane oscillatory mode calculated from

$$\omega_{xy} = \sqrt{\beta_1 + \sqrt{\beta_1^2 + \beta_2^2}}$$

$$\beta_1 = 2 - (U_{XX} + U_{YY})/2$$

$$\beta_2^2 = -U_{XX}U_{YY},$$

which means that once initial conditions $x(0)$ and $y(0)$ are selected, the corresponding initial velocity components cannot be chosen at will.

Although the choice of the z initial conditions is arbitrary, Wie states that choosing $x(0) = z(0) = 0$ and $\dot{z}(0) = -y(0)\omega_z$ (with $\omega_z = \sqrt{|U_{ZZ}|}$), the solution further reduces to a quasi-periodic Lissajous trajectory. We will not discuss this trajectory at this time. We just list his example initial condition.

Szebechely continues by noting Equations (7) - (8) do not hold when higher-order terms in the function U are retained. Nevertheless, the set of initial conditions given by these equations furnish the starting point of an iteration which leads to the proper initial condition for the nonlinear case. The closer the initial point $(x(0), y(0))$ is to the chosen libration point, the better a differential correction scheme will work to furnish the initial conditions desired for the establishment of periodic orbits in the nonlinear problem.

The linearization process allows only first-order terms in the coordinates and velocities; consequently, meaningful results must be connected with small values of these variables. Even when the initial conditions are chosen according to the linearized requirements, the spacecraft perform only one or two orbits before they depart from the area. Again, periodic orbits may be obtained by slight modification of the initial conditions which follow from the linearized solution. The point is that the orbits are very sensitive to changes in the initial conditions.

The linear model is amenable to linear analysis methods, which are more tractable than nonlinear solutions. The linear model is most helpful for preliminary control analysis as discussed by Hamilton. The nonlinear instabilities of this system must be restrained to maintain the desired periodic orbit motion.

6 Quadratic Equations for Circular Restricted Three-Body Problem

We went one-step beyond the linear dynamics model of Section 5. By further expanding U , we obtained a second-order model for the restricted problem. This model should yield trajectories closer to the nonlinear model than does the linear model.

$$\begin{aligned}
\ddot{x} - 2\omega\dot{y} - \omega^2x &= 2Ax - \frac{3}{2}B(2x^2 - y^2 - z^2) \\
\ddot{y} + 2\omega\dot{x} - \omega^2y &= -Ay + 3Bxy \\
\ddot{z} &= -Az + 3Bxz
\end{aligned}$$

where

$$\begin{aligned}
A &= \frac{\mu_1}{(X_0 + D_1)^3} + \frac{\mu_2}{(X_0 - D_2)^3} \\
B &= \frac{\mu_1}{(X_0 + D_1)^4} + \frac{\mu_2}{(X_0 - D_2)^4}
\end{aligned}$$

The initial conditions to be specified are

$$\begin{aligned}
x(0) \quad \dot{x}(0) \\
y(0) \quad \dot{y}(0) \\
z(0) \quad \dot{z}(0).
\end{aligned}$$

These equations are derived in Appendix D.

7 Linear Relative Motion Equations for Circular Restricted Three-Body Problem

Consider the linearized equations, with initial conditions selected such as to avoid exciting the divergent mode. The solution then takes the form

$$\mathbf{r} = \begin{bmatrix} x \\ y \\ z \end{bmatrix} = \begin{bmatrix} x_0 \cos \Omega(t - t_0) + \frac{y_0}{k} \sin \Omega(t - t_0) \\ -kx_0 \sin \Omega(t - t_0) + y_0 \cos \Omega(t - t_0) \\ z_0 \cos \omega(t - t_0) + \frac{\dot{z}_0}{\omega} \sin \omega(t - t_0) \end{bmatrix},$$

where subscript 0 refers to the value at time $t = t_0$. This solution can be written as a pair of decoupled matrix equations of similar form:

$$\begin{bmatrix} x \\ y \end{bmatrix} = \begin{bmatrix} \cos \Omega(t - t_0) & \frac{1}{k} \sin \Omega(t - t_0) \\ -k \sin \Omega(t - t_0) & \cos \Omega(t - t_0) \end{bmatrix} \begin{bmatrix} x_0 \\ y_0 \end{bmatrix} \quad (9)$$

$$\begin{bmatrix} z \\ \dot{z} \end{bmatrix} = \begin{bmatrix} \cos \omega(t - t_0) & \frac{1}{\omega} \sin \omega(t - t_0) \\ -\omega \sin \omega(t - t_0) & \cos \omega(t - t_0) \end{bmatrix} \begin{bmatrix} z_0 \\ \dot{z}_0 \end{bmatrix} \quad (10)$$

For notational convenience, let the vectors \mathbf{x} and \mathbf{z} refer, respectively, to $[x \ y]^T$ and $[z \ \dot{z}]^T$. Therefore, Equations (9) and (10) may be written as

$$\mathbf{x} = A_{k,\Omega}(t, t_0)\mathbf{x}_0 \quad (11)$$

$$\mathbf{z} = A_{\omega,\omega}(t, t_0)\mathbf{z}_0, \quad (12)$$

where

$$A_{k,\Omega}(t, t_0) = \begin{bmatrix} \cos \Omega(t - t_0) & \frac{1}{k} \sin \Omega(t - t_0) \\ -k \sin \Omega(t - t_0) & \cos \Omega(t - t_0) \end{bmatrix}$$

is the generic state transition matrix. Because of the obvious similarity, the relative motion solution may be developed for one of these matrix equations, and the result applied to the other.

7.1 Relative Motion of Two Objects on Same Trajectory

Now, say that there are two objects which satisfy this set of equations. Object 1 has the initial conditions which have been discussed, but object 2 trails object 1 by a time delay Δt . Therefore,

$$\mathbf{r}_2(t) = \mathbf{r}_1(t - \Delta t),$$

with the subscript referring to the object number. Let the relative motion be given by

$$\Delta \mathbf{r} = \mathbf{r}_1 - \mathbf{r}_2,$$

with the initial state

$$\mathbf{r}_1(t_0) = \mathbf{r}_2(t_0 + \Delta t) \triangleq \mathbf{r}_0.$$

First consider the in-plane motion of Equation (11). The in-plane motion of objects 1 and 2 is given by

$$\mathbf{x}_1 = A_{k,\Omega}(t, t_0)\mathbf{x}_0$$

$$\mathbf{x}_2 = A_{k,\Omega}(t - \Delta t, t_0)\mathbf{x}_0.$$

Therefore, the relative motion is

$$\Delta \mathbf{x} = [A_{k,\Omega}(t, t_0) - A_{k,\Omega}(t - \Delta t, t_0)]\mathbf{x}_0. \quad (13)$$

Now,

$$\begin{aligned}
 \Delta \mathbf{x}_0 = \Delta \mathbf{x}(t_0) &= \mathbf{x}_{10} - \mathbf{x}_{20} \\
 &= A_{k,\Omega}(t_0, t_0)\mathbf{x}_0 - A_{k,\Omega}(t_0 - \Delta t, t_0)\mathbf{x}_0 \\
 &= [I - A_{k,\Omega}(t_0 - \Delta t, t_0)]\mathbf{x}_0.
 \end{aligned}$$

And so,

$$\mathbf{x}_0 = [I - A_{k,\Omega}(t_0 - \Delta t, t_0)]^{-1}\Delta \mathbf{x}_0. \quad (14)$$

Substituting into Equation (13),

$$\Delta \mathbf{x} = [A_{k,\Omega}(t, t_0) - A_{k,\Omega}(t - \Delta t, t_0)][I - A_{k,\Omega}(t_0 - \Delta t, t_0)]^{-1}\Delta \mathbf{x}_0.$$

From the properties of the state transition matrix,

$$A_{k,\Omega}(t - \Delta t, t_0) = A_{k,\Omega}(t, t_0)A_{k,\Omega}(t_0 - \Delta t, t_0).$$

Therefore,

$$\begin{aligned}
 \Delta \mathbf{x} &= [A_{k,\Omega}(t, t_0) - A_{k,\Omega}(t, t_0)A_{k,\Omega}(t_0 - \Delta t, t_0)] \\
 &\quad [I - A_{k,\Omega}(t_0 - \Delta t, t_0)]^{-1}\Delta \mathbf{x}_0 \\
 &= A_{k,\Omega}(t, t_0)[I - A_{k,\Omega}(t_0 - \Delta t, t_0)][I - A_{k,\Omega}(t_0 - \Delta t, t_0)]^{-1}\Delta \mathbf{x}_0 \\
 &= A_{k,\Omega}(t, t_0)\Delta \mathbf{x}_0.
 \end{aligned}$$

The same result may be applied to Equation (12). The resulting relative motion equations are then

$$\begin{aligned}
 \Delta \mathbf{x} &= A_{k,\Omega}(t, t_0)\Delta \mathbf{x}_0 \\
 \Delta \mathbf{z} &= A_{w,\omega}(t, t_0)\Delta \mathbf{z}_0,
 \end{aligned}$$

with the full matrices as given in Equations (9) and (10).

It may be preferable to present the relative motion in terms of the relative position at the time of insertion of the second object — that is, at time $t_0 + \Delta t$. Referring to Equation (13),

$$\begin{aligned}
 \Delta \mathbf{x}(t_0 + \Delta t) &= [A_{k,\Omega}(t_0 + \Delta t, t_0) - A_{k,\Omega}(t_0, t_0)]\mathbf{x}_0 \\
 &= [A_{k,\Omega}(t_0 + \Delta t, t_0) - I]\mathbf{x}_0.
 \end{aligned}$$

Following the same logic as above,

$$\Delta \mathbf{x}_0 = [A_{k,\Omega}(t_0 + \Delta t, t_0) - I]^{-1} \Delta \mathbf{x}(t_0 + \Delta t),$$

and so

$$\begin{aligned} \Delta \mathbf{x} &= [A_{k,\Omega}(t, t_0) - A_{k,\Omega}(t - \Delta t, t_0)] \mathbf{x}_0 \\ &= [A_{k,\Omega}(t - \Delta t, t_0) A_{k,\Omega}(t_0 + \Delta t, t_0) - A_{k,\Omega}(t - \Delta t, t_0)] \\ &\quad [A_{k,\Omega}(t_0 + \Delta t, t_0) - I]^{-1} \Delta \mathbf{x}(t_0 + \Delta t). \\ &= A_{k,\Omega}(t - \Delta t, t_0) \Delta \mathbf{x}(t_0 + \Delta t). \end{aligned}$$

Once again, the same result applies to the out-of-plane motion, giving

$$\Delta \mathbf{z} = A_{\omega,\omega}(t - \Delta t, t_0) \Delta \mathbf{z}(t_0 + \Delta t).$$

Note that these results could also be written as

$$\begin{aligned} \Delta \mathbf{x} &= A_{k,\Omega}(t, t_0 + \Delta t) \Delta \mathbf{x}(t_0 + \Delta t) \\ \Delta \mathbf{z} &= A_{\omega,\omega}(t, t_0 + \Delta t) \Delta \mathbf{z}(t_0 + \Delta t). \end{aligned}$$

7.2 Relative Motion With Insertion Position or Time Error

Next, consider the possibility of an injection error for the second object, such that it does not in fact have the same initial state as the first. Let \mathbf{x}_{0b} refer to the in-plane state error at injection, such that

$$\mathbf{x}_2(t_0 + \Delta t) = \mathbf{x}_0 + \mathbf{x}_{0b}.$$

The resulting relative state is then, simply,

$$\Delta \mathbf{x} = A_{k,\Omega}(t, t_0 + \Delta t) (\Delta \mathbf{x}(t_0 + \Delta t)_a - \mathbf{x}_{0b}),$$

where $\Delta \mathbf{x}(t_0 + \Delta t)_a$ is the nominal relative state at the second object's injection time, as discussed above. Again, the same result applies to the out-of-plane motion, giving

$$\Delta \mathbf{z} = A_{\omega,\omega}(t, t_0 + \Delta t) (\Delta \mathbf{z}(t_0 + \Delta t)_a + \mathbf{z}_{0b}).$$

It may also be useful to examine an error in the injection time of the second object. Let the time error be Δt_b , such that

$$\Delta t = \Delta t_a + \Delta t_b,$$

where Δt_a refers to the nominal delay between the insertion of the first and second objects. In this case, the in-plane state of the second object is

$$\mathbf{x}_2 = A_{k,\Omega}(t - \Delta t_a - \Delta t_b).$$

The relative state is then

$$\Delta \mathbf{x} = [A_{k,\Omega}(t, t_0) - A_{k,\Omega}(t - \Delta t_a - \Delta t_b, t_0)]\mathbf{x}_0. \quad (15)$$

At the nominal injection time, $t_0 + \Delta t_a$, the relative state is

$$\Delta \mathbf{x}(t_0 + \Delta t_a) = [A_{k,\Omega}(t_0 + \Delta t_a, t_0) - A_{k,\Omega}(t_0 - \Delta t_b, t_0)]\mathbf{x}_0. \quad (16)$$

The second state transition matrix may be expanded in a Maclaurin series about $\Delta t_b = 0$. A first-order expansion gives

$$\begin{aligned} A_{k,\Omega}(t_0 - \Delta t_b, t_0) &= I + \begin{bmatrix} 0 & -\frac{\Omega}{k}\Delta t_b \\ k\Omega\Delta t_b & 0 \end{bmatrix} \\ &\triangleq I + B_{k,\Omega}(\Delta t_b). \end{aligned}$$

Substituting into Equation (16),

$$\Delta \mathbf{x}(t_0 + \Delta t_a) = [A_{k,\Omega}(t_0 + \Delta t_a, t_0) - I]\mathbf{x}_0 - B_{k,\Omega}(\Delta t_b)\mathbf{x}_0.$$

Note that the first term gives the nominal relative position at the nominal insertion time of the second object; the second term gives the error. Denote this first term as $\Delta \mathbf{x}(t_0 + \Delta t_a)_a$. Then,

$$\mathbf{x}_0 = [A_{k,\Omega}(t_0 + \Delta t_a, t_0) - I]^{-1}\Delta \mathbf{x}(t_0 + \Delta t_a)_a.$$

Substituting into Equation (15), and again invoking the properties of the state transition matrix,

$$\begin{aligned} \Delta \mathbf{x} &= [A_{k,\Omega}(t, t_0) - A_{k,\Omega}(t - \Delta t_a - \Delta t_b, t_0)] \\ &\quad [A_{k,\Omega}(t_0 + \Delta t_a, t_0) - I]^{-1}\Delta \mathbf{x}(t_0 + \Delta t_a)_a \end{aligned}$$

$$\begin{aligned}
&= [A_{k,\Omega}(t, t_0) - A_{k,\Omega}(t - \Delta t_a, t_0)A_{k,\Omega}(t_0 - \Delta t_b, t_0)] \\
&\quad [A_{k,\Omega}(t_0 + \Delta t_a, t_0) - I]^{-1} \Delta \mathbf{x}(t_0 + \Delta t_a)_a \\
&= \{A_{k,\Omega}(t, t_0) - A_{k,\Omega}(t - \Delta t_a, t_0)[I - B_{k,\Omega}(\Delta t_b)]\} \\
&\quad [A_{k,\Omega}(t_0 + \Delta t_a, t_0) - I]^{-1} \Delta \mathbf{x}(t_0 + \Delta t_a)_a \\
&= A_{k,\Omega}(t - \Delta t_a, t_0) \{A_{k,\Omega}(t_0 + \Delta t_a, t_0) - [I + B_{k,\Omega}(\Delta t)]\} \\
&\quad [A_{k,\Omega}(t_0 + \Delta t_a, t_0) - I]^{-1} \Delta \mathbf{x}(t_0 + \Delta t_a)_a \\
&= A_{k,\Omega}(t - \Delta t_a, t_0) \{I - B_{k,\Omega}(\Delta t)[A_{k,\Omega}(t_0 + \Delta t_a, t_0) - I]^{-1}\} \\
&\quad \Delta \mathbf{x}(t_0 + \Delta t_a)_a \\
&= A_{k,\Omega}(t - \Delta t_a, t_0) \Delta \mathbf{x}(t_0 + \Delta t_a)_a \\
&\quad - A_{k,\Omega}(t - \Delta t_a, t_0) B_{k,\Omega}(\Delta t) [A_{k,\Omega}(t_0 + \Delta t_a, t_0) - I]^{-1} \\
&\quad \Delta \mathbf{x}(t_0 + \Delta t_a)_a.
\end{aligned}$$

Here, note that the first term is again the nominal relative position, while the second term is the resulting error.

8 Some Examples

Currently, there are four different MATLAB scripts that present numerical solutions to these models:

- full equations of motion about L_2
- linear equations of motion about L_2
- quadratic equations of motion about L_2
- relative motion of two objects on the same trajectory.

We first duplicated Hamilton's results shown in his Section 8.1.1 to check the linear code.

For subsequent analysis, we used a consistent set physical quantities taken from Dunham and Muhonen [6].

Let us examine the same initial conditions applied to these four numerical solutions. We begin near the L_2 equilibrium point. Consider displacing the spacecraft 10,000 km away from L_2 along only the x direction, with $\dot{y}(0) = -1.127.8$ km/day as defined from Equation (8) of Section 5. All of y , $\dot{x}(0)$, z , and $\dot{z}(0)$ are zero. As noted earlier, motions in the Z-plane

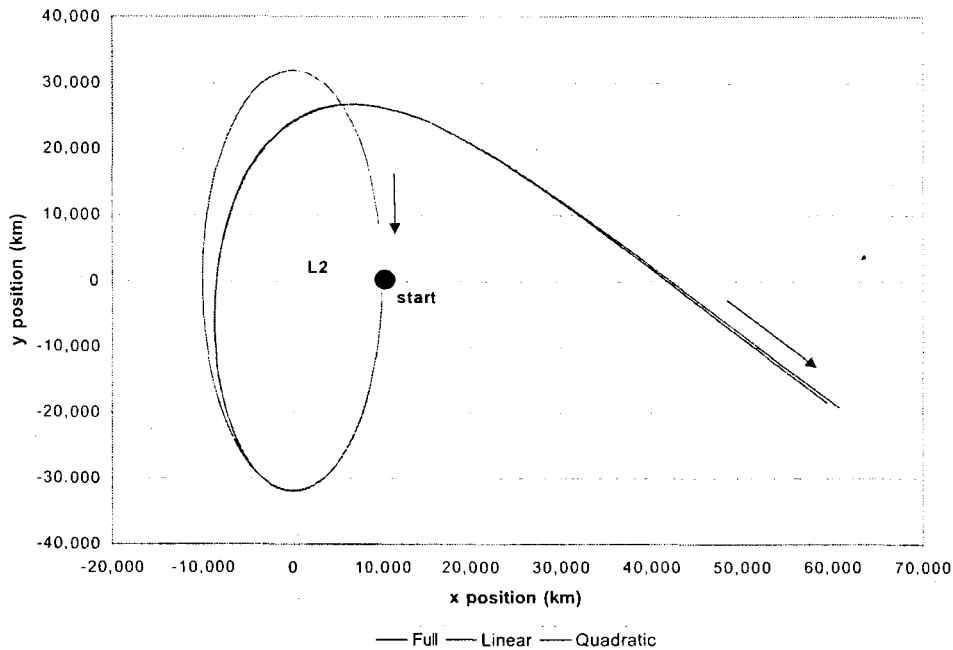


Figure 4: Solutions to Models Show Contrasting Fidelity.

are uncoupled from the X-Y plane; therefore, for these initial conditions, all motions will be in the X-Y plane.

Figure 4 contrasts the differences among the three models of the equations of motion as shown for 170 days (nearly a full period of 178 days). The full model does not even close on itself. For these initial conditions the full model diverges and the quadratic model shows very good agreement with the full model. The linear model does close on itself, but only represents the actual motion for about one-quarter of an orbit. Shown on the figure is the L_2 point, which is the origin, and the starting location. MATLAB's "ode45" solver was used, which is based on an explicit Runge-Kutta (4,5) formula. The print interval was one day.

Continuing with the same data produced for Figure 4, we turn to Figure 5. Here we take the component positions of the linear and quadratic models and subtract the corresponding position of the full model. Although plotted for 22 days beyond one period, we can see how rapidly the divergence grew as the second orbit began.

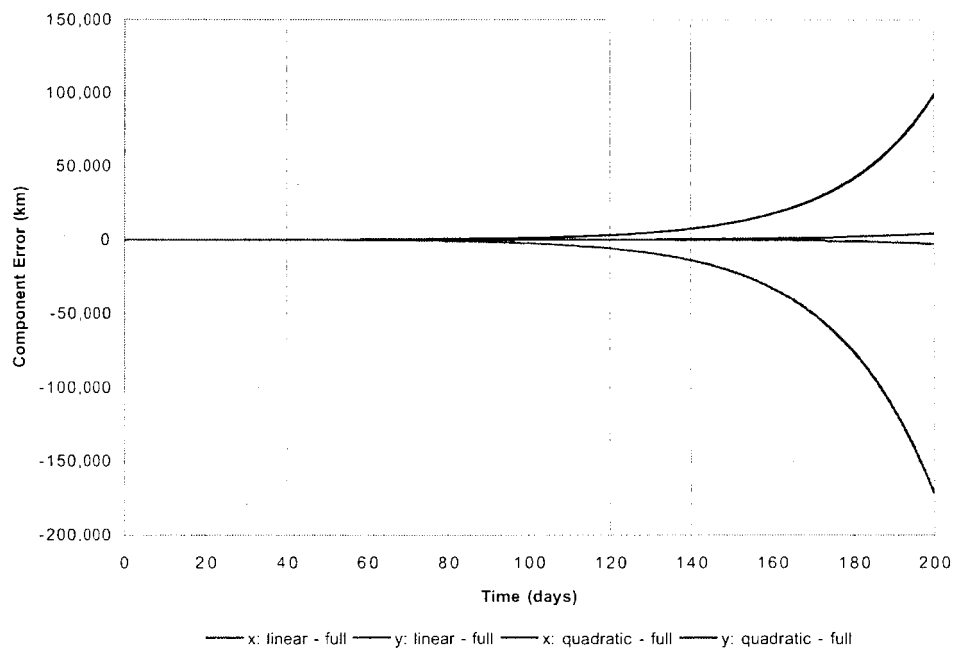


Figure 5: Relative Errors Among Models Show Significant Position Differences.

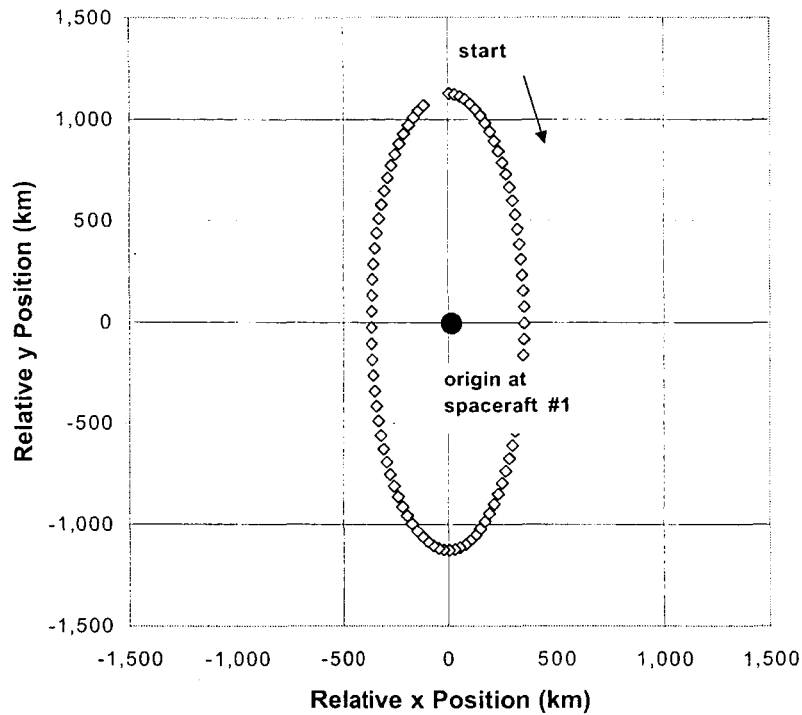


Figure 6: Relative Position of Two Spacecraft.

We move on to the analytic solution of the relative motion between two spacecraft. Here we used the linear solution coded from Equation (13) of Section 7.1. See Figure 6, which shows the motion of spacecraft #2 with respect to spacecraft #1. The calculations based on the initial conditions discussed above were made for each spacecraft. They have the same initial position and velocity conditions yet spacecraft #2 began one day after spacecraft #1. Each diamond on the figure shows the position of spacecraft #2 in steps of two days. You might consider yourself to be at the origin riding on spacecraft #1. With a one-day delay, the position of spacecraft #2 is plotted every two days (to offer clarity between plot symbols). At the orbit's beginning and halfway points, the relative change of position of spacecraft #2 is less than other orbit points.

Appendices

A Derivation of the Full NonLinear Equations of Motion for the Circular Restricted Three-Body Problem (relative to barycenter)

The development of the equations of motion will follow that of Hamilton. In our reading of his thesis to understand his work, we rederived the equations of motion. More details are given in these respective appendixes to maintain a record of our labors.

Returning to Figure 1, which is a rotating coordinate system, we find the need to add an inertial reference frame to define the rotation vector.

An inertial coordinate system is defined with origin at the system barycenter. The orthogonal basis vectors \hat{n}_1 , \hat{n}_2 , and \hat{n}_3 are fixed. Vectors \hat{n}_1 and \hat{n}_2 lie in the same plane as the rotating basis vectors \hat{a}_1 and \hat{a}_2 . The vector \hat{n}_3 is always aligned with \hat{a}_3 . Once every revolution, \hat{n}_1 is aligned with \hat{a}_1 at the same time that \hat{n}_2 is aligned with \hat{a}_2 . With respect to the inertial coordinate frame, the two large bodies are rotating about their barycenter with a constant angular velocity

$$\begin{aligned}\bar{\omega} &= \begin{bmatrix} 0 \\ 0 \\ \omega \end{bmatrix} \hat{n} \\ &= \omega \hat{n}_3\end{aligned}$$

where

$$\omega = \sqrt{\frac{G(m_1 + m_2)}{D^3}}$$

and G is the gravitational constant.

With rotating reference axes, the calculation of the spacecraft's velocity with respect to an inertial frame is

$$\frac{d\bar{r}}{dt_n} = \frac{d\bar{r}}{dt_a} + \bar{\omega} \times \bar{r}$$

where the position vector of the spacecraft in the rotating frame is

$$\bar{r} = X\hat{a}_1 + Y\hat{a}_2 + Z\hat{a}_3.$$

Substitute into the calculation and collect terms:

$$\frac{d\bar{r}}{dt_n} = \dot{X}\hat{a}_1 + \dot{Y}\hat{a}_2 + \dot{Z}\hat{a}_3 + \begin{vmatrix} \hat{a}_1 & \hat{a}_2 & \hat{a}_3 \\ 0 & 0 & \omega \\ X & Y & Z \end{vmatrix}$$

$$\dot{\bar{r}} = (\dot{X} - Y\omega)\hat{a}_1 + (\dot{Y} + X\omega)\hat{a}_2 + \dot{Z}\hat{a}_3.$$

With rotating reference axes, the calculation of the acceleration of vector \bar{r} with respect to an inertial frame is

$$\frac{d^2\bar{r}}{dt^2_n} = \dot{\omega} \times \bar{r}_a + \bar{\omega} \times (\bar{\omega} \times \bar{r}_a) + 2\bar{\omega} \times \frac{d\bar{r}}{dt_n} + \frac{d^2\bar{r}}{dt^2_n}$$

The first term is zero because the system rotates at constant angular speed.

Substitution into the equation yields

$$\begin{aligned} \frac{d^2\bar{r}}{dt^2_n} &= \bar{\omega} \times (-\omega Y\hat{a}_1 + \omega X\hat{a}_2) + 2\bar{\omega} \times (\dot{X}\hat{a}_1 + \dot{Y}\hat{a}_2 + \dot{Z}\hat{a}_3) \\ &\quad + (\ddot{X}\hat{a}_1 + \ddot{Y}\hat{a}_2 + \ddot{Z}\hat{a}_3) \\ &= \begin{vmatrix} \hat{a}_1 & \hat{a}_2 & \hat{a}_3 \\ 0 & 0 & \omega \\ -\omega Y & \omega X & 0 \end{vmatrix} + \begin{vmatrix} \hat{a}_1 & \hat{a}_2 & \hat{a}_3 \\ 0 & 0 & 2\omega \\ \dot{X} & \dot{Y} & \dot{Z} \end{vmatrix} + (\ddot{X}\hat{a}_1 + \ddot{Y}\hat{a}_2 + \ddot{Z}\hat{a}_3) \end{aligned}$$

$$\ddot{\bar{r}} = (\ddot{X} - 2\omega\dot{Y} - \omega^2 X)\hat{a}_1 + (\ddot{Y} + 2\omega\dot{X} - \omega^2 Y)\hat{a}_2 + \ddot{Z}\hat{a}_3$$

We associate the kinematics of $\ddot{\bar{r}}$ with the force of gravity acting on the system. Gravity is the only force acting on the system.

From Newton's second law, which states that the time rate of change of linear momentum is proportional to the force applied. For our fixed-mass system of interest

$$\bar{F} = m_3\ddot{\bar{r}} = -\frac{Gm_1m_3}{|r_1|^3}\bar{r}_1 - \frac{Gm_2m_3}{|r_2|^3}\bar{r}_2.$$

As a reminder, m_1 is the mass of the larger large body, m_2 is the mass of the smaller large body, and m_3 is the mass of the spacecraft. Now substitute into this expression the equations for $\ddot{\vec{r}}$, $\ddot{\vec{r}}_1$ and $\ddot{\vec{r}}_2$ and separate the vector equation into the three components.

$$\begin{aligned}
(\ddot{X} - 2\omega\dot{Y} - \omega^2 X)\hat{a}_1 + (\ddot{Y} + 2\omega\dot{X} - \omega^2 Y)\hat{a}_2 + \ddot{Z}\hat{a}_3 = \\
-\frac{Gm_1}{|r_1|^3}[(X + D_1)\hat{a}_1 + Y\hat{a}_2 + Z\hat{a}_3] - \frac{Gm_2}{|r_2|^3}r_2[(X - D_2)\hat{a}_1 + Y\hat{a}_2 + Z\hat{a}_3] \\
\ddot{X} - 2\omega\dot{Y} - \omega^2 X = -\frac{\mu_1(X + D_1)}{|r_1|^3} - \frac{\mu_2(X - D_2)}{|r_2|^3} \\
\ddot{Y} + 2\omega\dot{X} - \omega^2 Y = -\frac{\mu_1 Y}{|r_1|^3} - \frac{\mu_2 Y}{|r_2|^3} \\
\ddot{Z} = -\frac{\mu_1 Z}{|r_1|^3} - \frac{\mu_2 Z}{|r_2|^3}
\end{aligned}$$

From Wie [4] we note these equations of motion can also be expressed in terms of a pseudopotential $U = U(X, Y, Z)$ as follows:

$$\begin{aligned}
\ddot{X} - 2\omega\dot{Y} &= \frac{\partial U}{\partial X} \triangleq U_X \\
\ddot{Y} + 2\omega\dot{X} &= \frac{\partial U}{\partial Y} \triangleq U_Y \\
\ddot{Z} &= \frac{\partial U}{\partial Z} \triangleq U_Z.
\end{aligned}$$

where the pseudopotential U , which is the centrifugal plus gravitational force potential, is defined as

$$U = \frac{1}{2}\omega^2(X^2 + Y^2) + \frac{\mu_1}{r_1} + \frac{\mu_2}{r_2}.$$

Also

$$\begin{aligned}
r_1 &= \sqrt{(X + D_1)^2 + Y^2 + Z^2} \\
r_2 &= \sqrt{(X - D_2)^2 + Y^2 + Z^2}.
\end{aligned}$$

Again, the initial conditions to be specified are

$$\begin{aligned}
X(0) \quad \dot{X}(0) \\
Y(0) \quad \dot{Y}(0) \\
Z(0) \quad \dot{Z}(0).
\end{aligned}$$

B Derivation of the Full Nonlinear Equations of Motion for the Circular Restricted Three-Body Problem Near L_2

Begin with the results of the derivation of the full nonlinear equations of motion relative to barycenter, Equations (1)-(3):

$$\begin{aligned}\ddot{X} - 2\omega\dot{Y} - \omega^2 X &= -\frac{\mu_1(X + D_1)}{|r_1|^3} - \frac{\mu_2(X - D_2)}{|r_2|^3} \\ \ddot{Y} + 2\omega\dot{X} - \omega^2 Y &= -\frac{\mu_1 Y}{|r_1|^3} - \frac{\mu_2 Y}{|r_2|^3} \\ \ddot{Z} &= -\frac{\mu_1 Z}{|r_1|^3} - \frac{\mu_2 Z}{|r_2|^3}\end{aligned}$$

Substitute using (4)-(6):

$$\begin{aligned}X &= X_0 + x \\ Y &= Y_0 + y \\ Z &= Z_0 + z,\end{aligned}$$

to obtain

$$\begin{aligned}(\ddot{X}_0 + \ddot{x}) - 2\omega(\dot{Y}_0 + \dot{y}) - \omega^2(X_0 + x) &= -\frac{\mu_1(X_0 + x + D_1)}{|r_1|^3} - \frac{\mu_2(X_0 + x - D_2)}{|r_2|^3} \\ (\ddot{Y}_0 + \ddot{y}) - 2\omega(\dot{X}_0 + \dot{x}) - \omega^2(Y_0 + y) &= -\frac{\mu_1(Y_0 + y)}{|r_1|^3} - \frac{\mu_2(Y_0 + y)}{|r_2|^3} \\ (\ddot{Z}_0 + \ddot{z}) &= -\frac{\mu_1(Z_0 + z)}{|r_1|^3} - \frac{\mu_2(Z_0 + z)}{|r_2|^3}\end{aligned}$$

By definition the equilibrium point is stationary; therefore, many terms are zero.

$$\begin{aligned}\ddot{X}_0 &= 0 & \ddot{x} &= 0 \\ \ddot{Y}_0 &= 0 & \ddot{y} &= 0 \\ \ddot{Z}_0 &= 0 & \ddot{z} &= 0.\end{aligned}$$

The equations reduce to the following:

$$\ddot{x} - 2\omega\dot{y} - \omega^2(X_0 + x) = -\frac{\mu_1(X_0 + x + D_1)}{r_1^3} - \frac{\mu_2(X_0 + x - D_2)}{r_2^3}$$

$$\begin{aligned}\ddot{y} + 2\omega\dot{x} - \omega^2(Y_0 + y) &= -\frac{\mu_1(Y_0 + y)}{r_1^3} - \frac{\mu_2(Y_0 + y)}{r_2^3} \\ \ddot{z} &= -\frac{\mu_1(Z_0 + z)}{r_1^3} - \frac{\mu_2(Z_0 + z)}{r_2^3},\end{aligned}$$

where r_1 and r_2 are now defined below as

$$\begin{aligned}r_1 &= \sqrt{(X_0 + x + D_1)^2 + (Y_0 + y)^2 + (Z_0 + z)^2} \\ r_2 &= \sqrt{(X_0 + x - D_2)^2 + (Y_0 + y)^2 + (Z_0 + z)^2}.\end{aligned}$$

The initial conditions to be specified are

$$\begin{aligned}x(0) & \quad \dot{x}(0) \\ y(0) & \quad \dot{y}(0) \\ z(0) & \quad \dot{z}(0).\end{aligned}$$

C Derivation of the Linear Equations of Motion for the Circular Restricted Three-Body Problem Near L_2

We develop linear equations to have models applicable for linear analysis methods.

We document details not shown in Hamilton's thesis.

We repeat the nonlinear equations for convenience.

$$\begin{aligned}\ddot{X} - 2\omega\dot{Y} &= \frac{\partial U}{\partial X} \\ \ddot{Y} + 2\omega\dot{X} &= \frac{\partial U}{\partial Y} \\ \ddot{Z} &= \frac{\partial U}{\partial Z}\end{aligned}$$

where

$$U = \frac{1}{2}\omega^2(X^2 + Y^2) + \frac{\mu_1}{r_1} + \frac{\mu_2}{r_2}.$$

Also

$$\begin{aligned}r_1 &= \sqrt{(X + D_1)^2 + Y^2 + Z^2} \\ r_2 &= \sqrt{(X - D_2)^2 + Y^2 + Z^2}.\end{aligned}$$

We substitute the individual coordinates

$$\begin{aligned}X &= X_0 + x \\ Y &= Y_0 + y \\ Z &= Z_0 + z\end{aligned}$$

to obtain

$$\begin{aligned}(\ddot{X}_0 + \ddot{x}) - 2\omega(\dot{Y}_0 + \dot{y}) &= \frac{\partial U}{\partial X} = U_X \\ (\ddot{Y}_0 + \ddot{y}) - 2\omega(\dot{X}_0 + \dot{x}) &= \frac{\partial U}{\partial Y} = U_Y \\ (\ddot{Z}_0 + \ddot{z}) &= \frac{\partial U}{\partial Z} = U_Z\end{aligned}$$

Now, perform a Taylor series expansion on these partials of U , about the libration, equilibrium, point. The first two terms of this series for a function of one variable are

$$f(x) = f(X_0) + xf'(X_0).$$

For U_X , let $f(x, y, z) = \frac{\partial U}{\partial X}$

Note that because the function is already a first derivative, we stop the Taylor series at its first derivative so we can stop the series at the quadratic term. We have a function of three variables so the Taylor series is modified as follows (with L_2 substituting for subscript 0 as the chosen expansion and evaluation point)

$$f(x, y, z) = U_X|_{L_2} + x \frac{\partial}{\partial X} U_X \Big|_{L_2} + y \frac{\partial}{\partial Y} U_X \Big|_{L_2} + z \frac{\partial}{\partial Z} U_X \Big|_{L_2}$$

For U_Y , let $f(x, y, z) = \frac{\partial U}{\partial Y}$, then

$$f(x, y, z) = U_Y|_{L_2} + x \frac{\partial}{\partial X} U_Y \Big|_{L_2} + y \frac{\partial}{\partial Y} U_Y \Big|_{L_2} + z \frac{\partial}{\partial Z} U_Y \Big|_{L_2}$$

For U_Z , let $f(x, y, z) = \frac{\partial U}{\partial Z}$, then

$$f(x, y, z) = U_Z|_{L_2} + x \frac{\partial}{\partial X} U_Z \Big|_{L_2} + y \frac{\partial}{\partial Y} U_Z \Big|_{L_2} + z \frac{\partial}{\partial Z} U_Z \Big|_{L_2}$$

By definition at the equilibrium point, there is no motion. Many terms are zero.

$$\begin{aligned} \ddot{X}_{L_2} &= \dot{x}_{L_2} = U_X|_{L_2} = 0 \\ \ddot{Y}_{L_2} &= \dot{y}_{L_2} = U_Y|_{L_2} = 0 \\ \ddot{Z}_{L_2} &= \dot{z}_{L_2} = U_Z|_{L_2} = 0 \end{aligned}$$

Additionally, terms of U_X and U_Y involving the partial of Z are zero because motions in the Z -direction are uncoupled from the X - Y plane motions. Therefore

$$\begin{aligned} \ddot{x} - 2\omega\dot{y} &= xU_{XX}|_{L_2} + yU_{YX}|_{L_2} \\ \ddot{y} - 2\omega\dot{x} &= xU_{XY}|_{L_2} + yU_{YY}|_{L_2} \\ \ddot{z} &= zU_{ZZ}|_{L_2} \end{aligned}$$

The above equations are the first-order, or linear, coupled, equations of motion for the circular restricted three-body problem. These describe the motion of the spacecraft relative to an equilibrium point (X_0, Y_0, Z_0) . The equilibrium point rotates with a constant angular velocity.

$$U|_0 = \frac{\omega^2}{2}(X_0^2 + Y_0^2) + \frac{\mu_1}{|\sqrt{(X_0 + D_1)^2 + Y_0^2 + Z_0^2}|} + \frac{\mu_2}{|\sqrt{(X_0 - D_0)^2 + Y_0^2 + Z_0^2}|}$$

For the restricted three-body problem at L_2 , the Y_0 and Z_0 terms are zero and the equations reduce to

$$\begin{aligned} \ddot{x} - 2\omega\dot{y} &= xU_{XX}|_{L_2} \\ \ddot{y} + 2\omega\dot{x} &= yU_{YY}|_{L_2} \\ \ddot{z} &= zU_{ZZ}|_{L_2} \end{aligned}$$

Return to the general form of U as we first carry out the derivatives of U , then substitute for the libration point.

$$U = \frac{\omega^2}{2}(X^2 + Y^2) + \frac{\mu_1}{\sqrt{(X + D_1)^2 + Y^2 + Z^2}} + \frac{\mu_2}{\sqrt{(X - D_2)^2 + Y^2 + Z^2}}$$

For X :

$$\begin{aligned} \frac{\partial U}{\partial X} &= \frac{\partial U}{\partial X} \left[\frac{\omega^2}{2}(X^2 + Y^2) \right] \\ &\quad + \frac{\partial U}{\partial X} \left[\frac{\mu_1}{\sqrt{(X + D_1)^2 + Y^2 + Z^2}} \right] \\ &\quad + \frac{\partial U}{\partial X} \left[\frac{\mu_2}{\sqrt{(X - D_2)^2 + Y^2 + Z^2}} \right] \\ &= \omega^2 X \\ &\quad + \mu_1 \frac{\partial U}{\partial X} \left[((X + D_1)^2 + Y^2 + Z^2)^{-\frac{1}{2}} \right] \\ &\quad + \mu_2 \frac{\partial U}{\partial X} \left[((X - D_2)^2 + Y^2 + Z^2)^{-\frac{1}{2}} \right] \end{aligned}$$

Employ the differential $d(u^n) = nu^{n-1}du$ to calculate the last two terms of the equation $\frac{\partial U}{\partial X}$:

$$\begin{aligned} &\mu_1 \frac{\partial U}{\partial X} \left[((X + D_1)^2 + Y^2 + Z^2)^{-\frac{1}{2}} \right] \\ &= \mu_1 \left(-\frac{1}{2} \right) ((X + D_1)^2 + Y^2 + Z^2)^{-\frac{3}{2}} \frac{\partial}{\partial X} ((X + D_1)^2 + Y^2 + Z^2) \\ &= -\frac{\mu_1}{2} \frac{1}{\sqrt{(X + D_1)^2 + Y^2 + Z^2}^3} (2X + 2D_1) \\ &= -\frac{\mu_1(X + D_1)}{\sqrt{(X + D_1)^2 + Y^2 + Z^2}^3} \end{aligned}$$

Of course this calculation is similar for the term beginning with μ_2 . Here assign

$$\begin{aligned} r_1 &= \sqrt{(X + D_1)^2 + Y^2 + Z^2} \\ r_2 &= \sqrt{(X - D_2)^2 + Y^2 + Z^2} \end{aligned}$$

Finally

$$\frac{\partial U}{\partial X} = \omega^2 X - \frac{\mu_1(X + D_1)}{r_1^3} - \frac{\mu_2(X - D_2)}{r_2^3}.$$

Now take the second derivative using $d(uv) = u dv + v du$:

$$\begin{aligned} \frac{\partial^2 U}{\partial X^2} &= \omega^2 - \mu_1 \frac{\partial}{\partial X} \left[\overbrace{(X + D_1)}^u \overbrace{((X + D_1)^2 + Y^2 + Z^2)^{-\frac{3}{2}}}^v \right] \\ &\quad - \mu_2 \frac{\partial}{\partial X} \left[\overbrace{(X - D_2)}^u \overbrace{((X - D_2)^2 + Y^2 + Z^2)^{-\frac{3}{2}}}^v \right]. \end{aligned}$$

$$\begin{aligned} \frac{\partial^2 U}{\partial X^2} &= \omega^2 - \mu_1 \left\{ (X + D_1) \left[-\frac{3}{2} ((X + D_1)^2 + Y^2 + Z^2)^{-\frac{5}{2}} (2X + 2D_1) \right] \right. \\ &\quad \left. + ((X + D_1)^2 + Y^2 + Z^2)^{-\frac{3}{2}} (1) \right\} \\ &\quad - \mu_2 \left\{ (X - D_2) \left[-\frac{3}{2} ((X - D_2)^2 + Y^2 + Z^2)^{-\frac{5}{2}} (2X - 2D_2) \right] \right. \\ &\quad \left. + ((X - D_2)^2 + Y^2 + Z^2)^{-\frac{3}{2}} (1) \right\}. \end{aligned}$$

Now reduce the terms and substitute for r_1 and r_2

$$U_{XX} = \omega^2 - \mu_1 \left[\frac{1}{r_1^3} - \frac{3(X + D_1)^2}{r_1^5} \right] - \mu_2 \left[\frac{1}{r_2^3} - \frac{3(X - D_2)^2}{r_2^5} \right].$$

For Y :

$$\frac{\partial U}{\partial Y} = \omega^2 Y - \frac{\mu_1 Y}{r_1^3} - \frac{\mu_2 Y}{r_2^3}$$

and

$$U_{YY} = \omega^2 - \mu_1 \left[\frac{1}{r_1^3} - \frac{3Y^2}{r_1^5} \right] - \mu_2 \left[\frac{1}{r_2^3} - \frac{3Y^2}{r_2^5} \right].$$

For Z :

$$\frac{\partial U}{\partial Z} = -\frac{\mu_1 Z}{r_1^3} - \frac{\mu_2 Z}{r_2^3}$$

and

$$U_{ZZ} = -\mu_1 \left[\frac{1}{r_1^3} - \frac{3Z^2}{r_1^5} \right] - \mu_2 \left[\frac{1}{r_2^3} - \frac{3Z^2}{r_2^5} \right].$$

If desired, evaluate these at a collinear libration point, say L_2 where $X = X_0$, $Y = 0$, $Z = 0$.

$$\begin{aligned}U_{XX}|_{L_2} &= \omega^2 + \frac{2\mu_1}{(X_0 + D_1)^3} + \frac{2\mu_2}{(X_0 - D_2)^3} \\U_{YY}|_{L_2} &= \omega^2 - \frac{\mu_1}{(X_0 + D_1)^3} - \frac{\mu_2}{(X_0 - D_2)^3} \\U_{ZZ}|_{L_2} &= -\frac{\mu_1}{(X_0 + D_1)^3} - \frac{\mu_2}{(X_0 - D_2)^3}\end{aligned}$$

D Derivation of Quadratic Differential Equations for Circular Restricted Motion Near L_2

We repeat the nonlinear equations for convenience:

$$\ddot{X} - 2\omega\dot{Y} = \frac{\partial U}{\partial X} \quad (17)$$

$$\ddot{Y} + 2\omega\dot{X} = \frac{\partial U}{\partial Y} \quad (18)$$

$$\ddot{Z} = \frac{\partial U}{\partial Z} \quad (19)$$

where

$$U = \frac{\omega^2}{2}(X^2 + Y^2) + \frac{\mu_1}{r_1} + \frac{\mu_2}{r_2} \quad (20)$$

and

$$r_1^2 = (X + D_1)^2 + Y^2 + Z^2 \quad (21)$$

$$r_2^2 = (X - D_2)^2 + Y^2 + Z^2 \quad (22)$$

The right sides of the equations of motion can be formed from differentiation of Equation (20):

$$\frac{\partial U}{\partial X} = \omega^2 X - \frac{\mu_1}{r_1^2} \frac{\partial r_1}{\partial X} - \frac{\mu_2}{r_2^2} \frac{\partial r_2}{\partial X} \quad (23)$$

$$\frac{\partial U}{\partial Y} = \omega^2 Y - \frac{\mu_1}{r_1^2} \frac{\partial r_1}{\partial Y} - \frac{\mu_2}{r_2^2} \frac{\partial r_2}{\partial Y} \quad (24)$$

$$\frac{\partial U}{\partial Z} = -\frac{\mu_1}{r_1^2} \frac{\partial r_1}{\partial Z} - \frac{\mu_2}{r_2^2} \frac{\partial r_2}{\partial Z} \quad (25)$$

The required derivatives of r_1 and r_2 are formed by differentiating Equations (21) and (22):

$$\frac{\partial r_1}{\partial X} = \frac{X + D_1}{r_1}$$

$$\frac{\partial r_1}{\partial Y} = \frac{Y}{r_1}$$

$$\frac{\partial r_1}{\partial Z} = \frac{Z}{r_1}$$

$$\begin{aligned}\frac{\partial r_2}{\partial X} &= \frac{X - D_2}{r_2} \\ \frac{\partial r_2}{\partial Y} &= \frac{Y}{r_2} \\ \frac{\partial r_2}{\partial Z} &= \frac{Z}{r_2}\end{aligned}$$

Equations (23) – (25) are expanded in Taylor series expansions about the L_2 libration point, at coordinates $(X, Y, Z) = (X_0, 0, 0)$. Let

$$\begin{bmatrix} x \\ y \\ z \end{bmatrix} = \begin{bmatrix} X - X_0 \\ Y \\ Z \end{bmatrix} \quad (26)$$

give the displacement from L_2 . Denote $\partial U/\partial X$ by U_X , and similarly for U_Y and U_Z . Then, the Taylor series through second-order in x, y, z are given by

$$\begin{aligned}U_X &= U_X|_{L_2} + \left(\frac{\partial U_X}{\partial X} \Big|_{L_2} x + \frac{\partial U_X}{\partial Y} \Big|_{L_2} y + \frac{\partial U_X}{\partial Z} \Big|_{L_2} z \right) \\ &+ \frac{1}{2} \left(\frac{\partial^2 U_X}{\partial X^2} \Big|_{L_2} x^2 + \frac{\partial^2 U_X}{\partial Y^2} \Big|_{L_2} y^2 + \frac{\partial^2 U_X}{\partial Z^2} \Big|_{L_2} z^2 \right. \\ &\quad \left. - \frac{\partial^2 U_X}{\partial X \partial Y} \Big|_{L_2} xy + \frac{\partial^2 U_X}{\partial X \partial Z} \Big|_{L_2} xz + \frac{\partial^2 U_X}{\partial Y \partial Z} \Big|_{L_2} yz \right) \quad (27)\end{aligned}$$

$$\begin{aligned}U_Y &= U_Y|_{L_2} + \left(\frac{\partial U_Y}{\partial X} \Big|_{L_2} x + \frac{\partial U_Y}{\partial Y} \Big|_{L_2} y + \frac{\partial U_Y}{\partial Z} \Big|_{L_2} z \right) \\ &+ \frac{1}{2} \left(\frac{\partial^2 U_Y}{\partial X^2} \Big|_{L_2} x^2 + \frac{\partial^2 U_Y}{\partial Y^2} \Big|_{L_2} y^2 + \frac{\partial^2 U_Y}{\partial Z^2} \Big|_{L_2} z^2 \right. \\ &\quad \left. - \frac{\partial^2 U_Y}{\partial X \partial Y} \Big|_{L_2} xy + \frac{\partial^2 U_Y}{\partial X \partial Z} \Big|_{L_2} xz + \frac{\partial^2 U_Y}{\partial Y \partial Z} \Big|_{L_2} yz \right) \quad (28)\end{aligned}$$

$$\begin{aligned}U_Z &= U_Z|_{L_2} + \left(\frac{\partial U_Z}{\partial X} \Big|_{L_2} x + \frac{\partial U_Z}{\partial Y} \Big|_{L_2} y + \frac{\partial U_Z}{\partial Z} \Big|_{L_2} z \right) \\ &+ \frac{1}{2} \left(\frac{\partial^2 U_Z}{\partial X^2} \Big|_{L_2} x^2 + \frac{\partial^2 U_Z}{\partial Y^2} \Big|_{L_2} y^2 + \frac{\partial^2 U_Z}{\partial Z^2} \Big|_{L_2} z^2 \right. \\ &\quad \left. - \frac{\partial^2 U_Z}{\partial X \partial Y} \Big|_{L_2} xy + \frac{\partial^2 U_Z}{\partial X \partial Z} \Big|_{L_2} xz + \frac{\partial^2 U_Z}{\partial Y \partial Z} \Big|_{L_2} yz \right) \quad (29)\end{aligned}$$

A vertical bar with subscript L_2 indicates evaluation at the coordinates of the libration point.

The derivatives of U are constructed by differentiating Equations (23) – (25). Note that higher-order derivatives of r_1 and r_2 are required. These are given by

$$\begin{aligned}
\frac{\partial^2 r_1}{\partial X^2} &= \frac{1}{r_1} - \frac{(X + D_1)^2}{r_1^3} \\
\frac{\partial^2 r_1}{\partial Y^2} &= \frac{1}{r_1} - \frac{Y^2}{r_1^3} \\
\frac{\partial^2 r_1}{\partial Z^2} &= \frac{1}{r_1} - \frac{Z^2}{r_1^3} \\
\frac{\partial^2 r_1}{\partial X \partial Y} &= -\frac{(X + D_1)Y}{r_1^3} \\
\frac{\partial^2 r_1}{\partial X \partial Z} &= -\frac{(X + D_1)Z}{r_1^3} \\
\frac{\partial^2 r_1}{\partial Z \partial Z} &= -\frac{YZ}{r_1^3} \\
\frac{\partial^2 r_2}{\partial X^2} &= \frac{1}{r_2} - \frac{(X - D_2)^2}{r_2^3} \\
\frac{\partial^2 r_2}{\partial Y^2} &= \frac{1}{r_2} - \frac{Y^2}{r_2^3} \\
\frac{\partial^2 r_2}{\partial Z^2} &= \frac{1}{r_2} - \frac{Z^2}{r_2^3} \\
\frac{\partial^2 r_2}{\partial X \partial Y} &= -\frac{(X - D_2)Y}{r_2^3} \\
\frac{\partial^2 r_2}{\partial X \partial Z} &= -\frac{(X - D_2)Z}{r_2^3} \\
\frac{\partial^2 r_2}{\partial Z \partial Z} &= -\frac{YZ}{r_2^3}
\end{aligned}$$

The evaluated partial derivatives are then:

$$\begin{aligned}
\left. \frac{\partial U_X}{\partial X} \right|_{L_2} &= \omega^2 + \frac{2\mu_1}{(X_0 + D_1)^3} + \frac{2\mu_2}{(X_0 - D_2)^3} \\
\left. \frac{\partial U_Y}{\partial Y} \right|_{L_2} &= \omega^2 - \frac{\mu_1}{(X_0 + D_1)^3} - \frac{\mu_2}{(X_0 - D_2)^3}
\end{aligned}$$

$$\begin{aligned}
\left. \frac{\partial U_Z}{\partial Z} \right|_{L_2} &= -\frac{\mu_1}{(X_0 + D_1)^3} - \frac{\mu_2}{(X_0 - D_2)^3} \\
\left. \frac{\partial^2 U_X}{\partial X^2} \right|_{L_2} &= -\frac{6\mu_1}{(X_0 + D_1)^4} - \frac{6\mu_2}{(X_0 - D_2)^4} \\
\left. \frac{\partial^2 U_X}{\partial Y^2} \right|_{L_2} &= \frac{3\mu_1}{(X_0 + D_1)^4} + \frac{3\mu_2}{(X_0 - D_2)^4} \\
\left. \frac{\partial^2 U_X}{\partial Z^2} \right|_{L_2} &= \frac{3\mu_1}{(X_0 + D_1)^4} + \frac{3\mu_2}{(X_0 - D_2)^4}
\end{aligned}$$

and

$$\begin{aligned}
\left. \frac{\partial U_X}{\partial Y} \right|_{L_2} &= \left. \frac{\partial U_X}{\partial Z} \right|_{L_2} = \left. \frac{\partial U_Y}{\partial Z} \right|_{L_2} = \left. \frac{\partial^2 U_X}{\partial XY} \right|_{L_2} = \left. \frac{\partial^2 U_X}{\partial XZ} \right|_{L_2} \\
&= \left. \frac{\partial^2 U_X}{\partial YZ} \right|_{L_2} = \left. \frac{\partial^2 U_Y}{\partial Y^2} \right|_{L_2} = \left. \frac{\partial^2 U_Y}{\partial YZ} \right|_{L_2} = \left. \frac{\partial^2 U_Y}{\partial Z^2} \right|_{L_2} = \left. \frac{\partial^2 U_Z}{\partial Z^3} \right|_{L_2} = 0.
\end{aligned}$$

Note that, because of the continuity of the derivatives, any other derivatives are, in fact repeats of those listed. For example,

$$\begin{aligned}
\frac{\partial^2 U_Y}{\partial X^2} &= \frac{\partial^2}{\partial X^2} \left(\frac{\partial U}{\partial Y} \right) \\
&= \frac{\partial^3 U}{\partial X^2 \partial Y} \\
&= \frac{\partial^2}{\partial XY} \left(\frac{\partial U}{\partial X} \right) \\
&= \frac{\partial^2 U_X}{\partial XY}.
\end{aligned}$$

By definition, the L_2 coordinates satisfy the equilibrium condition of Equations (17) - (19). Therefore,

$$U_X|_{L_2} = U_Y|_{L_2} = U_X|_{L_2} = 0.$$

Substituting the derivatives into Equations (27) - (29),

$$U_X = \left[\omega^2 + \frac{2\mu_1}{(X_0 + D_1)^3} + \frac{2\mu_2}{(X_0 - D_2)^3} \right] x$$

$$-\frac{3}{2} \left[\frac{\mu_1}{(X_0 + D_1)^4} + \frac{\mu_2}{(X_0 - D_2)^3} \right] (2x^2 - y^2 - z^2) \quad (30)$$

$$U_Y = \left[\omega^2 - \frac{\mu_1}{(X_0 + D_1)^3} - \frac{\mu_2}{(X_0 - D_2)^3} \right] y \quad (31)$$

$$+ 3 \left[\frac{\mu_1}{(X_0 + D_1)^4} + \frac{\mu_2}{(X_0 - D_2)^3} \right] xy$$

$$U_Z = \left[-\frac{\mu_1}{(X_0 + D_1)^3} - \frac{\mu_2}{(X_0 - D_2)^3} \right] z \quad (32)$$

$$+ 3 \left[\frac{\mu_1}{(X_0 + D_1)^4} + \frac{\mu_2}{(X_0 - D_2)^3} \right] xz.$$

Define

$$A \triangleq \frac{\mu_1}{(X_0 + D_1)^3} + \frac{\mu_2}{(X_0 - D_2)^3} \quad (33)$$

$$B \triangleq \frac{\mu_1}{(X_0 + D_1)^4} + \frac{\mu_2}{(X_0 - D_2)^4}. \quad (34)$$

Then, substituting in Equations (30) - (32),

$$U_X = (\omega^2 + 2A)x - \frac{3}{2}B(2x^2 - y^2 - z^2)$$

$$U_Y = (\omega^2 - A)y + 3Bxy$$

$$U_Z = -Az + 3Bxz.$$

Substituting into Equations (17) - (18), and using Equation (26) on the left side, gives

$$\ddot{x} - 2\omega\dot{y} - \omega^2 x = 2Ax - \frac{3}{2}B(2x^2 - y^2 - z^2)$$

$$\ddot{y} + 2\omega\dot{x} - \omega^2 y = -Ay + 3Bxy$$

$$\ddot{z} = -Az + 3Bxz.$$

References

- [1] Hamilton, Nicholas H. "Formation Flying Satellite Control Around the L2 Sun-Earth Libration Point," Master's thesis, George Washington University, School of Engineering and Applied Science, 19 December 2001.
- [2] Vallado, David A. *Fundamentals of Astrodynamics and Applications*. 2nd ed. El Segundo, CA: Microcosm Press and Dordrecht, The Netherlands: Kluwer Academic Publishers, 2001.
- [3] Szebehely, Victor. *Theory of Orbits*. New York, NY: Academic Press Inc., 1967. [NRL Library: QB 355.S98]
- [4] Wie, Bong. *Space Vehicle Dynamics and Control*. Reston, VA: American Institute of Aeronautics and Astronautics, Inc., 1998.
- [5] Farquhar, Robert W. *The Control of Libration and Use of Libration-Point Satellites*. NASA TR R-346. Greenbelt, MD: Goddard Space Flight Center, September 1970.
- [6] Dunham, David W., and Daniel P. Muhonen. "Tables of Libration-Point Parameters for Selected Solar System Objects." *The Journal of the Astronautical Sciences* (January-March 2001): 197-217.

**Part 2: Linear and Quadratic
Modelling and Solution of the
Relative Motion**

Contents

1	Introduction	51
2	Problem Definition	52
3	Relative Motion Differential Equations	54
3.1	Series Expansion of Differential Equations	56
3.2	Magnitude Ordering	60
3.3	Linear Telescope Motion about the Hub	61
3.4	Halo Telescope Motion	63
4	Lindstedt-Poincaré Development	64
4.1	Order 1	67
4.2	Order 2	68
4.3	Order 3	72
4.4	Solution Summary	81
5	Simulation	81
5.1	Implementation Procedure	81
5.2	Simulation to Compare Results of Models	84
6	Summary	88
	Appendices	91
	A Constant Parameters	91
	References	95

List of Tables

1	Distance Ratios and Basic Accelerations	60
2	Relationship of Aperture Plane Roll Angle to i and j	79
3	Summary of Inputs and Resulting Values Used to Select Orbit Size and Orientation	83
4	Initial Conditions of Telescope With Respect to Hub Resulting From Analytical Solution	85
5	Initial Conditions of Hub With Respect to Sun-Earth L_2 Point	86
6	Physical Constants [3]	91
7	Derived Constants	91
8	Constants Specific to Sun-Earth L_2 Point [2]	91
9	Computed Values and Coefficients	93

List of Figures

1	Aperture Formation of MAXIM Pathfinder, Concept of June 2002.	52
2	Coordinate Axis Definition.	55
3	Compare 3 Solutions for Telescope Motion Along the x -axis. .	87
4	Compare 3 Solutions for Telescope Motion Along the y -axis. .	87
5	Compare 3 Solutions for Telescope Motion Along the z -axis. .	88

1 Introduction

Some continuing long-term goals of our sponsor are to develop high-fidelity equations of motion representing the formation flying of spacecraft near the Sun-Earth L_2 point and equations describing the relative motion between these constellation members. The equations are to be used to develop orbit control schemes.

This is our second report, which continues from Part 1 [1], with further derivations of analytical expressions for the relative motion between a formation of spacecraft orbiting near the Sun-Earth L_2 point. This research is loosely motivated by formation flying concepts for the MicroArcsecond X-ray Imaging Mission (MAXIM) Pathfinder.

To begin the understanding of the behavior of objects in formation near L_2 , we begin with the assumptions of a circular restricted three-body problem. In this report, we are not modeling the true eccentric orbit of the Earth and Moon about their respective primaries and other planetary and solar gravitational orbit perturbations.

In this report, we present a preliminary understanding of the relative motion between two spacecraft orbiting the chosen L_2 point. While components are further identified below, we describe the motion of a typical telescope spacecraft with respect to the central hub spacecraft of the constellation. The hub is treated as the constellation's reference point; its orbital path about L_2 was examined in Part 1. The description of motion of one telescope spacecraft with respect to the hub spacecraft can be applied to as many telescope spacecraft as needed.

After a significant literature search, we state that what we are uniquely contributing is a description of spacecraft in formation flight about the Sun-Earth L_2 point.

First, we list the components of the MAXIM mission. Second, we develop the differential equations of motion for the telescope spacecraft with respect to the hub. The resulting solution is developed using the Lindstedt-Poincaré perturbation method to ensure periodic motion. Periodic motion of the in-plane and out-of-plane orbit is desirable to maintain the formation. Finally, we provide analytic solutions of relative motion. This report thus contains the following:

- development of differential equations of motion for the telescope with respect to the hub

- description of the linear telescope motion about the hub
- discussion of the preference of a halo orbit (rather than a Lissajous orbit) of the hub about the L_2 point
- inclusion of linear hub motion effects upon the motion of the telescope relative to the hub
- inclusion of quadratic hub motion effects upon the relationships between the telescope frequency and amplitude

2 Problem Definition

The current configuration of the MAXIM Pathfinder mission is depicted and described below.

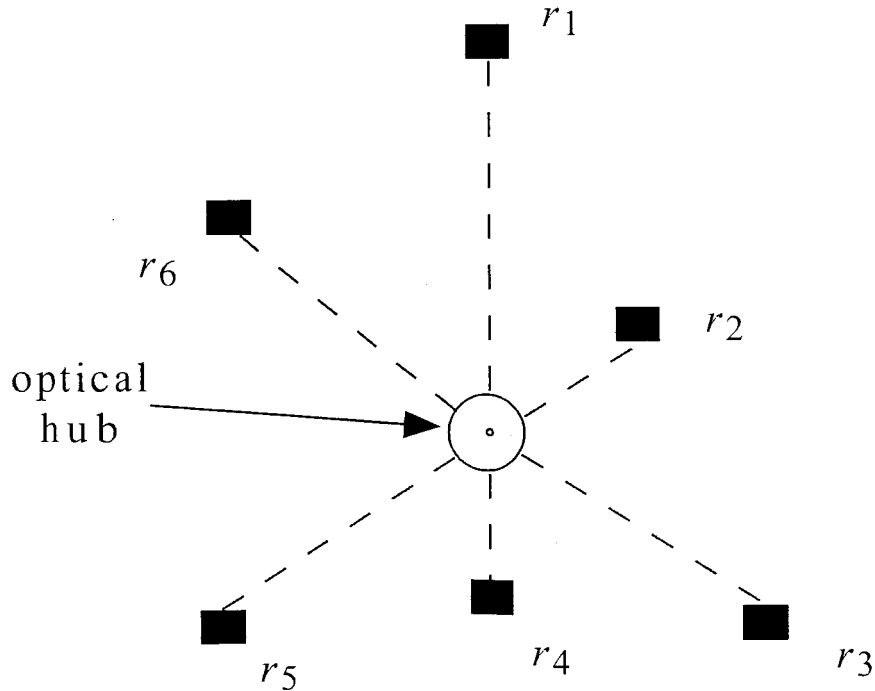


Figure 1: Aperture Formation of MAXIM Pathfinder, Concept of June 2002.

Seven spacecraft shown in Figure 1 are in the same plane forming a flat aperture. The optical hub is in the “center” of six free-flying spacecraft (telescopes). Dashed lines do not indicate a physical connection, but rather indicate random radial directions listed r_1 through r_6 . The scalar length of r ranges from 100 to 500 meters. Additionally, the six free-flying spacecraft are loosely spaced 60° from one another.

There is also a detector spacecraft located approximately 20,000 km and 90° out of the plane formed by the flat aperture. The entire system is in a Sun-Earth L_2 orbit, which has yet to be designed. The analysis of the detector’s orbit relative to the aperture plane was beyond the scope of this work.

At the beginning of this task, we were directed by the sponsor to investigate the following:

1. types and fidelity of models used to describe the relative orbits of the seven spacecraft forming the aperture
2. relative orbits of the seven spacecraft forming the flat aperture
3. slewing motions of the flat aperture

The optics hub slews only in attitude. The entire system points all over the sky — there is no nominal inertial orientation. Also, we may select any distance between L_2 and the optics hub. Additionally, the question was raised as to whether the motions of the telescope relative to the hub be described in cylindrical coordinates. This may be easier to describe when working with the project astronomers.

We were unable to do all of this with the funding available for this phase of the project. The work presented here covers the depth needed for items 1 and 2. We would need to continue to extend the development for one telescope into that for six telescopes. A computer-generated visualization of the aperture plane’s motion based on our equations of motion would be highly useful.

We have concerns about being able to arbitrarily select the distance between L_2 and the optics hub. We suggest that the MAXIM Pathfinder mission may best work in a halo-type orbit. A halo orbit is defined when the frequency ratio of out-of-plane to in-plane periods is a rational number. The

three-dimensional halo orbit closes on itself and is periodic, in contrast to a Lissajous orbit in which the trajectory does not close. In particular, we recommend a halo orbit in which the in-plane and out-of-plane periods are equal.

In Section 3 we form two sets of differential equations of relative motion: full nonlinear and truncated nonlinear equations.

In Section 4 we present an analytical solution to these equations.

In Section 5 we show simulations.

In Section 6 we summarize this report.

3 Relative Motion Differential Equations

In Part 1 of this research [1], the general second order differential equations of motion were constructed for an object near the Sun-Earth L_2 libration point, using the force model of the classical circular restricted three body problem. In this model, the Earth is treated as being in a circular orbit about the sun, the spacecraft mass is considered to be negligible as compared to the two primaries, and only point-mass gravitational forces are considered.

For this system, depicted in Figure 2, the differential equations of motion for an object (object i) near the Sun-Earth L_2 are given by

$$\ddot{\mathbf{r}}_i = - \left(\frac{\mu_1}{\rho_{1i}^3} + \frac{\mu_2}{\rho_{2i}^3} \right) \mathbf{r}_i - \left(\frac{\mu_1(x_e + D_1)}{\rho_{1i}^3} + \frac{\mu_2(x_e - D_2)}{\rho_{2i}^3} \right) \hat{\mathbf{x}} + n^2 x_e \hat{\mathbf{x}},$$

where

\mathbf{r}_i = vector from L_2 to object i

μ_1 = solar Keplerian constant

μ_2 = terrestrial Keplerian constant (Earth + Moon)

ρ_{1i} = distance from Sun to object i

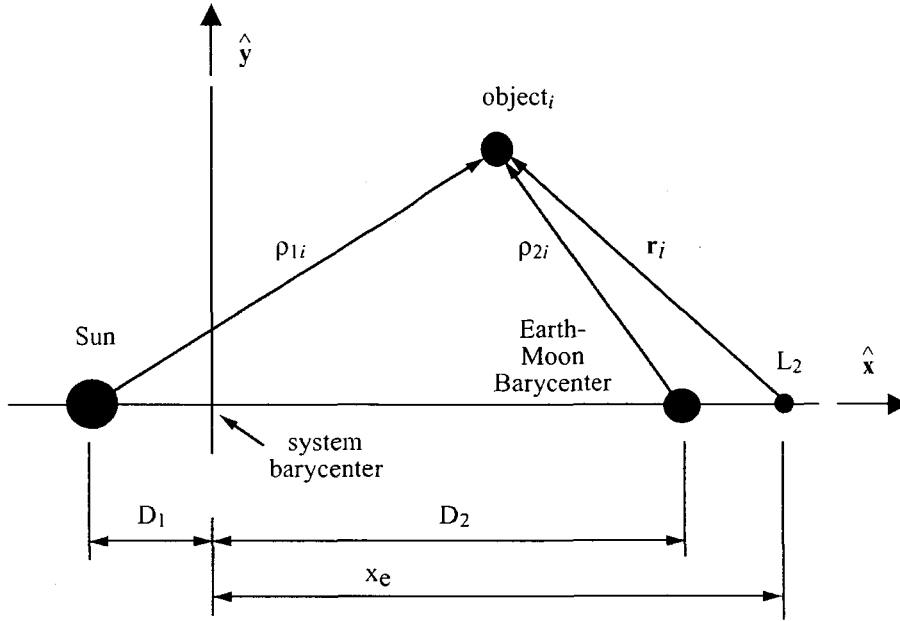


Figure 2: Coordinate Axis Definition.

ρ_{2i} = distance from Earth-Moon barycenter to object i

x_e = distance from system barycenter to L_2

D_1 = distance from system barycenter to sun

D_2 = distance from system barycenter to earth-moon barycenter

\hat{x} = unit vector parallel to sun-earth line of syzygy,
pointing in sun-to-earth direction

n = terrestrial mean motion about sun (assumed constant).

Let \mathbf{r}_h and \mathbf{r}_t denote, respectively, the vector from L_2 to the hub and to a telescope. Therefore, if \mathbf{r} is the vector from the hub to the telescope, the

differential equation of motion for the telescope relative to the hub is

$$\begin{aligned}
\ddot{\mathbf{r}} &= \ddot{\mathbf{r}}_t - \ddot{\mathbf{r}}_h \\
&= - \left(\frac{\mu_1}{\rho_{1t}^3} + \frac{\mu_2}{\rho_{2t}^3} \right) \mathbf{r}_t - \left(\frac{\mu_1(x_e + D_1)}{\rho_{1t}^3} + \frac{\mu_2(x_e - D_2)}{\rho_{2t}^3} \right) \hat{\mathbf{x}} \\
&\quad - \left(\frac{\mu_1}{\rho_{1h}^3} + \frac{\mu_2}{\rho_{2h}^3} \right) \mathbf{r}_h + \left(\frac{\mu_1(x_e + D_1)}{\rho_{1h}^3} + \frac{\mu_2(x_e - D_2)}{\rho_{2h}^3} \right) \hat{\mathbf{x}} \\
&= -\mu_1 \left(\frac{\mathbf{r}_t}{\rho_{1t}^3} - \frac{\mathbf{r}_h}{\rho_{1h}^3} \right) - \mu_2 \left(\frac{\mathbf{r}_t}{\rho_{2t}^3} - \frac{\mathbf{r}_h}{\rho_{2h}^3} \right) \\
&\quad - \mu_1(x_e + D_1) \left(\frac{1}{\rho_{1t}^3} - \frac{1}{\rho_{1h}^3} \right) \hat{\mathbf{x}} - \mu_2(x_e - D_2) \left(\frac{1}{\rho_{2t}^3} - \frac{1}{\rho_{2h}^3} \right) \hat{\mathbf{x}},
\end{aligned} \tag{1}$$

where now, in general, the subscripts h and t refer to the hub and telescope.

3.1 Series Expansion of Differential Equations

The differential equations of motion are now expanded in powers of the distances between L_2 and the hub, as well as between the hub and the telescope. This is done with the intention of developing an analytical solution in terms of these quantities, useful for performing a control system analysis.

First, the inverse powers of the ρ magnitudes are written in terms of these distances. If $\boldsymbol{\rho}_{1h}$ is the vector from the sun to the hub, then

$$\boldsymbol{\rho}_{1h} = (x_e + D_1)\hat{\mathbf{x}} + \mathbf{r}_h.$$

The square of its magnitude is then given by

$$\begin{aligned}
\rho_{1h}^2 &= \boldsymbol{\rho}_{1h} \cdot \boldsymbol{\rho}_{1h} \\
&= (x_e + D_1)^2 + r_h^2 + 2(x_e + D_1)(\mathbf{r}_h \cdot \hat{\mathbf{x}}) \\
&= (x_e + D_1)^2 + r_h^2 + 2(x_e + D_1)x_h \\
&= (x_e + D_1)^2 \left[1 + \left(\frac{r_h}{x_e + D_1} \right)^2 + \frac{2x_h}{x_e + D_1} \right].
\end{aligned}$$

where x_h is the x -component of \mathbf{r}_h . Then,

$$\begin{aligned}
\frac{1}{\rho_{1h}^3} &= \frac{1}{(x_e + D_1)^3} \left[1 + \left(\frac{r_h}{x_e + D_1} \right)^2 + \frac{2x_h}{x_e + D_1} \right]^{-3/2} \\
&= (x_e + D_1)^{-3} (1 + c_{1h})^{-3/2},
\end{aligned}$$

where

$$\epsilon_{1h} \triangleq \left(\frac{r_h}{x_e + D_1} \right)^2 + \frac{2x_h}{x_e + D_1}$$

is assumed to be less than unity. Using a binomial expansion,

$$\begin{aligned} \frac{1}{\rho_{1h}^3} &= \frac{1}{(x_e + D_1)^3} \sum_{k=0}^{\infty} \binom{-3/2}{k} \epsilon_{1h}^k \\ &= \frac{1}{(x_e + D_1)^3} \left[1 + \sum_{k=1}^{\infty} \binom{-3/2}{k} \epsilon_{1h}^k \right]. \end{aligned}$$

In the same fashion, for the telescope,

$$\frac{1}{\rho_{1t}^3} = \frac{1}{(x_e + D_1)^3} \left[1 + \sum_{k=1}^{\infty} \binom{-3/2}{k} \epsilon_{1t}^k \right], \quad (2)$$

where

$$\epsilon_{1t} \triangleq \left(\frac{r_t}{x_e + D_1} \right)^2 + \frac{2x_t}{x_e + D_1},$$

again assumed to be less than unity.

Now, r_t may be written in terms of r_h . Using

$$\mathbf{r}_t = \mathbf{r}_h + \mathbf{r},$$

$$\begin{aligned} r_t^2 &= (\mathbf{r}_h + \mathbf{r}) \cdot (\mathbf{r}_h + \mathbf{r}) \\ &= r_h^2 + r^2 + 2\mathbf{r}_h \cdot \mathbf{r}. \end{aligned}$$

Also,

$$x_t = x_h + x.$$

Therefore,

$$\begin{aligned} \epsilon_{1t} &= \left(\frac{r_t}{x_e + D_1} \right)^2 + \frac{2x_t}{x_e + D_1} \\ &= \frac{r_h^2 + r^2 + 2\mathbf{r}_h \cdot \mathbf{r}}{(x_e + D_1)^2} + \frac{2(x_h + x)}{x_e + D_1} \\ &= \left[\frac{r_h^2}{(x_e + D_1)^2} + \frac{2x_h}{x_e + D_1} \right] + \left[\frac{r^2 + 2\mathbf{r}_h \cdot \mathbf{r}}{(x_e + D_1)^2} + \frac{2x}{x_e + D_1} \right] \\ &= \epsilon_{1h} + \delta_1, \end{aligned}$$

where

$$\delta_1 \triangleq \frac{r^2 + 2\mathbf{r}_h \cdot \mathbf{r}}{(x_e + D_1)^2} + \frac{2x}{x_e + D_1}.$$

Again using a binomial expansion, the powers of ϵ_{1t} , as required in Equation (2), are given by

$$\begin{aligned} \epsilon_{1t}^k &= (\epsilon_{1h} + \delta_1)^k \\ &= \sum_{\ell=0}^k \binom{k}{\ell} \delta_1^\ell \epsilon_{1h}^{k-\ell} \\ &= \epsilon_{1h}^k + \sum_{\ell=1}^k \binom{k}{\ell} \delta_1^\ell \epsilon_{1h}^{k-\ell}. \end{aligned}$$

This expression may now be used in Equation (2), giving

$$\begin{aligned} \frac{1}{\rho_{1t}^3} &= \frac{1}{(x_e + D_1)^3} \left\{ 1 + \sum_{k=1}^{\infty} \binom{-3/2}{k} \left[\epsilon_{1h}^k + \sum_{\ell=1}^k \binom{k}{\ell} \delta_1^\ell \epsilon_{1h}^{k-\ell} \right] \right\} \\ &= \frac{1}{(x_e + D_1)^3} \left[1 + \sum_{k=1}^{\infty} \binom{-3/2}{k} \epsilon_{1h}^k \right] \\ &\quad + \frac{1}{(x_e + D_1)^3} \sum_{k=1}^{\infty} \binom{-3/2}{k} \sum_{\ell=1}^k \binom{k}{\ell} \delta_1^\ell \epsilon_{1h}^{k-\ell} \\ &= \frac{1}{\rho_{1h}^3} + \frac{1}{(x_e + D_1)^3} \sum_{k=1}^{\infty} \binom{-3/2}{k} \sum_{\ell=1}^k \binom{k}{\ell} \delta_1^\ell \epsilon_{1h}^{k-\ell}. \end{aligned}$$

Therefore, for use in Equation (1),

$$\frac{1}{\rho_{1t}^3} - \frac{1}{\rho_{1h}^3} = \frac{1}{(x_e + D_1)^3} \sum_{k=1}^{\infty} \binom{-3/2}{k} \sum_{\ell=1}^k \binom{k}{\ell} \delta_1^\ell \epsilon_{1h}^{k-\ell}. \quad (3)$$

Additionally,

$$\begin{aligned} \frac{\mathbf{r}_t}{\rho_{1t}^3} - \frac{\mathbf{r}_h}{\rho_{1h}^3} &= \frac{\mathbf{r}_h + \mathbf{r}}{\rho_{1t}^3} - \frac{\mathbf{r}_h}{\rho_{1h}^3} \\ &= \mathbf{r}_h \left(\frac{1}{\rho_{1t}^3} - \frac{1}{\rho_{1h}^3} \right) + \frac{\mathbf{r}}{\rho_{1t}^3}. \end{aligned} \quad (4)$$

An identical development may be used to form the following relationships for distances involving the earth:

$$\frac{1}{\rho_{2t}^3} - \frac{1}{\rho_{2h}^3} = \frac{1}{(x_e - D_2)^3} \sum_{k=1}^{\infty} \binom{-3/2}{k} \sum_{\ell=1}^k \binom{k}{\ell} \delta_2^\ell c_{2h}^{k-\ell} \quad (5)$$

and

$$\frac{\mathbf{r}_t}{\rho_{2t}^3} - \frac{\mathbf{r}_h}{\rho_{2h}^3} = \mathbf{r}_h \left(\frac{1}{\rho_{2t}^3} - \frac{1}{\rho_{2h}^3} \right) + \frac{\mathbf{r}}{\rho_{2t}^3}, \quad (6)$$

where

$$\epsilon_{2h} \triangleq \left(\frac{r_h}{x_e - D_2} \right)^2 + \frac{2x_h}{x_e - D_2}$$

and

$$\delta_2 \triangleq \frac{r^2 + 2\mathbf{r}_h \cdot \mathbf{r}}{(x_e - D_2)^2} + \frac{2x}{x_e - D_2}.$$

Substituting Equations (3) (6) into Equation (1), the telescope motion relative to the hub is then given by

$$\begin{aligned} \ddot{\mathbf{r}} &= -\mu_1 \left[(\mathbf{r}_h + (x_e + D_1)\hat{\mathbf{x}}) \left(\frac{1}{\rho_{1t}^3} - \frac{1}{\rho_{1h}^3} \right) + \frac{\mathbf{r}}{\rho_{1t}^3} \right] \\ &\quad - \mu_2 \left[(\mathbf{r}_h + (x_e - D_2)\hat{\mathbf{x}}) \left(\frac{1}{\rho_{2t}^3} - \frac{1}{\rho_{2h}^3} \right) + \frac{\mathbf{r}}{\rho_{2t}^3} \right] \\ &= -\mu_1 \left[\frac{\mathbf{r}_h + (x_e + D_1)\hat{\mathbf{x}}}{(x_e + D_1)^3} \sum_{k=1}^{\infty} \binom{-3/2}{k} \sum_{\ell=1}^k \binom{k}{\ell} \delta_1^\ell \epsilon_{1h}^{k-\ell} \right. \\ &\quad \left. + \frac{\mathbf{r}}{(x_e + D_1)^3} \sum_{k=0}^{\infty} \binom{-3/2}{k} \sum_{\ell=0}^k \binom{k}{\ell} \delta_1^\ell \epsilon_{1h}^{k-\ell} \right] \\ &\quad - \mu_2 \left[\frac{\mathbf{r}_h + (x_e - D_2)\hat{\mathbf{x}}}{(x_e - D_2)^3} \sum_{k=1}^{\infty} \binom{-3/2}{k} \sum_{\ell=1}^k \binom{k}{\ell} \delta_2^\ell \epsilon_{2h}^{k-\ell} \right. \\ &\quad \left. + \frac{\mathbf{r}}{(x_e - D_2)^3} \sum_{k=0}^{\infty} \binom{-3/2}{k} \sum_{\ell=0}^k \binom{k}{\ell} \delta_2^\ell \epsilon_{2h}^{k-\ell} \right]. \end{aligned} \quad (7)$$

3.2 Magnitude Ordering

A magnitude ordering system is now employed in order to truncate Equation (7), prior to forming the solution. It is noted that the motion of the system takes place on two separate distance scales. There is a large distance scale, in which the motion of the hub about L_2 is described, relative to the motion of L_2 within the context of the three-body problem. Then, there is a small distance scale, in which the motion of the telescope about the hub is described, relative to the motion of the hub about L_2 .

Table 1: Distance Ratios and Basic Accelerations

r/r_h	8.333×10^{-7}
$r_h/(x_e + D_1)$	3.971×10^{-3}
$r_h/(x_e - D_2)$	3.980×10^{-1}
$r/(x_e + D_1)$	3.309×10^{-9}
$r/(x_e - D_2)$	3.316×10^{-7}
$\mu_1/(x_e + D_1)^2$	$5.812 \times 10^{-6} \text{ km/s}^2$
$\mu_2/(x_e - D_2)^2$	$1.775 \times 10^{-7} \text{ km/s}^2$

For ordering purposes, consider the hub motion about L_2 to be on the order of 600,000 km, and the telescope motion about the hub to be on the order of 500 m. Using the constants of Appendix A, the relative distances are approximated by the ratios of Table 1. In the differential equations, these ratios scale the basic acceleration quantities which also appear in the table. Terms involving these basic accelerations scaled by $r_h/(x_e + D_1)$ and $r_h/(x_e - D_2)$ are now designated as being of order 1; terms involving the basic accelerations scaled by $r/(x_e + D_1)$ and $r/(x_e - D_2)$ are designated as being of order 3.

Retaining terms in Equation (7) only through order 3, substantial algebra gives the truncated differential equations as

$$\begin{aligned}
 \ddot{\mathbf{r}} = & A[-\mathbf{r} + 3x\dot{\mathbf{x}}] \\
 & + B[3x\mathbf{r}_h + 3x_h\mathbf{r} + (3\mathbf{r}_h \cdot \mathbf{r} - 15xx_h)\dot{\mathbf{x}}] \\
 & + C[(3\mathbf{r}_h \cdot \mathbf{r} - 15xx_h)\mathbf{r}_h + \frac{3}{2}(r_h^2 - 5x_h^2)\mathbf{r} \\
 & \quad - \frac{15}{2}(2x_h\mathbf{r}_h \cdot \mathbf{r} - 7xx_h^2 + xr_h^2)\dot{\mathbf{x}}],
 \end{aligned} \tag{8}$$

where

$$A = \frac{\mu_1}{(x_e + D_1)^3} + \frac{\mu_2}{(x_e - D_2)^3} \quad (9)$$

$$B = \frac{\mu_1}{(x_e + D_1)^4} + \frac{\mu_2}{(x_e - D_2)^4} \quad (10)$$

$$C = \frac{\mu_1}{(x_e + D_1)^5} + \frac{\mu_2}{(x_e - D_2)^5}. \quad (11)$$

Note that this truncation includes terms which are linear in the coordinates of \mathbf{r} and no more than cubic in the coordinates of \mathbf{r}_h . Terms involving A , B , and C are, respectively, of orders 3, 4, and 5; lower order terms do not appear.

The acceleration vector $\ddot{\mathbf{r}}$ may be written relative to a rotating coordinate system which rotates at the constant angular rate n about the z -axis normal to the ecliptic, and with the x direction as previously defined. This gives

$$\ddot{\mathbf{r}} = \begin{bmatrix} \ddot{x} - 2n\dot{y} - n^2x \\ \ddot{y} + 2n\dot{x} - n^2y \\ \ddot{z} \end{bmatrix}.$$

where the column vector notation is used to indicate the xyz vector components.

3.3 Linear Telescope Motion about the Hub

Consider now the linear motion of the telescope about the hub. From Equation (8), the linear differential equations are given by

$$\ddot{\mathbf{r}} = A[-\mathbf{r} + 3x\hat{\mathbf{x}}],$$

or, in component form,

$$\begin{bmatrix} \ddot{x} - 2n\dot{y} - (n^2 + 2A)x \\ \ddot{y} + 2n\dot{x} - (n^2 - A)y \\ \ddot{z} + Az \end{bmatrix} = \mathbf{0}. \quad (12)$$

As would be expected, these differential equations take exactly the same form as the linearized hub equations discussed in [1], with the same fundamental frequencies; the same solution approach may be followed. Clearly, the out-of-plane motion in the z direction is decoupled from the motion in the

xy plane. The z equation describes simple harmonic motion, with a solution that may be written as

$$z = A_z \sin(\nu t + \psi),$$

where $\nu^2 = A$.

Following the standard linear analysis, the in-plane motion is assumed to exhibit a solution of the form

$$\begin{bmatrix} x \\ y \end{bmatrix} = \begin{bmatrix} a \\ b \end{bmatrix} e^{st}.$$

Accordingly, the fourth-degree characteristic equation for s is

$$s^4 - (A - 2n^2)s^2 - (n^2 + 2A)(A - n^2) = 0. \quad (13)$$

Keeping in mind the relative magnitudes of n (≈ 0.0172 rad/day) and A (≈ 0.0012 rad/day), the solution to this equation has four distinct roots. One root is positive real, and corresponds to a divergent mode:

$$s_d = \sqrt{\frac{A}{2} - n^2 + \sqrt{\left(\frac{A}{2} - n^2\right)^2 + (n^2 + 2A)(A - n^2)}}.$$

A second, negative real, root corresponds to a convergent mode:

$$s_c = -s_d.$$

The remaining two roots are a purely imaginary conjugate pair, corresponding to oscillatory motion with natural frequency λ given by

$$\lambda^2 = -\frac{A}{2} + n^2 + \sqrt{\left(\frac{A}{2} - n^2\right)^2 + (n^2 + 2A)(A - n^2)}.$$

Each mode shape is described by the eigenvector associated with the corresponding eigenvalue s .

As in the analysis of [1], periodic motion occurs if the in-plane initial conditions are selected so as to excite only the oscillatory linear modes. From the solution of the eigenvalue problem, placing this requirement upon the initial conditions gives

$$\begin{aligned} \dot{x}(0) &= \frac{\lambda}{k} y(0) \\ \dot{y}(0) &= -k\lambda x(0). \end{aligned}$$

where

$$k = \frac{\lambda^2 + n^2 + 2A}{2\lambda n}.$$

Under this relationship among the initial conditions, the complete linear solution for the telescope motion about the hub may now be written in the form

$$\begin{aligned} x &= -A_x \cos(\lambda t + \phi) \\ y &= kA_x \sin(\lambda t + \phi) \\ z &= A_z \sin(\nu t + \psi). \end{aligned}$$

3.4 Halo Telescope Motion

It is desired that the constellation of telescope spacecraft remain in approximately the same specified plane over the few days' duration required for observations. To achieve this orientation, a halo-type orbit of the telescopes about the hub is selected. Such an orbit provides periodic motion in the aperture plane, with the out-of-ecliptic-plane fundamental frequency equal to λ , the fundamental frequency of the xy -planar motion.

In order to do this, the inclusion of higher-order forces is used to adjust the out-of-plane fundamental frequency. Consider the z -component of Equation (8):

$$\begin{aligned} \ddot{z} &= -Az \\ &+ B(3xz_h + 3zx_h) \\ &+ C(-12xx_h z_h + 3yy_h z_h - 6zx_h^2 + \frac{3}{2}zy_h^2 + \frac{9}{2}zz_h^2). \end{aligned}$$

Recall that $A = \nu^2$, and define Δ such that

$$\Delta = \lambda^2 - \nu^2.$$

Then, this differential equation may be written as

$$\begin{aligned} \ddot{z} + \lambda^2 z &= \Delta z + B(3xz_h + 3zx_h) \\ &+ C(-12xx_h z_h + 3yy_h z_h - 6zx_h^2 + \frac{3}{2}zy_h^2 + \frac{9}{2}zz_h^2). \end{aligned}$$

Here, the magnitude of Δ allows the term Δz to be treated as a higher order term, grouped with the terms containing the coefficient C . Using this formulation, the linear solution now becomes

$$z = A_z \sin(\lambda t + \psi),$$

with the same fundamental period as the in-plane motion.

Together with the x and y components of Equation (8), the system differential equations are

$$\begin{aligned} \ddot{x} - 2n\dot{y} - n^2x &= -2Ax \\ &+ B(-6xx_h + 3yy_h + 3zz_h) \\ &+ C(12xx_h^2 - 12yx_hy_h - 12zx_hz_h - 6xy_h^2 - 6xz_h^2) \end{aligned} \quad (14a)$$

$$\begin{aligned} \ddot{y} + 2n\dot{x} - n^2y &= -Ay \\ &+ B(3xy_h + 3yx_h) \\ &+ C(-12xx_hy_h + \frac{9}{2}yy_h^2 + 3zy_hz_h - 6yx_h^2 + \frac{3}{2}yz_h^2) \end{aligned} \quad (14b)$$

$$\begin{aligned} \ddot{z} + \lambda^2z &= \Delta z + B(3xz_h + 3zx_h) \\ &+ C(-12xx_hz_h + 3yy_hz_h - 6zx_h^2 + \frac{3}{2}zy_h^2 + \frac{9}{2}zz_h^2). \end{aligned} \quad (14c)$$

4 Lindstedt-Poincaré Development

The analytical solution to the expanded equations of motion of Equations (14) is now developed using a modified version of the Lindstedt-Poincaré method. This method provides for the sequential solution of a system of differential equations, ordered by magnitude of the terms, while simultaneously placing restrictions on the initial conditions, in order to ensure periodic motion. In this development, the equations are expanded through third order in the small quantities, which is defined as terms that are at most linear in the motion of the telescope relative to the hub, and quadratic in the motion of the hub relative to L_2 .

Introduce the non-linear frequency terms by series expansion, and change the independent variable from t to τ , where

$$\tau = \omega t$$

and

$$\omega = 1 + \omega_1 + \omega_2 + \dots,$$

assumed to be an asymptotic series, is used to scale the linear frequency. Using primes to denote differentiation with respect to τ , the left side of Equations (14) become

$$\begin{bmatrix} \omega^2 x'' - 2\omega n y' - n^2 x \\ \omega^2 y'' + 2\omega n x' - n^2 y \\ \omega^2 z'' + \lambda^2 z \end{bmatrix}.$$

Recall that the forcing terms in the differential Equations (8) are ordered such that the terms involving A , B , and C are, respectively, of orders 3, 4, and 5. Now, for notational convenience, these terms are reordered as orders 1, 2, and 3. The solution vector is assumed to take the form of an asymptotic series, such that

$$\begin{bmatrix} x \\ y \\ z \end{bmatrix} = \begin{bmatrix} x_1 + x_2 + x_3 + \cdots \\ y_1 + y_2 + y_3 + \cdots \\ z_1 + z_2 + z_3 + \cdots \end{bmatrix},$$

where the ordering by subscript is consistent with the reordering of the terms of the differential equations; the order of a given term is specified by the subscript.

This expansion is then substituted into the differential equations of Equations (14), and terms collected by order. The resulting first-order equations for x_1 , y_1 , and z_1 , are given by

$$\begin{bmatrix} x_1'' - 2ny_1' - (n^2 - 2A)x_1 \\ y_1'' + 2nx_1' + (A - n^2)y_1 \\ z_1'' + \lambda^2 z_1 \end{bmatrix} = \mathbf{0}. \quad (15)$$

Note that these equations are identical in form to the linear equations of Equation (12), with λ replacing ν in the z component equation.

The second order equations contain contributions from the motion of the hub about L_2 . As shown by Richardson [2], the hub motion relative to L_2 may also be expressed in a series form:

$$\begin{bmatrix} x_h \\ y_h \\ z_h \end{bmatrix} = \begin{bmatrix} x_{1h} + x_{2h} + \cdots \\ y_{1h} + y_{2h} + \cdots \\ z_{1h} + z_{2h} + \cdots \end{bmatrix}.$$

In the second order equations, only x_{1h} , y_{1h} , and z_{1h} are included; at third order, the $2h$ terms contribute as well.

The second order equations for x_2 , y_2 , and z_2 , containing terms which are linear in the position of the hub, are then

$$\begin{bmatrix} x_2'' - 2ny_2' - (n^2 + 2A)x_2 \\ y_2'' + 2nx_2' + (A - n^2)y_2 \\ z_2'' + \lambda^2 z_2 \end{bmatrix} = \begin{bmatrix} -2\omega_1(x_1'' - ny_1') - 6Bx_1x_{1h} + 3B(y_1y_{1h}h + z_1z_{1h}) \\ -2\omega_1(y_1'' + nx_1') + 3B(x_1y_{1h} + y_1x_{1h}) \\ -2\omega_1z_1'' + 3B(x_1z_{1h} + z_1x_{1h}) \end{bmatrix}. \quad (16)$$

Here, the telescope motion terms on the right side are now assumed to be known from the solution to the linear equations.

Next, the third order equations for x_3 , y_3 , and z_3 , containing terms linear in the $2h$ hub position terms and quadratic in the $1h$ terms, are

$$\begin{aligned} x_3'' - 2ny_3' - (n^2 + 2A)x_3 = & \\ & - 2\omega_1(x_2'' - ny_2') - 2\omega_2(x_1'' - ny_1') - \omega_1^2 x_1'' \\ & + 3B(y_2 y_{1h} + z_2 z_{1h} - 2x_2 x_{1h} - 2x_1 x_{2h} + y_1 y_{2h} + z_1 z_{2h}) \\ & + 6C[x_1(2x_{1h}^2 - y_{1h}^2 - z_{1h}^2) - 2y_1 x_{1h} y_{1h} - 2z_1 x_{1h} z_{1h}] \end{aligned} \quad (17a)$$

$$\begin{aligned} y_3'' - 2nx_3' + (A - n^2)y_3 = & \\ & - 2\omega_1(y_2'' + nx_2') - 2\omega_2(y_1'' + nx_1') - \omega_1^2 y_1'' \\ & + 3B(x_2 y_{1h} + y_2 x_{1h} + x_1 y_{2h} + y_1 x_{2h}) \\ & + 3C[-4x_1 x_{1h} y_{1h} + y_1(-2x_{1h}^2 + \frac{3}{2}y_{1h}^2 + \frac{1}{2}z_{1h}^2) + z_1 y_{1h} z_{1h}] \end{aligned} \quad (17b)$$

$$\begin{aligned} z_3'' + \lambda^2 z_3 = & \\ & - 2\omega_1 z_2'' - (2\omega_2 + \omega_1^2)z_1'' + \Delta z_1 \\ & + 3B(x_2 z_{1h} + z_2 x_{1h} + x_1 z_{2h} + z_1 x_{2h}) \\ & + 3C[-4x_1 x_{1h} z_{1h} + y_1 y_{1h} z_{1h} + z_1(-2x_{1h}^2 + \frac{1}{2}y_{1h}^2 + \frac{3}{2}z_{1h}^2)]. \end{aligned} \quad (17c)$$

Again, the right side terms are assumed to be known from the lower order solutions.

Note that the left side terms at each order take an identical form. Therefore, a particular solution may be formed for a general periodic forcing function. That solution may then be applied to each of the actual forcing terms, and the complete solution given by superposition. Higher order homogeneous solutions are not required, as they are identical in form to the terms of the linear solution, and thus are already present in the complete solution.

Accordingly, consider the general case of the forced system, given by

$$\begin{bmatrix} x'' - 2ny' - (n^2 + 2A)x \\ y'' - 2nx' - (A - n^2)y \\ z'' + \lambda^2 z \end{bmatrix} = \begin{bmatrix} \mathcal{A} \cos(q\tau + \theta) \\ \mathcal{B} \sin(q\tau + \theta) \\ \mathcal{F} \sin(p\tau + \gamma) \end{bmatrix}. \quad (18)$$

This vector is representative of all forcing terms which occur, where q and p are integers. Next, following the method of undetermined coefficients, the particular solution is assumed to take the form

$$\begin{bmatrix} x \\ y \\ z \end{bmatrix} = \begin{bmatrix} R_x \cos(q\tau + \theta) \\ R_y \sin(q\tau + \theta) \\ R_z \sin(p\tau + \gamma) \end{bmatrix}.$$

Substituting into the general system of Equation (18), and solving for the solution amplitudes,

$$\begin{aligned} R_x &= \frac{2nq\mathcal{B} - \mathcal{A}(q^2 + n^2 - A)}{q^4 + (A - 2n^2)q^2 - (A - n^2)(n^2 + 2A)} \\ R_y &= \frac{2nq\mathcal{A} - \mathcal{B}(q^2 + n^2 + 2A)}{q^4 + (A - 2n^2)q^2 - (A - n^2)(n^2 + 2A)} \\ R_z &= \frac{\mathcal{F}}{\lambda^2 - p^2}. \end{aligned} \quad (19)$$

Note that the denominator of R_x and R_y is, in fact, the characteristic equation of the linear system, as seen in Equation (13), where s^2 has been replaced by $-q^2$. Therefore, upon examination of this particular solution, either q or p equaling λ corresponds to the resonance condition. In that case, the forcing function has the same frequency as the homogeneous solution, and so the particular solution must instead have an amplitude which is secular in τ . However, in order for the solution to be bounded for all τ , such secular terms may not appear. Therefore, restrictions are placed on the solution, such that secular terms do not arise.

For the case that $p = \lambda$, it is required that $\mathcal{F} = 0$. For $q = \lambda$, the general x and y -component differential equations are combined into a single fourth-order differential equation:

$$\begin{aligned} x'''' - (A - 2n^2)x'' - (A - n^2)(n^2 + 2A)x = \\ [2n\mathcal{B}q + (A - n^2 - q^2)\mathcal{A}] \cos(q\tau + \theta). \end{aligned} \quad (20)$$

It is then required that the forcing amplitude be zero, giving ¹

$$2n\mathcal{B}q + (A - n^2 - q^2)\mathcal{A} = 0. \quad (21)$$

4.1 Order 1

The solution to the first order system of Equation (15) is once again given by

$$\begin{bmatrix} x_1 \\ y_1 \\ z_1 \end{bmatrix} = \begin{bmatrix} -A_x \cos(\lambda\tau + \phi) \\ kA_x \sin(\lambda\tau + \phi) \\ A_z \sin(\lambda\tau + \psi) \end{bmatrix}, \quad (22)$$

¹Of course, the equations could instead be combined into a y'''' equation, which would give a different form of the required relationship. However, under the condition that q satisfy the characteristic equation, the two relationships are equivalent.

where here the solution is taken as a function of τ .

4.2 Order 2

Here, in the second order equations, as previously mentioned, x_{1h} , y_{1h} , and z_{1h} appear. Again from the earlier analysis, the linear hub solution may be written as

$$\begin{bmatrix} x_{1h} \\ y_{1h} \\ z_{1h} \end{bmatrix} = \begin{bmatrix} -A_{xh} \cos(\lambda_h t + \phi_h) \\ kA_{xh} \sin(\lambda_h t + \phi_h) \\ A_{zh} \sin(\nu_h t + \psi_h) \end{bmatrix}. \quad (23)$$

Also, the hub frequencies λ_h and ν_h may be written using a nonlinear asymptotic frequency scaling function ω_h , where

$$\omega_h = 1 + \omega_{1h} + \omega_{2h} + \dots$$

As already seen, the linear hub frequency is the same as that of the telescope; therefore $\lambda_h = \lambda\omega_h$ and $\nu_h = \nu\omega_h$. For now, also assume that $\omega_{1h} = \omega_1$.

Typically, a Lindstedt-Poincaré analysis is employed for autonomous systems. Here, however, the forcing function is an explicit function of time, arising from the assumed solution for the hub motion. In the linear hub solution of Equation (23), the independent variable t must now be written in terms of τ , as

$$\begin{aligned} t &= \tau/\omega \\ &= \frac{\tau}{1 + \omega_1 + \omega_2 + \dots} \\ &= \tau(1 - \omega_1 - \omega_2 + \omega_1^2 + \dots). \end{aligned}$$

Then, in the hub solution,

$$\begin{aligned} \lambda_h t &= \lambda\omega_h t \\ &= \lambda(1 + \omega_1 + \omega_{2h} + \dots)t \\ &= \lambda(1 + \omega_1 + \omega_{2h} + \dots)(1 - \omega_1 - \omega_2 + \omega_1^2 + \dots)\tau \\ &= \lambda(1 + \omega_{2h} - \omega_2 + \dots)\tau. \end{aligned}$$

Define the second order contribution to this frequency correction as

$$\Delta\omega_2 = \omega_{2h} - \omega_2,$$

giving

$$\lambda_h t = \lambda(1 + \Delta\omega_2 + \dots)\tau.$$

Similarly, for the out of plane frequency,

$$\begin{aligned}\nu_h t &= \nu_h(1 - \omega_1 - \omega_2 + \omega_1^2 + \dots)\tau \\ &= \nu_h(1 - \bar{\omega} + \dots)\tau,\end{aligned}$$

where $\bar{\omega}$ represents the frequency correction through order 2.

Also, write the hub phase angles ϕ_h and ψ_h in terms of the telescope angles as

$$\phi_h = \phi + \Delta\phi$$

and

$$\psi_h = \psi + \Delta\psi,$$

where $\Delta\phi$ and $\Delta\psi$ represent the offset in phase angles between the hub and telescope motion. Substituting into the linear hub solution of Equation (23), and retaining the frequency correction through ω_2 and ω_{2h} ,

$$\begin{bmatrix} x_{1h} \\ y_{1h} \\ z_{1h} \end{bmatrix} = \begin{bmatrix} -A_{xh} \cos(\lambda(1 + \Delta\omega_2)\tau + \phi + \Delta\phi) \\ kA_{xh} \sin(\lambda(1 + \Delta\omega_2)\tau + \phi + \Delta\phi) \\ A_{zh} \sin(\nu_h(1 - \bar{\omega})\tau + \psi + \Delta\psi) \end{bmatrix}. \quad (24)$$

This linear hub solution and the first order telescope solution of Equation (22) are substituted into the right side of the second order telescope equation, Equation (16). After resolving the angles, the three component equations are then written as

$$\begin{aligned}x_2'' - 2ny_2' - (n^2 + 2A)x_2 &= -2\omega_1\lambda(\lambda - nk)A_x \cos(\lambda\tau + \phi) \\ &\quad - 3\left(1 + \frac{k^2}{2}\right)BA_xA_{xh} \\ &\quad \cos(\lambda(2 + \Delta\omega_2)\tau + 2\phi + \Delta\phi) \\ &\quad - 3\left(1 - \frac{k^2}{2}\right)BA_xA_{rh} \cos(\lambda\Delta\omega_2\tau + \Delta\phi) \\ &\quad + \frac{3}{2}BA_zA_{zh} \cos((\lambda - \nu_h(1 - \bar{\omega}))\tau - \Delta\psi) \\ &\quad - \frac{3}{2}BA_zA_{zh} \cos((\lambda + \nu_h(1 - \bar{\omega}))\tau + 2\psi + \Delta\psi)\end{aligned} \quad (25a)$$

$$\begin{aligned}y_2'' + 2nx_2' + (A - n^2)y_2 &= -2\omega_1\lambda(-k\lambda + n)A_x \sin(\lambda\tau + \phi) \\ &\quad - 3BkA_xA_{xh} \sin(\lambda(2 + \Delta\omega_2)\tau + 2\phi + \Delta\phi)\end{aligned} \quad (25b)$$

$$\begin{aligned}
z_2'' + \lambda^2 z_2 &= 2\omega_1 \lambda^2 A_z \sin(\lambda\tau + \psi) \\
&\quad - \frac{3}{2} B A_x A_{zh} \sin((\lambda + \nu_h(1 - \bar{\omega}))\tau + \phi + \psi + \Delta\psi) \\
&\quad + \frac{3}{2} B A_x A_{zh} \sin((\lambda - \nu_h(1 - \bar{\omega}))\tau + \phi - \psi - \Delta\psi) \\
&\quad - \frac{3}{2} B A_z A_{xh} \sin(\lambda(2 + \Delta\omega_2)\tau + \psi + \phi + \Delta\phi) \\
&\quad + \frac{3}{2} B A_z A_{xh} \sin(\lambda\Delta\omega_2\tau - \psi + \phi + \Delta\phi).
\end{aligned} \tag{25c}$$

Within Equations (25), each term of the forcing function is treated in the manner of the general approach given in Equations (18) and (19). First, consider the potentially resonant terms in Equations (25a) and (25b). Using the notation of Equation (18),

$$\begin{aligned}
\mathcal{A} &= -2\omega_1 \lambda(\lambda - nk)A_x \\
\mathcal{B} &= -2\omega_1 \lambda(-k\lambda + n)A_x \\
q &= \lambda \\
\theta &= \phi.
\end{aligned}$$

The condition of Equation (21), to avoid resonance terms, gives

$$-2\omega_1 \lambda A_x [2n(-k\lambda + n)\lambda + (A - n^2 - \lambda^2)(\lambda - nk)] = 0.$$

In general, this condition can only be satisfied for $\omega_1 = 0$. Next, consider the resonant-type terms in Equation (25c). Here,

$$\begin{aligned}
\mathcal{F} &= 2\omega_1 \lambda^2 A_z \\
p &= \lambda \\
\gamma &= \psi.
\end{aligned}$$

The condition to avoid resonance is

$$2\omega_1 \lambda^2 A_z = 0$$

and, again, this can only be satisfied for $\omega_1 = 0$. Accordingly, ω_1 is now taken to be zero. Note that this requirement also gives $\bar{\omega} = \omega_2$, which will be used from this point forward.

The particular solution to Equations (25) is then built using the method of undetermined coefficients, as previously described. The resulting solution

takes the form

$$\begin{aligned}
x_2 = & \rho_{21} A_x A_{xh} \cos(\lambda(2 + \Delta\omega_2)\tau + 2\phi + \Delta\phi) \\
& + \rho_{22} A_x A_{xh} \cos(\lambda\Delta\omega_2\tau + \Delta\phi) \\
& + \rho_{23} A_z A_{zh} \cos((\lambda - \nu_h(1 - \omega_2))\tau - \Delta\psi) \\
& + \rho_{24} A_z A_{zh} \cos((\lambda + \nu_h(1 - \omega_2))\tau + 2\psi + \Delta\psi)
\end{aligned} \tag{26a}$$

$$\begin{aligned}
y_2 = & \sigma_{21} A_x A_{xh} \sin(\lambda(2 + \Delta\omega_2)\tau + 2\phi + \Delta\phi) \\
& + \sigma_{22} A_x A_{xh} \sin(\lambda\Delta\omega_2\tau + \Delta\phi) \\
& + \sigma_{23} A_z A_{zh} \sin((\lambda - \nu_h(1 - \omega_2))\tau - \Delta\psi) \\
& + \sigma_{24} A_z A_{zh} \sin((\lambda + \nu_h(1 - \omega_2))\tau + 2\psi + \Delta\psi)
\end{aligned} \tag{26b}$$

$$\begin{aligned}
z_2 = & \kappa_{21} A_x A_{zh} \sin((\lambda + \nu_h(1 - \omega_2))\tau + \phi + \psi + \Delta\psi) \\
& + \kappa_{22} A_x A_{zh} \sin((\lambda - \nu_h(1 - \omega_2))\tau + \phi - \psi - \Delta\psi) \\
& + \kappa_{23} A_z A_{xh} \sin(\lambda(2 + \Delta\omega_2)\tau + \psi + \phi + \Delta\phi) \\
& + \kappa_{24} A_z A_{xh} \sin(\lambda\Delta\omega_2\tau - \psi + \phi + \Delta\phi),
\end{aligned} \tag{26c}$$

where the coefficients are

$$\begin{aligned}
\rho_{21} = & \frac{3B[-2n\lambda k(2 + \Delta\omega_2) + (1 + \frac{k^2}{2})(\lambda^2(2 + \Delta\omega_2)^2 + n^2 - A)]}{\lambda^4(2 + \Delta\omega_2)^4 + (A - 2n^2)\lambda^2(2 + \Delta\omega_2)^2 - (A - n^2)(n^2 + 2A)} \\
\rho_{22} = & \frac{3(1 - \frac{k^2}{2})B(\lambda^2\Delta\omega_2^2 + n^2 - A)}{\lambda^4\Delta\omega_2^4 + (A - 2n^2)\lambda^2\Delta\omega_2^2 - (A - n^2)(n^2 + 2A)} \\
\rho_{23} = & \frac{-\frac{3}{2}B((\lambda - \nu_h(1 - \omega_2))^2 + n^2 - A)}{(\lambda - \nu_h(1 - \omega_2))^4 + (A - 2n^2)(\lambda - \nu_h(1 - \omega_2))^2 - (A - n^2)(n^2 + 2A)} \\
\rho_{24} = & \frac{\frac{3}{2}B((\lambda + \nu_h(1 - \omega_2))^2 + n^2 - A)}{(\lambda + \nu_h(1 - \omega_2))^4 + (A - 2n^2)(\lambda + \nu_h(1 - \omega_2))^2 - (A - n^2)(n^2 + 2A)} \\
\sigma_{21} = & \frac{3B[-2n\lambda(2 + \Delta\omega_2)(1 + \frac{k^2}{2}) + k(\lambda^2(2 + \Delta\omega_2)^2 + n^2 + 2A)]}{\lambda^4(2 + \Delta\omega_2)^4 + (A - 2n^2)\lambda^2(2 + \Delta\omega_2)^2 - (A - n^2)(n^2 + 2A)} \\
\sigma_{22} = & \frac{-6n\lambda\Delta\omega_2(1 - \frac{k^2}{2})B}{\lambda^4\Delta\omega_2^4 + (A - 2n^2)\lambda^2\Delta\omega_2^2 - (A - n^2)(n^2 + 2A)} \\
\sigma_{23} = & \frac{3n(\lambda - \nu_h(1 - \omega_2))B}{(\lambda - \nu_h(1 - \omega_2))^4 + (A - 2n^2)(\lambda - \nu_h(1 - \omega_2))^2 - (A - n^2)(n^2 + 2A)} \\
\sigma_{24} = & \frac{-3n(\lambda + \nu_h(1 - \omega_2))B}{(\lambda + \nu_h(1 - \omega_2))^4 + (A - 2n^2)(\lambda + \nu_h(1 - \omega_2))^2 - (A - n^2)(n^2 + 2A)}
\end{aligned}$$

$$\begin{aligned}\kappa_{21} &= \frac{3B}{2\nu_h(1-\omega_2)(2\lambda+\nu_h(1-\omega_2))} \\ \kappa_{22} &= \frac{3B}{2\nu_h(1-\omega_2)(2\lambda-\nu_h(1-\omega_2))} \\ \kappa_{23} &= \frac{3B}{2\lambda^2(1+\Delta\omega_2)(3+\Delta\omega_2)} \\ \kappa_{24} &= \frac{3B}{2\lambda^2(1-\Delta\omega_2^2)}\end{aligned}$$

4.3 Order 3

The solution procedure at order 3 is much the same as for order 2, with much more complicated expressions. The previously determined lower order telescope motion is substituted into Equations (17), along with expressions for the hub motion.

For now, the differential equations are examined only for potentially resonant terms — those terms in which λ appears as the frequency in the τ domain. Analysis of these terms will provide relationships between the acceptable values of A_x and A_z , as well as corresponding expressions for ω_2 . (Further research will allow the development of the actual order-3 solution terms.)

Denoting the Cartesian components of these potentially resonant terms by \mathcal{R}_x , \mathcal{R}_y , and \mathcal{R}_z :

$$\begin{aligned}\mathcal{R}_x &= \left[-2\omega_2\lambda(\lambda - nk) + 3C((k^2 - 2)A_{xh}^2 + A_{zh}^2) \right. \\ &\quad \left. + \frac{3}{2}B[A_{xh}^2(k\sigma_{21} + k\sigma_{22} + 2\rho_{21} + 2\rho_{22}) \right. \\ &\quad \left. + A_{zh}^2(\kappa_{21} - \kappa_{22}) \right] A_x \cos(\lambda\tau + \phi)\end{aligned}\tag{27a}$$

$$\begin{aligned}\mathcal{R}_y &= \left[2\omega_2\lambda(\lambda k - n) + \frac{3}{4}kC[A_{xh}^2(3k^2 - 4) + A_{zh}^2] \right. \\ &\quad \left. - \frac{3}{2}BA_{xh}^2(-k\rho_{21} + k\rho_{22} - \sigma_{21} + \sigma_{22}) \right] A_x \sin(\lambda\tau + \phi)\end{aligned}\tag{27b}$$

$$\begin{aligned}\mathcal{R}_z &= \left[2\omega_2\lambda^2 + \frac{3}{4}C((k^2 - 4)A_{xh}^2 + 3A_{zh}^2) \right. \\ &\quad \left. - \frac{3}{2}B(A_{xh}^2(\rho_{23} - \rho_{21}) - A_{zh}^2(\kappa_{23} - \kappa_{21})) + \Delta \right] A_z \sin(\lambda\tau + \psi).\end{aligned}\tag{27c}$$

Note that \mathcal{R}_x and \mathcal{R}_y contain A_x as a factor, and \mathcal{R}_z contains A_z .

Now examine the conditions to avoid resonance, given by Equation (21), and the simpler z -component condition. It is clear that the coefficients of Equations (27) cannot satisfy these conditions with any degree of flexibility in the oscillation amplitudes — either or both of A_x and A_z would be required to be zero. Therefore, it is necessary to pursue an alternative.

It is possible to increase the flexibility among the orbital parameters by introducing additional resonance-inducing terms. One way to do this is to require that the hub be in a halo orbit about L_2 . This means that $\nu_h = \lambda_h$, which gives

$$\nu_h(1 - \omega_2) = \lambda(1 + \Delta\omega_2). \quad (28)$$

Making this requirement introduces the following additional resonant terms:

$$\begin{aligned} \mathcal{R}_x' = & 3\{C[\cos(\lambda\tau - \Delta\psi + \phi + \Delta\phi) - \cos(\lambda\tau + 2\psi + \Delta\psi - \phi - \Delta\phi)] \\ & + \frac{1}{2}B[(k\sigma_{23} + \kappa_{23} + 2\rho_{23})\cos(\lambda\tau - \Delta\psi + \phi + \Delta\phi) \\ & + (k\sigma_{24} + \kappa_{24} + 2\rho_{24})\cos(\lambda\tau + 2\psi + \Delta\psi - \phi - \Delta\phi)]\} \\ & A_z A_{xh} A_{zh} \end{aligned} \quad (29a)$$

$$\begin{aligned} \mathcal{R}_y' = & \frac{3}{4}\{Ck[\sin(\lambda\tau + 2\psi + \Delta\psi - \phi - \Delta\phi) + \sin(\lambda\tau - \Delta\psi + \phi + \Delta\phi)] \\ & + 2B[(k\rho_{23} - \sigma_{23})\sin(\lambda\tau - \Delta\psi + \phi + \Delta\phi) \\ & - (k\rho_{24} + \sigma_{24})\sin(\lambda\tau + 2\psi + \Delta\psi - \phi - \Delta\phi)]\} \\ & A_z A_{xh} A_{zh} \end{aligned} \quad (29b)$$

$$\begin{aligned} \mathcal{R}_z' = & \frac{3}{4}\{C[(k^2 - 4)\sin(\lambda\tau + \psi + \Delta\psi - \Delta\phi) \\ & + (k^2 + 4)\sin(\lambda\tau - \psi - \Delta\psi + 2\phi + \Delta\phi)] \\ & + 2B[(\rho_{22} - \kappa_{21})\sin(\lambda\tau + \psi + \Delta\psi - \Delta\phi) \\ & - (\rho_{21} + \kappa_{22})\sin(\lambda\tau - \psi - \Delta\psi + 2\phi + \Delta\phi)]\} \\ & A_x A_{xh} A_{zh}. \end{aligned} \quad (29c)$$

It can clearly be seen that the addition of these terms introduces more flexibility. In particular, note that A_x appears in \mathcal{R}_z' , while it is not in \mathcal{R}_z ; similarly, A_z is introduced into the x and y direction terms.

Next, in order to allow these new terms to combine with the original resonance terms, it is required that the phase angles match. All in-plane

trigonometric arguments are now required to be $\lambda\tau + \phi$: out-of-plane arguments are required to be $\lambda\tau + \psi$. This leads to the following six relationships:

$$\cos(\lambda\tau + 2\psi + \Delta\psi - \phi - \Delta\phi) = \pm \cos(\lambda\tau + \phi) \quad (30a)$$

$$\cos(\lambda\tau - \Delta\psi + \phi + \Delta\phi) = \pm \cos(\lambda\tau + \phi) \quad (30b)$$

$$\sin(\lambda\tau + 2\psi + \Delta\psi - \phi - \Delta\phi) = \pm \sin(\lambda\tau + \phi) \quad (30c)$$

$$\sin(\lambda\tau - \Delta\psi + \phi + \Delta\phi) = \pm \sin(\lambda\tau + \phi) \quad (30d)$$

$$\sin(\lambda\tau + \psi + \Delta\psi - \Delta\phi) = \pm \sin(\lambda\tau + \psi) \quad (30e)$$

$$\sin(\lambda\tau - \psi - \Delta\psi + 2\phi + \Delta\phi) = \pm \sin(\lambda\tau + \psi). \quad (30f)$$

From the hub halo motion analysis of [2], the hub phase angles must satisfy the relationship

$$\psi_h - \phi_h = \frac{j}{2}\pi,$$

for arbitrary integer j . With this in mind, Equations (30) lead to the requirement

$$\psi - \phi = (\ell + \frac{j}{2})\pi. \quad (31)$$

for arbitrary integer ℓ .

Richardson [2] also indicates that j must be odd (1 or 3) in order to avoid enormous hub motion amplitudes which would violate the series expansions being employed. Therefore, the same assumption is made here, that j must be odd. Applying these relationships to Equations (30) gives

$$\cos(\lambda\tau + 2\psi + \Delta\psi - \phi - \Delta\phi) = -(-1)^\ell \cos(\lambda\tau + \phi)$$

$$\cos(\lambda\tau - \Delta\psi + \phi + \Delta\phi) = (-1)^\ell \cos(\lambda\tau + \phi)$$

$$\sin(\lambda\tau + 2\psi + \Delta\psi - \phi - \Delta\phi) = -(-1)^\ell \sin(\lambda\tau + \phi)$$

$$\sin(\lambda\tau - \Delta\psi + \phi + \Delta\phi) = (-1)^\ell \sin(\lambda\tau + \phi)$$

$$\sin(\lambda\tau + \psi - \Delta\psi - \Delta\phi) = (2 - j) \cos(\lambda\tau + \phi)$$

$$\sin(\lambda\tau - \psi - \Delta\psi + 2\phi + \Delta\phi) = -(2 - j) \cos(\lambda\tau + \phi).$$

Using these results and augmenting Equations (27) with Equations (29),

$$\begin{aligned} \mathcal{R}_x = & \left[-2\omega_2\lambda(\lambda - nk)A_x + 3CA_x (k^2 A_{xh}^2 - 2A_{xh}^2 + A_{zh}^2) \right. \\ & + \frac{3}{2}BA_x [(k\sigma_{21} + k\sigma_{22} + 2\rho_{21} + 2\rho_{22})A_{xh}^2 + (\kappa_{21} - \kappa_{22})A_{zh}^2] \\ & + 6(-1)^\ell CA_z A_{xh} A_{zh} \\ & \left. + \frac{3}{2}(-1)^\ell B(-k\sigma_{23} + \kappa_{23} + 2\rho_{23} - k\sigma_{24} - \kappa_{24} - 2\rho_{24})A_z A_{xh} A_{zh} \right] \\ & \cos(\lambda\tau + \phi) \end{aligned} \quad (32a)$$

$$\begin{aligned} \mathcal{R}_y = & \left[2\omega_2\lambda(\lambda k - n)A_x + \frac{3}{4}kCA_x (3k^2 A_{xh}^2 - 4A_{xh}^2 + A_{zh}^2) \right. \\ & + \frac{3}{2}BA_x A_{xh}^2 (-k\rho_{21} + k\rho_{22} - \sigma_{21} + \sigma_{22}) \\ & \left. + \frac{3}{2}(-1)^\ell B(k\rho_{23} - \sigma_{23} + k\rho_{24} + \sigma_{24})A_z A_{xh} A_{zh} \right] \\ & \sin(\lambda\tau + \phi) \end{aligned} \quad (32b)$$

$$\begin{aligned} \mathcal{R}_z = & \left[2\omega_2\lambda^2 A_z + \frac{3}{4}CA_z (k^2 A_{xh}^2 - 4A_{xh}^2 + 3A_{zh}^2) \right. \\ & + \frac{3}{2}BA_z [(\rho_{23} - \rho_{24})A_{zh}^2 - (\kappa_{23} - \kappa_{24})A_{xh}^2] + \Delta A_z \\ & - 6(-1)^\ell CA_x A_{xh} A_{zh} \\ & \left. + \frac{3}{2}(-1)^\ell B(\rho_{22} + \rho_{21} + \kappa_{22} - \kappa_{21})A_x A_{xh} A_{zh} \right] \\ & (2 - j)(-1)^\ell \cos(\lambda\tau + \phi). \end{aligned} \quad (32c)$$

The relationship between ν_h and λ , given by Equation (28) may now be used in the ρ , σ , and κ functions, changing some of their forms to

$$\begin{aligned} \rho_{23} &= \frac{-\frac{3}{2}B(\lambda^2\Delta\omega_2^2 + n^2 - A)}{\lambda^4\Delta\omega_2^4 + (A - 2n^2)\lambda^2\Delta\omega_2^2 - (A - n^2)(n^2 + 2A)} \\ \rho_{21} &= \frac{\frac{3}{2}B(\lambda^2(2 + \Delta\omega_2)^2 + n^2 - A)}{\lambda^4(2 + \Delta\omega_2)^4 + (A - 2n^2)\lambda^2(2 + \Delta\omega_2)^2 - (A - n^2)(n^2 + 2A)} \\ \sigma_{23} &= \frac{-3n\lambda\Delta\omega_2 B}{\lambda^4\Delta\omega_2^4 + (A - 2n^2)\lambda^2\Delta\omega_2^2 - (A - n^2)(n^2 + 2A)} \\ \sigma_{24} &= \frac{-3n\lambda(2 + \Delta\omega_2)B}{\lambda^4(2 + \Delta\omega_2)^4 + (A - 2n^2)\lambda^2(2 + \Delta\omega_2)^2 - (A - n^2)(n^2 + 2A)} \\ \kappa_{21} &= \frac{3B}{2\lambda^2(1 + \Delta\omega_2)(3 + \Delta\omega_2)} \end{aligned}$$

$$\kappa_{22} = \frac{3B}{2\lambda^2(1 - \Delta\omega_2^2)}$$

For use in the equations at third order, the ρ , σ , and κ functions need only be expanded through linear terms in $\Delta\omega_2$. When linearized, the functions become

$$\begin{aligned} \rho_{21} = & \frac{3}{2d}B\{-8nk\lambda - (2 + k^2)(4\lambda^2 + n^2 - A)\} \\ & + \left[-\frac{4}{d}(8\lambda^2 + A - 2n^2)\lambda^2\{-8nk\lambda + (2 + k^2)(4\lambda^2 + n^2 - A)\}\right. \\ & \left. + 4(-nk\lambda + (2 + k^2)\lambda^2)\right]\Delta\omega_2\} \end{aligned}$$

$$\stackrel{\Delta}{=} \rho_{21a} + \rho_{21b}\Delta\omega_2$$

$$\rho_{22} = \frac{3(2 - k^2)B}{2(n^2 + 2A)}$$

$$\stackrel{\Delta}{=} \rho_{22a}$$

$$\rho_{23} = -\frac{3B}{2(n^2 + 2A)}$$

$$\stackrel{\Delta}{=} \rho_{23a}$$

$$\begin{aligned} \rho_{24} = & \frac{3}{2d}B\{(4\lambda^2 + n^2 - A) \\ & - \frac{4}{d}\lambda^2[16\lambda^4 + 8(n^2 - A)\lambda^2 + (A - n^2)(3n^2 + A)]\Delta\omega_2\} \end{aligned}$$

$$\stackrel{\Delta}{=} \rho_{24a} + \rho_{24b}\Delta\omega_2$$

$$\begin{aligned} \sigma_{21} = & \frac{3}{d}B\{-2n\lambda(2 + k^2) + k(4\lambda^2 + n^2 + 2A)\} \\ & + \left[-\frac{4}{d}(8\lambda^2 + A - 2n^2)\lambda^2\{-2n\lambda(2 + k^2) + k(4\lambda^2 + n^2 + 2A)\}\right. \\ & \left. + (-n\lambda(2 + k^2) + 4k\lambda^2)\right]\Delta\omega_2\} \end{aligned}$$

$$\stackrel{\Delta}{=} \sigma_{21a} + \sigma_{21b}\Delta\omega_2$$

$$\sigma_{22} = \frac{3n\lambda\Delta\omega_2(2 - k^2)B}{(A - n^2)(n^2 + 2A)}$$

$$\stackrel{\Delta}{=} \sigma_{22b}\Delta\omega_2$$

$$\sigma_{23} = \frac{3n\lambda\Delta\omega_2B}{(A - n^2)(n^2 + 2A)}$$

$$\stackrel{\Delta}{=} \sigma_{23b}\Delta\omega_2$$

$$\sigma_{24} = -\frac{3n}{d}\lambda B\left\{2 - \frac{1}{d}[48\lambda^4 + 4(A - 2n^2)\lambda^2 - (n^2 - A)(n^2 + 2A)]\Delta\omega_2\right\}$$

$$\stackrel{\Delta}{=} \sigma_{24a} + \sigma_{24b}\Delta\omega_2$$

$$\begin{aligned}
\kappa_{21} &= \frac{B}{6\lambda^2} (3 - 4\Delta\omega_2) \\
&\stackrel{\Delta}{=} \kappa_{21a} + \kappa_{21b}\Delta\omega_2 \\
\kappa_{22} &= \frac{3B}{2\lambda^2} \\
&\stackrel{\Delta}{=} \kappa_{22a} \\
\kappa_{23} &= \frac{B}{6\lambda^2} (3 - 4\Delta\omega_2) \\
&\stackrel{\Delta}{=} \kappa_{23a} + \kappa_{23b}\Delta\omega_2 \\
\kappa_{24} &= \frac{3B}{2\lambda^2} \\
&\stackrel{\Delta}{=} \kappa_{23a},
\end{aligned}$$

where

$$d = 16\lambda^4 + 4(A - 2n^2)\lambda^2 - (A - n^2)(n^2 + 2A).$$

The subscripts b and a respectively denote those terms involving and not involving $\Delta\omega_2$.

Keeping this in mind, and recalling that $\Delta\omega_2$ is defined as the difference between ω_{2h} and ω_2 , Equations (32) may be written in the form

$$\begin{aligned}
\mathcal{R}_x &= (\alpha_{1a}A_x + \alpha_{1b}\omega_2A_x + \alpha_{2a}A_z + \alpha_{2b}\omega_2A_z) \cos(\lambda\tau + \phi) \\
\mathcal{R}_y &= (\beta_{1a}A_x + \beta_{1b}\omega_2A_x + \beta_{2a}A_z + \beta_{2b}\omega_2A_z) \sin(\lambda\tau + \phi) \\
\mathcal{R}_z &= (\gamma_{1a}A_x + \gamma_{1b}\omega_2A_x + \gamma_{2a}A_z + \gamma_{2b}\omega_2A_z)(2 - j)(-1)^\ell \cos(\lambda\tau + \phi),
\end{aligned}$$

where the α , β , and γ coefficients are functions of constants and the the hub solution parameters ω_{2h} , A_{xh} , and A_{zh} . Using a tilde to indicate substitution

of ω_{2h} for $\Delta\omega_2$, these functions are

$$\begin{aligned}
\alpha_{1a} &= 3C(k^2 A_{xh}^2 - 2A_{xh}^2 + A_{zh}^2) \\
&\quad + \frac{3}{2}B[(k\tilde{\sigma}_{21} + k\tilde{\sigma}_{22} + 2\tilde{\rho}_{21} + 2\tilde{\rho}_{22})A_{xh}^2 + (\tilde{\kappa}_{21} - \tilde{\kappa}_{22})A_{zh}^2] \\
\alpha_{1b} &= -2\lambda(\lambda - nk) - \frac{3}{2}B[(k\tilde{\sigma}_{21b} + k\tilde{\sigma}_{22b} + 2\tilde{\rho}_{21b})A_{xh}^2 + \tilde{\kappa}_{21b}A_{zh}^2] \\
\alpha_{2a} &= \frac{3}{2}(-1)^\ell [4C + B(-k\tilde{\sigma}_{23} + \tilde{\kappa}_{23} + 2\tilde{\rho}_{23} - k\tilde{\sigma}_{24} - \tilde{\kappa}_{24} - 2\tilde{\rho}_{24})]A_{xh}A_{zh} \\
\alpha_{2b} &= -\frac{3}{2}(-1)^\ell B(-k\tilde{\sigma}_{23b} + \tilde{\kappa}_{23b} - k\tilde{\sigma}_{24b} - 2\tilde{\rho}_{24b})A_{xh}A_{zh} \\
\beta_{1a} &= \frac{3}{4}kC(3k^2 A_{xh}^2 - 4A_{xh}^2 + A_{zh}^2) + \frac{3}{2}BA_{xh}^2(-k\tilde{\rho}_{21} + k\tilde{\rho}_{22} - \tilde{\sigma}_{21} + \tilde{\sigma}_{22}) \\
\beta_{1b} &= 2\lambda(\lambda k - n) + \frac{3}{2}BA_{xh}^2(k\tilde{\rho}_{21b} + \tilde{\sigma}_{21b} - \tilde{\sigma}_{22b}) \\
\beta_{2a} &= \frac{3}{2}(-1)^\ell B(k\tilde{\rho}_{23} - \tilde{\sigma}_{23} + k\tilde{\rho}_{24} + \tilde{\sigma}_{24})A_{xh}A_{zh} \\
\beta_{2b} &= \frac{3}{2}(-1)^\ell B(\tilde{\sigma}_{23b} - k\tilde{\rho}_{24b} - \tilde{\sigma}_{24b})A_{xh}A_{zh} \\
\gamma_{1a} &= (-1)^\ell [-6C + \frac{3}{2}B(\tilde{\rho}_{22} + \tilde{\rho}_{21} + \tilde{\kappa}_{22} - \tilde{\kappa}_{21})]A_{xh}A_{zh} \\
\gamma_{1b} &= \frac{3}{2}(-1)^\ell B(\tilde{\kappa}_{21b} - \tilde{\rho}_{21b})A_{xh}A_{zh} \\
\gamma_{2a} &= \frac{3}{4}\left[C(k^2 A_{xh}^2 - 4A_{xh}^2 + 3A_{zh}^2) \right. \\
&\quad \left. + 2B[(\tilde{\rho}_{23} - \tilde{\rho}_{24})A_{zh}^2 - (\tilde{\kappa}_{23} - \tilde{\kappa}_{24})A_{xh}^2]\right] - \Delta \\
\gamma_{2b} &= 2\lambda^2 + \frac{3}{2}B(\tilde{\rho}_{24b}A_{zh}^2 + \tilde{\kappa}_{23b}A_{xh}^2).
\end{aligned} \tag{33}$$

Recall that the conditions to avoid resonance are as specified by Equation (21) and by the requirement that the z component of the resonant forcing function have zero amplitude. Here, these requirements now take the form

$$\begin{aligned}
2n(\beta_{1a}A_x + \beta_{1b}\omega_2A_x + \beta_{2a}A_z + \beta_{2b}\omega_2A_z)\lambda \\
+ (A - n^2 - \lambda^2)(\alpha_{1a}A_x + \alpha_{1b}\omega_2A_x + \alpha_{2a}A_z + \alpha_{2b}\omega_2A_z) = 0
\end{aligned} \tag{34}$$

and

$$\gamma_{1a}A_x + \gamma_{1b}\omega_2A_x + \gamma_{2a}A_z + \gamma_{2b}\omega_2A_z = 0. \tag{35}$$

Equation (34) may be written in the form

$$\zeta_{1a}A_x - \zeta_{1b}\omega_2A_x + \zeta_{2a}A_z + \zeta_{2b}\omega_2A_z = 0, \tag{36}$$

where

$$\begin{aligned}
\zeta_{1a} &= 2n\beta_{1a}\lambda + (A - n - \lambda^2)\alpha_{1a} \\
\zeta_{2a} &= 2n\beta_{2a}\lambda + (A - n - \lambda^2)\alpha_{2a} \\
\zeta_{1b} &= 2n\beta_{1b}\lambda + (A - n - \lambda^2)\alpha_{1b} \\
\zeta_{2b} &= 2n\beta_{2b}\lambda + (A - n - \lambda^2)\alpha_{2b}.
\end{aligned} \tag{37}$$

Equations (35) and (36) provide two equations in the three variables A_x , A_z , and ω_2 . However, a third relationship may be introduced. Consider the order-1 solution of Equation (22). Using the frequency and phase relationships of this section gives

$$\begin{bmatrix} x_1 \\ y_1 \\ z_1 \end{bmatrix} = \begin{bmatrix} -A_x \cos(\lambda\tau + \phi) \\ kA_x \sin(\lambda\tau + \phi) \\ (2-j)(-1)^\ell A_z \cos(\lambda\tau + \phi) \end{bmatrix},$$

with j either 1 or 3, and ℓ either 0 or 1. This part of the solution corresponds to the case where the aperture plane maintains a roll angle ξ about the y -axis. The range of this roll angle is related to the integers j and ℓ in the fashion shown in Table 2.

Table 2: Relationship of Aperture Plane Roll Angle to i and j

j	ℓ	ξ
1	0	$(0, \pi/2)$
1	1	$(-\pi/2, 0)$
3	0	$(-\pi/2, 0)$
3	1	$(0, \pi/2)$.

Therefore, the ratio $(2-j)(-1)^\ell A_z/A_x$ may be taken as an approximation to $\tan \xi$. Let η represent A_z/A_x . Assuming A_x to be nonzero, Equations (35) and (36) may be written in terms of η as

$$\gamma_{1a} + \gamma_{1b}\omega_2 + \gamma_{2a}\eta + \gamma_{2b}\omega_2\eta = 0. \tag{38}$$

and

$$\zeta_{1a} + \zeta_{1b}\omega_2 + \zeta_{2a}\eta + \zeta_{2b}\omega_2\eta = 0 \tag{39}$$

These two equations may be solved simultaneously for ω_2 and η . The combination of the equations leads to a quadratic, with two sets of solutions for ω_2 and η . Depending on the hub motion amplitudes, the solutions for η correspond to approximate aperture plane roll angles from $-\pi/2$ to $\pi/2$. The solution for ω_2 is then

$$\omega_2 = \frac{-\bar{B} \pm \sqrt{\bar{B}^2 - 4\bar{A}\bar{C}}}{2\bar{A}}, \quad (40)$$

where

$$\begin{aligned} \bar{A} &= \gamma_{1b}\zeta_{2b} - \gamma_{2b}\zeta_{1b} \\ \bar{B} &= \gamma_{1a}\zeta_{2b} + \gamma_{1b}\zeta_{2a} - \gamma_{2a}\zeta_{1b} - \gamma_{2b}\zeta_{1a} \\ \bar{C} &= \gamma_{1a}\zeta_{2a} - \gamma_{2a}\zeta_{1a} \end{aligned}$$

and the corresponding η is

$$\eta = -\frac{\zeta_{1a} + \zeta_{1b}\omega_2}{\zeta_{2a} + \zeta_{2b}\omega_2} = -\frac{\gamma_{1a} + \gamma_{1b}\omega_2}{\gamma_{2a} + \gamma_{2b}\omega_2}. \quad (41)$$

In turn, each value of η is associated with an infinite set of (A_x, A_z) pairs, each of which is, in turn, associated with a set of initial conditions for the relative telescope motion.

A rule of thumb may be developed in order to bound the selection of A_x and A_z . Examining the solution to the linear telescope equations, given by Equation (22), it can be seen that the approximate maximum distance of a telescope from the hub is

$$d_{\max} = \max(\sqrt{A_x^2 + A_z^2}, kA_x) \quad (42)$$

$$= A_x \max(\sqrt{1 + \eta^2}, k). \quad (43)$$

Therefore, if the maximum distance is required to be no greater than a distance $\overline{d_{\max}}$, A_x may be selected such that

$$A_x \leq \frac{\overline{d_{\max}}}{\max(\sqrt{1 + \eta^2}, k)},$$

and then $A_z = \eta A_x$.

4.4 Solution Summary

The solution is now constructed by adding Equations (22) and (26), and using the frequency and phase angle relationships of Section 4.3. This combined solution through order 2 is then

$$\begin{aligned}
 x = & -A_x \cos(\lambda\tau + \phi) \\
 & + (\rho_{21}A_xA_{xh} - \rho_{24}A_zA_{zh}(-1)^\ell) \cos(\lambda(2 + \Delta\omega_2)\tau + \phi_h + \phi) \quad (44a) \\
 & + (\rho_{22}A_xA_{xh} + \rho_{23}A_zA_{zh}(-1)^\ell) \cos(\lambda\Delta\omega_2\tau + \phi_h - \phi)
 \end{aligned}$$

$$\begin{aligned}
 y = & kA_x \sin(\lambda\tau + \phi) \\
 & + (\sigma_{21}A_xA_{xh} - \sigma_{24}A_zA_{zh}(-1)^\ell) \sin(\lambda(2 + \Delta\omega_2)\tau + \phi_h + \phi) \quad (44b) \\
 & + (\sigma_{22}A_xA_{xh} - \sigma_{23}A_zA_{zh}(-1)^\ell) \sin(\lambda\Delta\omega_2\tau + \phi_h - \phi)
 \end{aligned}$$

$$\begin{aligned}
 z = & [(-1)^\ell A_z \cos(\lambda\tau + \phi) \\
 & + (\kappa_{21}A_xA_{zh} + \kappa_{23}A_zA_{xh}(-1)^\ell) \cos(\lambda(2 + \Delta\omega_2)\tau + \phi_h + \phi) \\
 & - (\kappa_{22}A_xA_{zh} + \kappa_{24}A_zA_{xh}(-1)^\ell) \cos(\lambda\Delta\omega_2\tau + \phi_h - \phi)](2 - j), \quad (44c)
 \end{aligned}$$

where $\tau = (1 + \omega_2 t)$. The coefficients are as given following Equations (26), with the modifications which follow Equations (32).

5 Simulation

5.1 Implementation Procedure

Various representations of the telescope equations of motion were coded in MATLAB to examine the differences among the solutions. Some of the results are presented in this section. The motions of the hub and only one telescope were simulated because of programming and interpretation simplicity at this point. In the future, a visualization could be developed based on selection of initial conditions and results from the simulations.

The selection of the initial state is not arbitrary because the resulting uncontrolled orbit path is likely to be unsatisfactory. The solutions of these models show that the hub's trajectory diverges from a closed, periodic orbit in typically 150 to 200 days. Exploration of initial conditions has been a time consuming portion of this research.

Additionally, the uncontrolled telescope motion will diverge from the nearby reference path about the hub.

Difficulties in finding initial conditions that produced useful trajectories motivated short duration time frames. Assume that as the aperture plane orbits the L_2 point, a typical observation will last only a few days, before reorienting the plane to observe some other target. By simulating runs of 20 days duration, small diverging motions from the nominal halo motion were maintained.

The baseline solution is the numerical integration of the full equations of the hub subtracted from that of the telescope, as shown in Equation (1). In essence, there are two separate vehicles orbiting the L_2 point with very similar initial conditions. The slight differences in initial conditions are due to the placement of the telescope with respect to the hub.

One cannot arbitrarily specify initial hub and telescope positions for either the full, or the truncated nonlinear model, or the analytical model, and obtain closed or nearly closed orbits about the L_2 point.

To begin the process, implement the lengthy algorithms shown in Section 4.3:

- begin with a selection of A_{zh} , the amplitude of the motion along the z -axis of the hub with respect to L_2
- use a consistent set of physical quantities taken from Dunham and Muhonen [3] for the constants used in computing A , B , C of Equations (8) and for λ and k
- compute the α , β , γ terms of Equations (33)
- compute the ζ terms from Equations (37)
- solve for both of the ω_2 solutions from Equation (40)
- maintain two solutions for η (Equation (41)) based on two ω_2 terms
- then $A_z = \eta A_x$ yields two choices

Table 3 shows three combinations of amplitude selection, selections of j , and the results of calculations based on these selections. The application of Equation (G-1) from Richardson [2] constrains the A_{xh} corresponding to the selected A_{zh} . (This equation is plotted in Richardson's Figure H-1.)

Table 3: Summary of Inputs and Resulting Values Used to Select Orbit Size and Orientation

A_{zh} (km)	A_{zh} (km)	j	ω_2^-	ω_2^+	η^-	η^+	ξ^- (deg)	ξ^+ (deg)	A_z^- (m)	A_z^+ (km)
280,667	550,459	1	-0.29211	-0.29185	1.6115	1.6147	-58.18	-58.23	80.58	0.08073
280,667	550,459	3	-0.29211	-0.29185	1.6115	1.6147	58.18	58.23	80.58	0.08073
227,219	250,000	1	-0.26069	-0.11043	0.45009	3.9851	-24.23	-75.92	22.50	0.1993
227,219	250,000	3	-0.26069	-0.11043	0.45009	3.9851	24.23	75.92	22.50	0.1993
211,126	1,000	1	-0.23166	-0.07373	0.00178	905.98	-0.1020	-89.94	0.08902	45.30
211,126	1,000	3	-0.23166	-0.07373	0.00178	905.98	0.1020	89.94	0.08902	45.30

The amplitude of the hub motion along the z -axis was first chosen and then the amplitude of the hub motion along the x -axis is constrained by this relationship, which assures halo orbit solution via correct frequency selection.

The choice of A_{zh} of 550,459 km is the largest z -value that can be selected and yield real roots for ω_2 . An intermediate value of 250,000 km and a very small value of 1,000 km were also selected for presentation. The appendix shows the results of many calculations of this example.

There are only two acceptable choices for j , which controls the sign on the z -position equation. The selection of $j = 1$ corresponds to a left roll orientation of the aperture plane; the selection of $j = 3$ corresponds to a right roll. This table shows the results of calculations based on fixing $\ell = 1$ and $A_x = 50\text{m}$. (Results for $\ell = 0$ are not shown because the η values would be negative in Table 3 and lead to negative values of A_z .)

Because the equation for ω_2 admits two roots, these two values are carried forward to see their effects upon the calculation for η . The superscripts $-$ and $+$ refer to the sign on the square root in each solution. Two values are calculated for η and, in turn, two values of the arctangent of η to yield the approximate aperture plane roll angle, ξ .

The resulting magnitudes of the η terms, and their corresponding angle values should be highlighted. As stated above, the large value of A_{zh} is associated with the case in which the two roots for ω_2 approach a single double root. Accordingly, the resulting values of η , ξ , and A_z are also nearly identical.

For the intermediate value of A_{zh} , the ω_2 values are different. The roll angles, of the two solutions, are quite different. Finally, at the smallest value of A_{zh} , the ω_2 solutions are quite different. The roll angles of the two

solutions are at extreme values – based on η^- , the halo plane is nearly in the ecliptic (x - y) plane and based on η^+ , the halo plane is nearly in the y - z plane.

Because the user can select either A_{zh} or the desired roll orientation, the user does not have control over the combination of halo plane size and orientation. When considering the roll orientation of the aperture plane, from $-\pi/2$ to $\pi/2$, the user should realize that three months later, the orbit will have moved about the Sun such that the initial roll angle appears as a pitch rotation. This offers some orientation flexibility.

Again, the user does not have total control over hub position and, of course, the aperture plane location with respect to L_2 .

Continue with the implementation of these algorithms:

- compute the ρ , σ , κ terms on pages 76 – 77
- compute the analytical expressions of Equations (44)

Equations (44) are the analytical expressions for the motion of the telescope with respect to the hub. By taking the derivatives of these equations, one can compute the full state as a function of time. These equations may be used by trajectory control designers.

Also at $t = 0$, Equations (44) may be used to determine the initial state for use by two comparison solutions requiring numerical integration:

- Solution of Equation (1) – full nonlinear equations of motion of the telescope with respect to the hub
- Solution of Equation (8) – truncated, to second order in the distance of the hub from L_2 , nonlinear equations of motion of the telescope with respect to the hub

5.2 Simulation to Compare Results of Models

Here is an example that compares the results of the three solution methods for calculating the motion of the telescope with respect to the hub.

“Full” refers to the numerical integration of the separate equations of motion for the telescope and the hub, each spacecraft with respect to L_2 , and then subtracting the hub motion from that of the telescope. This represents the implementation of Equation (1).

Table 4: Initial Conditions of Telescope With Respect to Hub Resulting From Analytical Solution

$x(0)$	- 64.7796 m
$y(0)$	0.0 m
$z(0)$	26.4452 m
$\dot{x}(0)$	0.0 m/day
$\dot{y}(0)$	4.4205 m/day
$\dot{z}(0)$	0.0 m/day

“Truncated” refers to the numerical integration of the truncated equations of motion for the telescope with respect to the hub. This represents the implementation of Equation (8) with the terms that have a subscript h referring to the linear expressions for the motion of the hub. The linear hub solution is given by Equation (23), which was further simplified to give a halo orbit setting both frequencies to the same value and setting both phase angles to zero.

The initial conditions for both the full and truncated numerical integrations are obtained from the calculation, at $t = 0$, of the analytical solution.

“Analytical” refers to the second order solution, which is an explicit function of time, given by Equations (44).

From the intermediate case of Table 3, select the out-of-plane hub amplitude from the L_2 point to be 250,000 km (A_{zh}). Using Equation (G-1) of Richardson [2], the resulting value of A_{xh} is 227,219.42 km. Select the row with $j = 1$ or 3, corresponding to the desired aperture roll direction. The roll direction is implemented in the solution via Equation (44c). The roll angle direction is also indicated in Table 2. Remembering that Table 3 was computed using $\ell = 1$, choose $j = 1$ for a negative roll or choose $j = 3$ for a positive roll. In this simulation, $j = 3$.

Select the initial amplitude between the hub and the telescope to be $A_x = 50$ m, along the x -axis. The A_z^- choice initially gives the telescope a linear amplitude of 22.5 m away from the hub along the z -axis.

The analytical solution was first evaluated at $t = 0$ to obtain the initial conditions (of the telescope relative to the hub, Table 4) for the full and truncated solutions.

The initial conditions for the hub are listed in Table 5 with the equations

Table 5: Initial Conditions of Hub With Respect to Sun-Earth L_2 Point

$x_h(0)$	227,219.42 km
$y_h(0)$	0.00 km
$z_h(0)$	250,000.00 km
ϕ	0.00 rad
ϕ_h	0.00 rad
$\dot{x}_h(0)$	$(\lambda/k)y_h(0)$ km/day
$\dot{y}_h(0)$	$-k\lambda x_h(0)$ km/day
$\dot{z}_h(0)$	$-(2-j)\lambda A_{z_h} \sin(\phi_h)$ km/day

for \dot{x} , \dot{y} , and \dot{z} reproduced here for convenience. These were given earlier in Section 3.3.

The complete initial conditions for the telescope with respect to the L_2 point are given below:

$$x_t(0) = x_h(0) + x(0)$$

$$y_t(0) = y_h(0) + y(0)$$

$$z_t(0) = z_h(0) + z(0)$$

$$\dot{x}_t(0) = \dot{x}_h(0) + \dot{x}(0)$$

$$\dot{y}_t(0) = \dot{y}_h(0) + \dot{y}(0)$$

$$\dot{z}_t(0) = \dot{z}_h(0) + \dot{z}(0)$$

The following plots show the small differences among the three solution types over a 20-day duration. The plots show the telescope motion with respect to the hub. The origin of the coordinate system represents the position of the hub. Scales are expanded for the x and z positions.

Returning to the discussion that began in the introduction to Section 5.1, we note that over 5 days each solution yields almost the same result. The analytical solution is quite accurate for trajectory control analysis. We assume that as the aperture plane orbits the L_2 point, a typical observation will last only a few days, before reorienting the plane to observe some other target. By simulating runs of 20 days duration, we can see small diverging motions from the reference numerical solution.

In Figure 3, observe that both the full and truncated solutions are essentially the same. Considering the scale of the axis labeled “x position”, the

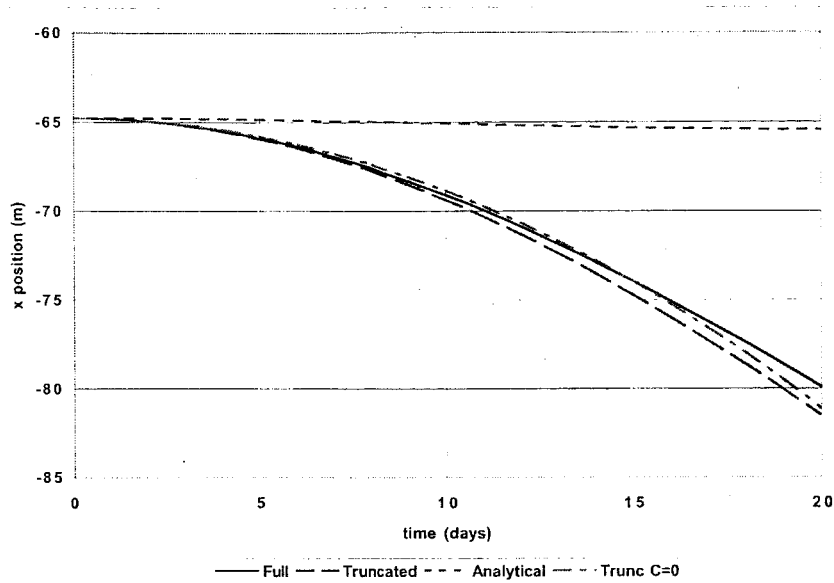


Figure 3: Compare 3 Solutions for Telescope Motion Along the x -axis.

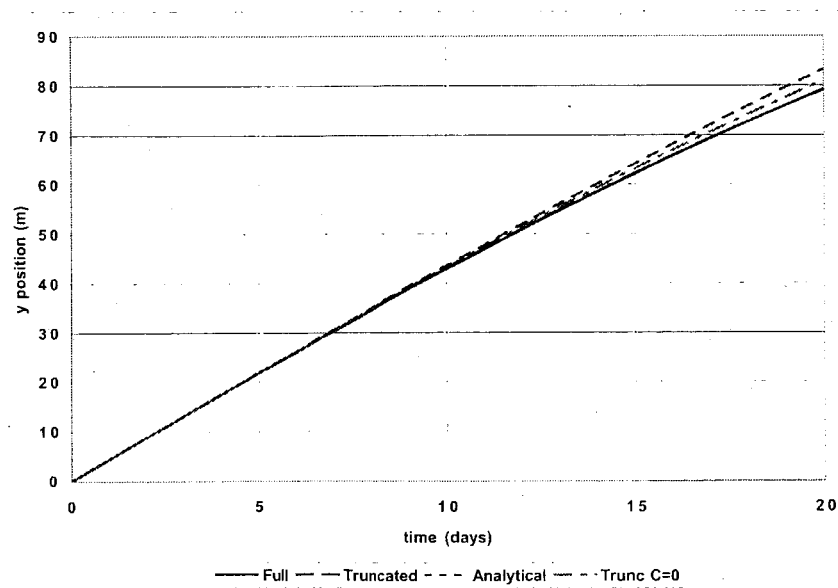


Figure 4: Compare 3 Solutions for Telescope Motion Along the y -axis.

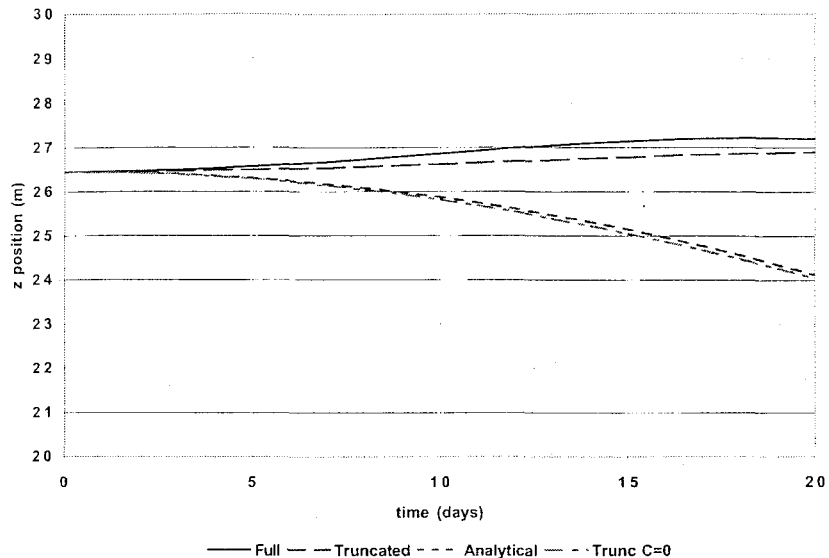


Figure 5: Compare 3 Solutions for Telescope Motion Along the z -axis.

analytical expression is close to the other solutions over 5 days. The curve labeled “Trunc $C=0$ ” shows that when the lowest order term of the truncated solution is set equal to zero, the effects are not significant in the x -direction.

In Figure 4, observe that all solutions are essentially the same for the scale shown.

In Figure 5, we see that both the full and truncated solutions are essentially the same. The analytical solution stays close to these solutions over 5 days. Remember the truncated solution has all of terms A, B, and C included. The highlight is the curve labeled “Trunc $C=0$ ” showing nearly the same result as the analytical solution. Now the importance of the “C” term is evident. It indicates that a more complete analytic solution would include higher order terms.

6 Summary

This report details the preliminary work describing the formation flying between spacecraft near the Sun-Earth L_2 libration point, beginning with the circular restricted three-body problem for the hub motion about L_2 .

The halo orbit was specified as a desirable aperture plane orbit, instead of a Lissajous orbit, because it is periodic. Additionally, over a one or two day observation period, the spacecraft telescopes of the aperture plane will minimally separate due to natural motions.

The analytical solution, Equations (44), for the motion of a typical telescope relative to the hub is presented, including terms which are linear in the hub motion. We anticipate feedback from our sponsor concerning the utility of these equations for use in orbit control system design.

We developed a full non-linear solution of hub motion, with respect to L_2 , subtracted from telescope motion, with respect to L_2 , as a reference trajectory.

We developed a truncated non-linear solution to the telescope motion with respect to the hub. Both the non-linear model and the truncated model are solved by numerical integration.

All three models produce trajectories that diverge from a closed path over the course of one orbit (roughly 200 days). We compared the three models over a shorter duration of 20 days expecting that a science observation would be on the order of a few days, before reorienting the aperture plane.

The analytical solution algorithm is quite lengthy. One example was presented and used to compare the accuracy of the solution compared to the reference trajectory. Over 5 days, the analytical solution is very close to the reference trajectory.

Appendices

A Constant Parameters

Table 6: Physical Constants [3]

μ_1	132,712,440,017.987 km ³ /s ²
μ_2	403,503.236 km ³ /s ²
n	0.199106385 × 10 ⁻⁶ rad/s

Table 7: Derived Constants

x_e	151,105,099.094445 km
D_1	454.84086785372 km
D_2	149,597,415.850132 km

Table 8: Constants Specific to Sun-Earth L_2 Point [2]

ℓ_1	-14.82882087	1/(DU ² -TU ²)
ℓ_2	1.673691389	1/(DU ² -TU ²)
s_1	-0.7444513767	1/(DU-TU ²)
s_2	0.1250471558	1/(DU-TU ²)
DU	1.507683382 × 10 ⁶ km	
TU	58.13235527	days

Richardson's algorithm ([2], page 2-31) for computing A_{xh} given A_{zh} and for computing ω_{2h} are given here:

$$\ell_1 A_{xh}^2 + \ell_2 A_{zh}^2 + \Delta = 0$$

$$\omega_{2h} = s_1 A_{xh}^2 + s_2 A_{zh}^2$$

These are the modifications used to dimensionalize Richardson's algorithms:

$$A_{xh} = DU \sqrt{(-\ell_2(A_{zh}/DU)^2 - \Delta TU^2)/\ell_1}$$
$$\omega_{2h} = s_1(A_{xh}/DU)^2 + s_2(A_{zh}/DU)^2$$

Where in Table 8, the constants "DU" refers to distance unit and "TU" refers to time unit.

Table 9: Computed Values and Coefficients

A	$1.16605228517927 \times 10^{-3}$	1/day ²
B	$5.84853993419721 \times 10^{-10}$	1/(km-day ²)
C	$3.86667873919725 \times 10^{-16}$	1/(km ² -day ²)
λ	$3.53850956958284 \times 10^{-2}$	rad/day
k	3.18712225987377	
ν^2	$1.16605228517927 \times 10^{-3}$	rad/day ²
Δ	$8.60527122236636 \times 10^{-5}$	1/day ²
d	$2.56733055729898 \times 10^{-5}$	1/day ⁴
ρ_{21a}	$1.18887100881492 \times 10^{-6}$	1/km
ρ_{21b}	$-6.40826960245161 \times 10^{-7}$	1/km
ρ_{22a}	$-2.72318375685819 \times 10^{-6}$	1/km
ρ_{22b}	0	1/km
ρ_{23a}	$-3.33815613931628 \times 10^{-7}$	1/km
ρ_{23b}	0	1/km
ρ_{24a}	$1.41409729921967 \times 10^{-7}$	1/km
ρ_{24b}	$-1.21027861225803 \times 10^{-7}$	1/km
σ_{21a}	$6.51772783060505 \times 10^{-7}$	1/km
σ_{21b}	$-7.61518233174130 \times 10^{-7}$	1/km
σ_{22a}	0	1/km
σ_{22b}	$-3.81021051605070 \times 10^{-6}$	1/km
σ_{23a}	0	1/km
σ_{23b}	$4.67066447286556 \times 10^{-7}$	1/km
σ_{24a}	$-8.32024709778584 \times 10^{-8}$	1/km
σ_{24b}	$1.30305530510727 \times 10^{-7}$	1/km
κ_{21a}	$2.33548302511691 \times 10^{-7}$	1/km
κ_{21b}	$-3.11397736682255 \times 10^{-7}$	1/km
κ_{22a}	$7.00644907535074 \times 10^{-7}$	1/km
κ_{22b}	0	1/km
κ_{23a}	$2.33548302511691 \times 10^{-7}$	1/km
κ_{23b}	$-3.11397736682255 \times 10^{-7}$	1/km
κ_{24a}	$7.00644907535074 \times 10^{-7}$	1/km
κ_{24b}	0	1/km

References

- [1] Segerman, Alan M. and Zedd, Michael F., "Investigations of Spacecraft Orbits Around the L_2 Sun-Earth Libration Point—Part 1," April, 2002.
- [2] Richardson, David L. *Periodic Orbits About the L_1 and L_2 Collinear Points in the Circular-Restricted Problem*. Prepared for Goddard Space Flight Center by Computer Sciences Corporation, Report CSC/TR-78/6002, March 1978.
- [3] Dunham, David W., and Daniel P. Muhonen. "Tables of Libration-Point Parameters for Selected Solar System Objects." *The Journal of the Astronautical Sciences* (January–March 2001): 197-217.

Part 3: Modelling the Perturbations
— **Elliptical Earth Orbit, Lunar Gravity, Solar Radiation Pressure, Thrusters**

Contents

1	Introduction and Problem Definition	105
2	Equations of Motion	109
2.1	Circular Restricted Three-Body Problem	109
2.2	Elliptical Restricted Three-Body Problem	111
2.2.1	Elliptical Problem Libration Point Analog	111
2.2.2	Relative Motion Equation Derivation	112
2.3	Lunar Gravitational Effects	116
2.4	Solar Radiation Pressure Effects	117
2.5	Spacecraft Thruster Effects	118
2.6	Summary	121
3	Expanded Equations of Motion	126
3.1	Circular Restricted Three-Body Problem	126
3.2	Elliptical Restricted Three-Body Problem	126
3.3	Lunar Gravitational Effects	129
3.4	Summary	134
4	Modeling Uncertainties	136
4.1	Elliptical Restricted Three-Body Problem	136
4.2	Lunar Gravitational Effects	137
5	Sensitivity Summary	138
6	Summary and Conclusion	139
	Appendices	143
A	Sensitivity of Telescope Motion to Errors in Hub Position	143
A.1	Derivation of Variational Equations	143
A.2	Linear Equations	147
A.3	Solution Development	148
A.3.1	Non-secular Solution	149
A.3.2	Secular Solution	150
A.3.3	State Transition Matrix	153
A.4	Out-of-Plane Solution	153
A.4.1	Secular	154

A.4.2 Non-Secular	156
A.5 In-Plane Particular Solution	157
A.5.1 Secular	158
A.5.2 Non-Secular	161
A.6 Summary	163
B Relative Motion Near Earth-Moon L_2 Libration Point	164
C Calculation of Luminosity Reduction Due to Partial Eclipse	165
D Constant Parameters	171
References	172

List of Tables

1	Acceleration due to Solar Radiation Pressure vs. Surface Area	122
2	Example Initial Conditions	124
3	Along-Ellipsoid Effect of Sun-Earth Perturbation on Solution (90 days)	127
4	Along-Ellipsoid Effect of Lunar Perturbation on Solution (90 days)	133
5	Along-Ellipsoid Effect of Earth-Moon Perturbation on Solu- tion (15 days)	164
6	Physical Constants	171
7	Computed Values and Coefficients	171

List of Figures

1	Aperture Formation of MAXIM Pathfinder, Concept of June 2002.	106
2	Coordinate Axis Definition	109
3	Coordinate Axis Definition (including Moon)	117
4	Vehicle Thrust in Body-Fixed Frame	119
5	Frame Rotation from Body to Rotating Frames	121
6	Effects of Perturbations on Relative Distance — Full Equations	125
7	Effects of Perturbations on Relative Distance — Expanded Equations	135
8	Relative Motion Error Caused by 1.7 km Initial Hub Position Error	139
9	Relative Motion Error Caused by 17.3 km Initial Hub Position Error	140
10	$\partial z/\partial x_h$ and $\partial z/\partial z_h$ with resonance	156
11	$\partial z/\partial z_h$ without resonance	157
12	$\partial x/\partial y_h$ and $\partial y/\partial y_h$ with resonance	160
13	$\partial x/\partial x_h$ and $\partial y/\partial x_h$ with resonance	161
14	$\partial x/\partial z_h$ and $\partial y/\partial z_h$ with resonance	162
15	$\partial x/\partial z_h$ and $\partial y/\partial z_h$ without resonance	162
16	Solar Radiation Shadowing Geometry	165
17	Earth Obscuration and Solar Disk Geometry	166

1 Introduction and Problem Definition

Some continuing long-term goals of our sponsor are to develop high-fidelity equations of motion representing the formation flying of a spacecraft constellation near the Sun-Earth L_2 point and equations describing the relative motion between these constellation members.

This is our third report, which continues from Part 1 [1] and Part 2 [2]. In this report, we further the work of Part 2 by developing the elliptical restricted three-body problem from the previous work with the circular restricted three-body problem. Additionally, this new work includes the force perturbations of lunar gravitation, solar radiation, and spacecraft thrusters. The effects of the elliptical orbit of the Earth-Moon system about the sun and the force perturbations are incorporated as additive perturbations to the circular restricted three-body problem.

This work builds from the previously developed circular restricted three-body problem formulation. The familiarity of the formulations gained from Part 2 is maintained here. We present the development of the full nonlinear baseline model, which includes these perturbations:

- begin with circular restricted three-body problem
- then adding terms describing the elliptical orbit of Earth around the sun
- then adding terms describing the moon's motion about Earth
- then adding terms incorporating the force due to solar radiation
- finally adding terms for spacecraft thrust

We identify the magnitude of the contribution of each perturbation to the solution, in order to help determine when it should be included in the computations. We identify substantial modeling uncertainties. In addition to identifying the magnitudes of the effects of the included perturbations, we identify the magnitudes of what is dropped in the truncation process.

The development continues with the expanded form of the full nonlinear baseline to sufficiently high order such as to capture the relevant contributions to the model. The presentation of the perturbations is organized in similar fashion to the baseline presentation so the reader can easily compare and contrast the models.

This research is loosely motivated by formation flying concepts for the MicroArcsecond X-ray Imaging Mission (MAXIM) Pathfinder. A concept configuration of the MAXIM mission is depicted and described below.

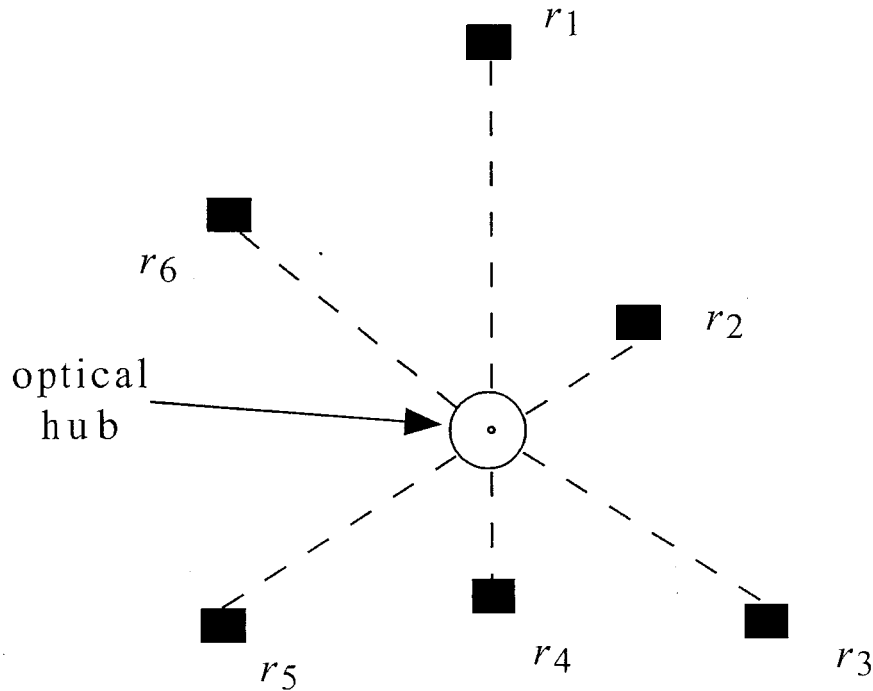


Figure 1: Aperture Formation of MAXIM Pathfinder. Concept of June 2002.

Seven spacecraft shown in Figure 1 are in the same plane forming a flat aperture. The optical hub is in the “center” of six free-flying spacecraft (telescopes). Dashed lines do not indicate a material connection, but rather indicate random radial directions listed r_1 through r_6 . The scalar length of r ranges from 100 to 500 meters. Additionally, the six free-flying spacecraft are loosely spaced 60° from one another.

There is also a detector spacecraft located approximately 20,000 km and 90° out of the plane formed by the flat aperture. The entire system is in a Sun-Earth L_2 orbit, which has yet to be designed by the mission team. The analysis of the detector’s orbit relative to the aperture plane is beyond the scope of this work.

In Section 2.1, we present the circular restricted three-body problem's equations of motion, the coordinate frame that describes the motion, and define terms used in the formulation.

In each section below, as appropriate, we explain the effects of those terms retained and dropped from the derivation in the course of the truncation process.

- In Section 2.2, we present the elliptical restricted three-body problem, which is used as the baseline for the subsequent development.
- In Section 2.3, we incorporate the effects of the lunar gravity.
- In Section 2.4, we incorporate the effects of the solar radiation pressure.
- In Section 2.5, we incorporate the terms used to include spacecraft thrusters.
- In Section 2.6, we consolidate the equations into one location. There is further discussion to compare the relative magnitude of the terms so that they may be turned on or off.
- In Section 3.1, we present the expanded form of the circular full nonlinear baseline.
- In Section 3.2, we present the derivation of the expanded form of the elliptical full nonlinear baseline.
- In Section 3.3, we incorporate the effects of the lunar gravity.
- In Section 3.4, we consolidate the equations into one location. There is further discussion to compare the relative magnitude of the terms so that they may be turned on or off.

Because there is no expansion of the forces from solar radiation pressure and spacecraft thrust, the contributions presented in Sections 2.4 and 2.5 are merely restated in Section 3.4.

One important measurement of the hub-telescope concept is knowledge of the distance between the spacecraft to within millimeters or even smaller. However, while many of the equations of motion presented in Sections 2 and 3 have terms that require numerical values which are listed in readily available

publications, some values of the needed physical parameters are given to a number of significant figures with uncertainties in their knowledge or measurement. A certain value may be defined one way in one text and a different way in another text. This will produce different results in the numerical calculations. Examples of these uncertainties applicable to the equations in this report are shown in Section 4. Some discussion is provided indicating the impact to the simulation results due to differences in the calculations.

Section 5 summarizes the results of Appendix A, which contains a detailed discussion of the sensitivity of the relative motion to small errors in the assumed position of the hub.

Appendix B fulfills a request by the sponsor to minimally address relative motion at the L_2 point of the Earth-Moon system.

Appendix C explains the eclipse geometry and corresponding shadow model used in the application of solar radiation pressure.

2 Equations of Motion

2.1 Circular Restricted Three-Body Problem

In Parts 1 and 2 of this research [1, 2], the general second order differential equations of motion were constructed for an object near the Sun-Earth L_2 libration point, using the force model of the classical circular restricted three-body problem. In this model, Earth is treated as being in a circular orbit about the sun, the spacecraft mass is considered to be negligible as compared to the two primaries, and only point-mass gravitational forces are considered.

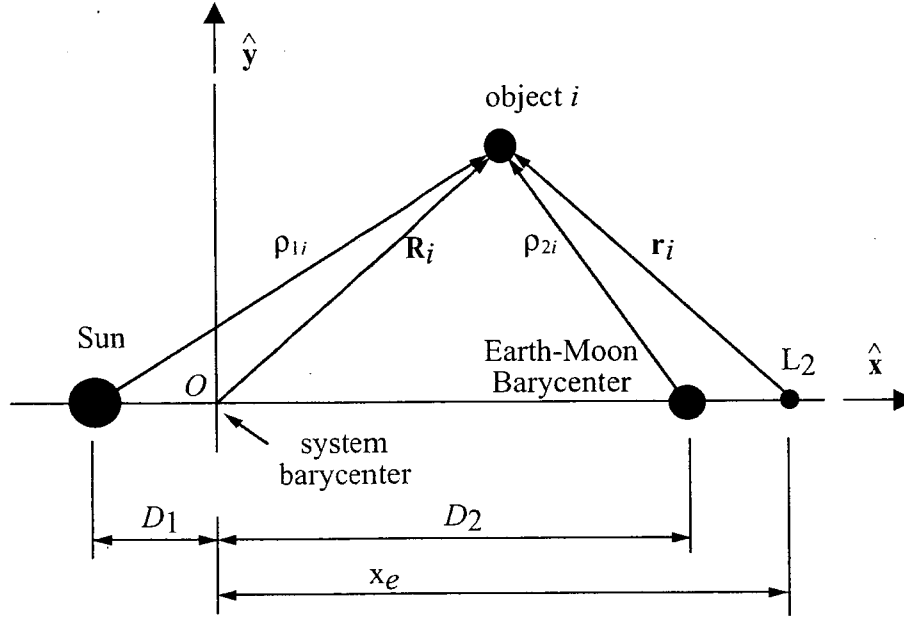


Figure 2: Coordinate Axis Definition

For this system, depicted in Figure 2, the differential equations of motion for an object (object i) near the Sun-Earth L_2 are given by

$$\ddot{\mathbf{r}}_i = - \left(\frac{\mu_1}{\rho_{1i}^3} + \frac{\mu_2}{\rho_{2i}^3} \right) \mathbf{r}_i - \left(\frac{\mu_1(x_e + D_1)}{\rho_{1i}^3} + \frac{\mu_2(x_e - D_2)}{\rho_{2i}^3} \right) \hat{\mathbf{x}} + n^2 x_e \hat{\mathbf{x}},$$

where

- \mathbf{r}_i = vector from L_2 to object i
- μ_1 = solar Keplerian constant
- μ_2 = terrestrial Keplerian constant (Earth + Moon)
- ρ_{1i} = distance from Sun to object i
- ρ_{2i} = distance from Earth-Moon barycenter to object i
- x_e = distance from system barycenter to L_2
- D_1 = distance from system barycenter to Sun
- D_2 = distance from system barycenter to Earth-Moon barycenter
- $\hat{\mathbf{x}}$ = unit vector parallel to Sun-Earth line of syzygy,
pointing in Sun-to-Earth direction
- n = terrestrial mean motion about Sun (assumed constant).

The coordinate frame of Figure 2 is a rotating reference frame with origin O at the system barycenter. The x -axis points along the Sun-Earth line of syzygy and the z -axis is parallel to the system angular momentum; the y -axis completes the dextral coordinate system.

Let \mathbf{r}_h and \mathbf{r}_t denote, respectively, the vector from L_2 to the hub and to a telescope. Therefore, if \mathbf{r} is the vector from the hub to the telescope, the differential equation of motion for the telescope relative to the hub is

$$\begin{aligned}
 \ddot{\mathbf{r}} &= \ddot{\mathbf{r}}_t - \ddot{\mathbf{r}}_h \\
 &= -\left(\frac{\mu_1}{\rho_{1t}^3} + \frac{\mu_2}{\rho_{2t}^3}\right)\mathbf{r}_t - \left(\frac{\mu_1(x_e + D_1)}{\rho_{1t}^3} + \frac{\mu_2(x_e - D_2)}{\rho_{2t}^3}\right)\hat{\mathbf{x}} \\
 &\quad - \left(\frac{\mu_1}{\rho_{1h}^3} + \frac{\mu_2}{\rho_{2h}^3}\right)\mathbf{r}_h + \left(\frac{\mu_1(x_e + D_1)}{\rho_{1h}^3} + \frac{\mu_2(x_e - D_2)}{\rho_{2h}^3}\right)\hat{\mathbf{x}} \\
 &= -\mu_1\left(\frac{\mathbf{r}_t}{\rho_{1t}^3} - \frac{\mathbf{r}_h}{\rho_{1h}^3}\right) - \mu_2\left(\frac{\mathbf{r}_t}{\rho_{2t}^3} - \frac{\mathbf{r}_h}{\rho_{2h}^3}\right) \\
 &\quad - \mu_1(x_e + D_1)\left(\frac{1}{\rho_{1t}^3} - \frac{1}{\rho_{1h}^3}\right)\hat{\mathbf{x}} - \mu_2(x_e - D_2)\left(\frac{1}{\rho_{2t}^3} - \frac{1}{\rho_{2h}^3}\right)\hat{\mathbf{x}},
 \end{aligned} \tag{1}$$

where now, in general, the subscripts h and t refer to the hub and telescope.

2.2 Elliptical Restricted Three-Body Problem

The extension to Equation (1) is now developed for the case of the elliptical restricted three-body problem. First, it is necessary to locate the point which is analogous to the libration point L_2 in the circular restricted problem. As would be expected, such a point exists; as the Sun-Earth distance varies, the location of the point oscillates along the x -axis.

2.2.1 Elliptical Problem Libration Point Analog

Say that there is an elliptical analog to the L_2 point and that its position relative to the (assumed inertial) system barycenter is given by

$$\mathbf{R}_e = x_e \hat{\mathbf{x}} + y_e \hat{\mathbf{y}} + z_e \hat{\mathbf{z}}.$$

Letting f refer to the true anomaly of Earth's orbit about the sun, the coordinate system has angular velocity

$$\boldsymbol{\omega}_e = f \hat{\mathbf{z}},$$

which now is considered to be varying throughout the year. Differentiating \mathbf{R}_e ,

$$\dot{\mathbf{R}}_e = \begin{bmatrix} \dot{x}_e - f y_e \\ \dot{y}_e + f x_e \\ \dot{z}_e \end{bmatrix}, \quad \ddot{\mathbf{R}}_e = \begin{bmatrix} \ddot{x}_e - \dot{f} y_e - 2f \dot{y}_e - f^2 x_e \\ \ddot{y}_e + \dot{f} x_e + 2f \dot{x}_e - f^2 y_e \\ \ddot{z}_e \end{bmatrix},$$

where the column vector notation is used to indicate the xyz vector components.

The Newtonian gravitational force per unit mass acting on an object at this point is given by

$$\mathbf{F}_e/m = \begin{bmatrix} -\frac{\mu_1(x_e + D_1)}{r_{1e}^3} - \frac{\mu_2(x_e - D_2)}{r_{2e}^3} \\ -\frac{\mu_1 y_e}{r_{1e}^3} - \frac{\mu_2 y_e}{r_{2e}^3} \\ -\frac{\mu_1 z_e}{r_{1e}^3} - \frac{\mu_2 z_e}{r_{2e}^3} \end{bmatrix},$$

where

$$\mathbf{r}_{1e} = (x_e + D_1) \hat{\mathbf{x}} + y_e \hat{\mathbf{y}} + z_e \hat{\mathbf{z}} \quad \text{and} \quad \mathbf{r}_{2e} = (x_e - D_2) \hat{\mathbf{x}} + y_e \hat{\mathbf{y}} + z_e \hat{\mathbf{z}}.$$

and D_1 and D_2 now refer to the time-varying locations of Sun and Earth along the line of syzygy.

Clearly, as in the circular restricted case, the z equation is decoupled, and admits a solution $z_e = 0$. If, as anticipated, the desired solution involves $y_e = 0$, the x and y components of the force-acceleration equation become:

$$\begin{aligned}\dot{\mathbf{x}} : \ddot{x}_e - f^2 x_e + \frac{\mu_1}{(x_e + D_1)^2} + \frac{\mu_2}{(x_e - D_2)^2} &= 0 \\ \dot{\mathbf{y}} : \ddot{y}_e + 2\dot{f}\dot{y}_e = \frac{1}{x_e} \frac{d}{dt}(x_e^2 \dot{f}) &= 0.\end{aligned}$$

From the y -component equation, $x_e^2 \dot{f}$ is therefore constant. However, conservation of the Sun-Earth two-body angular momentum per unit mass h , gives

$$D^2 \dot{f} = h,$$

where D is the varying Sun-Earth distance $D_1 + D_2$. Of course, unlike the case of the circular restricted problem, this distance varies throughout the year. Substitution for \dot{f} in the y -component equation gives

$$\left(\frac{x_e}{D}\right)^2 = \text{constant}.$$

For later convenience, define this constant in terms of the constant γ , such that

$$\left(\frac{x_e}{D}\right)^2 = \left(\gamma + \frac{D_2}{D}\right)^2.$$

Taking the positive root, this gives the definition of γ as

$$\gamma \triangleq \frac{x_e - D_2}{D}.$$

In the case of the Sun-Earth system, γ is approximately 0.01007824; x_e varies between 1.486×10^8 and 1.536×10^8 km throughout the course of the year.

2.2.2 Relative Motion Equation Derivation

Let \mathbf{R}_i denote the position vector from the system barycenter (point O) to spacecraft m_i . Referring again to Figure 2,

$$\mathbf{R}_i = x_e \dot{\mathbf{x}} + \mathbf{r}_i.$$

As above, the coordinate system has angular velocity

$$\omega_c = f\hat{\mathbf{z}}.$$

Differentiating \mathbf{R}_i ,

$$\begin{aligned}\dot{\mathbf{R}}_i &= \dot{x}_e\hat{\mathbf{x}} + f x_e\hat{\mathbf{y}} + \dot{\mathbf{r}}_i \\ \ddot{\mathbf{R}}_i &= (\ddot{x}_e - f^2 x_e)\hat{\mathbf{x}} + (2f\dot{x}_e + \ddot{f}x_e)\hat{\mathbf{y}} + \ddot{\mathbf{r}}_i.\end{aligned}$$

The distance x_e and its time derivatives may be written in terms of the varying Sun-Earth distance D and its derivatives, using the following definitions of the constants γ and ρ , and the associated relationships:

$$\begin{aligned}\gamma &\triangleq \frac{x_e - D_2}{D} & \rho &\triangleq \frac{\mu_2}{\mu} & D_1 &= \rho D \\ \gamma + 1 &= \frac{x_e + D_1}{D} & 1 - \rho &= \frac{\mu_1}{\mu} & D_2 &= (1 - \rho)D,\end{aligned}$$

where

$$\mu = \mu_1 + \mu_2.$$

Then,

$$\begin{aligned}x_e &= \gamma D + D_2 \\ &= (\gamma + 1 - \rho)D \\ \dot{x}_e &= (\gamma + 1 - \rho)\dot{D} \\ \ddot{x}_e &= (\gamma + 1 - \rho)\ddot{D}.\end{aligned}$$

This gives the acceleration vector $\ddot{\mathbf{R}}_i$ as

$$\ddot{\mathbf{R}}_i = (\gamma + 1 - \rho)(\ddot{D} - f^2 D)\hat{\mathbf{x}} + (\gamma + 1 - \rho)(2f\dot{D} + \ddot{f}D)\hat{\mathbf{y}} + \ddot{\mathbf{r}}_i. \quad (2)$$

Similarly, two-body relationships may be used to write \dot{D} and \ddot{D} in terms of \dot{f} and \ddot{f} . Using the two-body equations of motion for the sun (could use

Earth):

$$\begin{aligned}
\mathbf{R}_1 &= -D_1 \hat{\mathbf{x}} \\
&= -\rho D \hat{\mathbf{x}} \\
\omega_c &= f \hat{\mathbf{z}} \\
\dot{\mathbf{R}}_1 &= -\rho \dot{D} \hat{\mathbf{x}} - \rho f D \dot{\mathbf{y}} \\
\ddot{\mathbf{R}}_1 &= (-\rho \ddot{D} + \rho f^2 D) \hat{\mathbf{x}} + (-2\rho f \dot{D} - \rho \ddot{f} D) \hat{\mathbf{y}} \\
&= \rho (f^2 D - \ddot{D}) \hat{\mathbf{x}} - \rho (\ddot{f} D + 2f \dot{D}) \hat{\mathbf{y}} \\
&= \frac{\mu_2}{D^2} \hat{\mathbf{x}} \quad (\text{two-body force})
\end{aligned}$$

This gives the component equations

$$\begin{aligned}
\hat{\mathbf{x}} : \rho (f^2 D - \ddot{D}) &= \frac{\mu_2}{D^2} \\
\hat{\mathbf{y}} : -\rho (\ddot{f} D + 2f \dot{D}) &= -\frac{\rho}{D} \frac{d}{dt} (D^2 f) = 0,
\end{aligned}$$

which yield

$$\begin{aligned}
\ddot{D} - f^2 D &= -\frac{\mu_2}{\rho D^2} \\
2f \dot{D} + \ddot{f} D &= 0.
\end{aligned}$$

Substituting into Equation (2), the acceleration becomes

$$\begin{aligned}
\ddot{\mathbf{R}}_i &= -(\gamma + 1 - \rho) \frac{\mu_2}{\rho D^2} \hat{\mathbf{x}} + \ddot{\mathbf{r}}_i \\
&= \left[-(\gamma + 1) \frac{\mu}{D^2} + \frac{\mu_2}{D^2} \right] \hat{\mathbf{x}} + \ddot{\mathbf{r}}_i \\
&= \left[-(\gamma + 1) \frac{\mu_1}{D^2} - \gamma \frac{\mu_2}{D^2} \right] \hat{\mathbf{x}} + \ddot{\mathbf{r}}_i.
\end{aligned}$$

Introducing the two-body forces,

$$\ddot{\mathbf{R}}_i = \left[-(\gamma + 1) \frac{\mu_1}{D^2} - \gamma \frac{\mu_2}{D^2} \right] \hat{\mathbf{x}} + \ddot{\mathbf{r}}_i = -\frac{\mu_1}{\rho_{1i}^3} \boldsymbol{\rho}_{1i} - \frac{\mu_2}{\rho_{2i}^3} \boldsymbol{\rho}_{2i}. \quad (3)$$

Note that the explicit appearance of the time derivatives of f has now been removed.

Next, the vectors ρ_{1i} and ρ_{2i} may be written as

$$\begin{aligned}\rho_{1i} &= (x_e + D_1)\hat{\mathbf{x}} + \mathbf{r}_i \\ &= (\gamma + 1)D\hat{\mathbf{x}} + \mathbf{r}_i\end{aligned}\quad \text{and} \quad \begin{aligned}\rho_{2i} &= (x_e - D_2)\hat{\mathbf{x}} + \mathbf{r}_i \\ &= \gamma D\hat{\mathbf{x}} + \mathbf{r}_i.\end{aligned}$$

Substituting into Equation (3),

$$\begin{aligned}\ddot{\mathbf{R}}_i &= -\left[(\gamma + 1)\frac{\mu_1}{D^2} + \gamma\frac{\mu_2}{D^2}\right]\hat{\mathbf{x}} + \ddot{\mathbf{r}}_i \\ &= -\frac{\mu_1}{\rho_{1i}^3}[(\gamma + 1)D\hat{\mathbf{x}} + \mathbf{r}_i] - \frac{\mu_2}{\rho_{2i}^3}[\gamma D\hat{\mathbf{x}} + \mathbf{r}_i] \\ &= -\left(\frac{\mu_1}{\rho_{1i}^3} + \frac{\mu_2}{\rho_{2i}^3}\right)\mathbf{r}_i - \left[(\gamma + 1)\frac{\mu_1}{\rho_{1i}^3} + \gamma\frac{\mu_2}{\rho_{2i}^3}\right]D\hat{\mathbf{x}}.\end{aligned}$$

In the rotating frame, \mathbf{r}_i and its time derivatives are given by

$$\mathbf{r}_i = \begin{bmatrix} x_i \\ y_i \\ z_i \end{bmatrix}, \quad \dot{\mathbf{r}}_i = \begin{bmatrix} \dot{x}_i - \dot{f}y_i \\ \dot{y}_i + \dot{f}x_i \\ \dot{z}_i \end{bmatrix}, \quad \ddot{\mathbf{r}}_i = \begin{bmatrix} \ddot{x}_i - \ddot{f}y_i - 2\dot{f}\dot{y}_i - \dot{f}^2x_i \\ \ddot{y}_i + \ddot{f}x_i + 2\dot{f}\dot{x}_i - \dot{f}^2y_i \\ \ddot{z}_i \end{bmatrix}.$$

Note that vectors ρ_{1i} , ρ_{2i} , and \mathbf{r}_i are dependent upon the eccentricity of Earth's orbit, as is D . To avoid this dependence, redefine these vectors relative to reference positions of Sun, Earth, and L_2 along the line of syzygy. Denoting the reference distances by an overbar,

$$\begin{aligned}\mathbf{R}_i &= \bar{x}_e\hat{\mathbf{x}} + \mathbf{r}_i \\ \omega_c &= \dot{f}\hat{\mathbf{z}} \\ \dot{\mathbf{R}}_i &= \dot{f}\bar{x}_e\hat{\mathbf{y}} + \dot{\mathbf{r}}_i \\ \ddot{\mathbf{R}}_i &= -\dot{f}^2\bar{x}_e\hat{\mathbf{x}} + \ddot{f}\bar{x}_e\hat{\mathbf{y}} + \ddot{\mathbf{r}}_i.\end{aligned}$$

Again using the definitions of γ and ρ , $\bar{x}_e = (\gamma + 1 - \rho)\bar{D}$.

Using this form of the acceleration,

$$\begin{aligned}\ddot{\mathbf{R}}_i &= (\gamma + 1 - \rho)(-\dot{f}^2\hat{\mathbf{x}} + \ddot{f}\hat{\mathbf{y}})\bar{D} + \ddot{\mathbf{r}}_i \\ &= -\left(\frac{\mu_1}{\rho_{1i}^3} + \frac{\mu_2}{\rho_{2i}^3}\right)\mathbf{r}_i - \left[(\gamma + 1)\frac{\mu_1}{\rho_{1i}^3} + \gamma\frac{\mu_2}{\rho_{2i}^3}\right]\bar{D}\hat{\mathbf{x}},\end{aligned}\quad (4)$$

where

$$\rho_{1i} = (\gamma + 1)\bar{D}\hat{\mathbf{x}} + \mathbf{r}_i \quad \text{and} \quad \rho_{2i} = \gamma\bar{D}\hat{\mathbf{x}} + \mathbf{r}_i.$$

Vectors \mathbf{r}_i and $\ddot{\mathbf{r}}_i$ take the same forms as before, now relative to the reference L_2 location.

For the relative motion, let

$$\mathbf{r} = \mathbf{r}_t - \mathbf{r}_h = \mathbf{R}_t - \mathbf{R}_h.$$

Then,

$$\begin{aligned} \ddot{\mathbf{r}} = & -\mu_1 \left(\frac{\mathbf{r}_t}{\rho_{1t}^3} - \frac{\mathbf{r}_h}{\rho_{1h}^3} \right) - \mu_2 \left(\frac{\mathbf{r}_t}{\rho_{2t}^3} - \frac{\mathbf{r}_h}{\rho_{2h}^3} \right) \\ & - \left[\mu_1(\gamma + 1) \left(\frac{1}{\rho_{1t}^3} - \frac{1}{\rho_{1h}^3} \right) + \mu_2\gamma \left(\frac{1}{\rho_{2t}^3} - \frac{1}{\rho_{2h}^3} \right) \right] \bar{D}\dot{\mathbf{x}}, \end{aligned} \quad (5)$$

as in Equation (1).

2.3 Lunar Gravitational Effects

This section discusses the lunar contribution to the telescope motion relative to the hub. Terms corresponding to the gravitational force of the moon upon the hub and telescope spacecraft are included in the relative equations of motion (telescope relative to hub). The resulting contribution is then cast as an additive perturbation to the elliptical restricted three-body problem equations, such that when the lunar motion is ignored, the contribution reverts to the lunar mass placed at the Earth position. The moon is treated as a point mass.

As shown in Figure 3, let ρ_{3i} denote the vector from the moon to spacecraft i , either the hub or a telescope, and let μ_3 denote the lunar Keplerian constant. The lunar force per unit mass on spacecraft i is then given by

$$-\mu_3 \frac{\rho_{3i}}{\rho_{3i}^3}. \quad (6)$$

Therefore, the contribution to the equations of motion of the telescope relative to the hub is

$$\mathbf{F}_m = -\mu_3 \left(\frac{\rho_{3t}}{\rho_{3t}^3} - \frac{\rho_{3h}}{\rho_{3h}^3} \right), \quad (7)$$

where the subscripts h and t refer respectively to the hub and telescope.

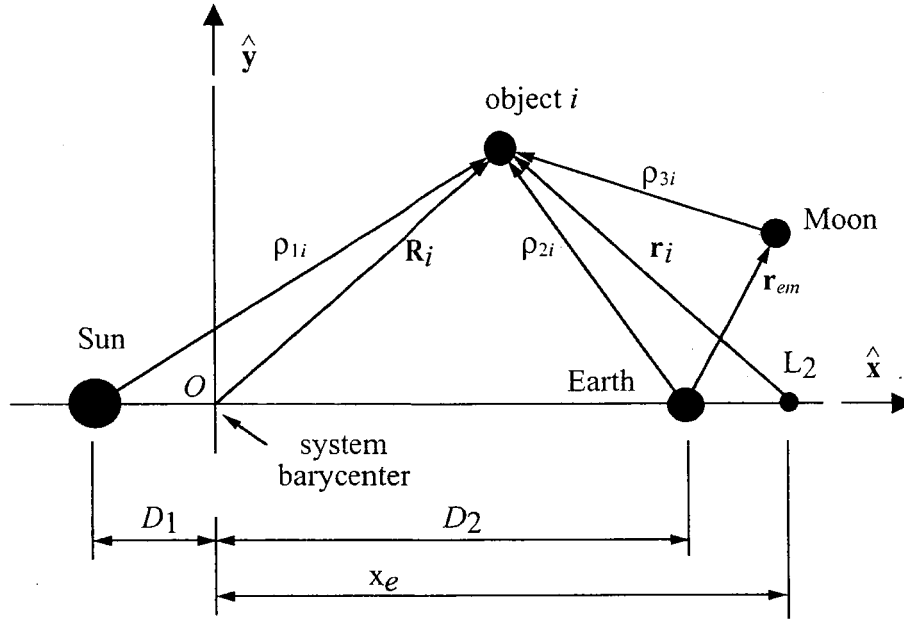


Figure 3: Coordinate Axis Definition (including Moon)

2.4 Solar Radiation Pressure Effects

The work presented in this section and in Appendix C was prepared by Professor David Richardson of the University of Cincinnati, under subcontract for this project [3].

The pressure from solar radiation imparts a tiny force on a telescope spacecraft. Depending upon spacecraft design and distance from the sun, the force can perturb both the spacecraft's attitude and orbit. The force can also be harnessed to beneficially propel the spacecraft.

We present a model to compute the force on a spacecraft, accounting for the force reduction when the spacecraft orbits through the terrestrial shadow.

At a distance ρ_{1i} from the sun, the solar flux I (the irradiance) acting on the spacecraft is given by

$$I = \frac{L}{4\pi\rho_{1i}^2},$$

where

$$L = 3.842 \times 10^{26} \text{ watts}$$

is the solar luminosity (total emitted radiation).

If A is the cross-sectional area of a spacecraft of mass m projected normal to the spacecraft-Sun line, then the solar radiation force F_s per unit mass acting on the spacecraft is

$$F_s = \frac{C_R LA}{4\pi mc\rho_{1t}^2} = \frac{1.0198 \times 10^{17} C_R A}{m\rho_{1t}^2} \text{ N/unit mass,}$$

where c is the speed of light and $0 \leq C_R \leq 2$ is the parameter characteristic of the reflectivity of the spacecraft surface facing the sun:

$$\begin{aligned} C_R = 0 & \quad \text{translucent,} \\ C_R = 1 & \quad \text{perfectly absorbent,} \\ C_R = 2 & \quad \text{perfectly reflective.} \end{aligned}$$

For trajectory motion that passes through any portion of Earth's shadow, the full disk of the sun will be partially obscured. In the vicinity of L_2 , this will occur at distances normal to the line of syzygy of approximately 13,420 km or less. In such cases, the force expression above must be scaled by a "luminosity reduction factor" σ which ranges from zero (total eclipse) to unity (full sunlight). The appropriate expression for the force per unit mass is then written:

$$\mathbf{F}_s = \frac{1.0198 \times 10^{17} C_R A \sigma}{m\rho_{1t}^2} \boldsymbol{\rho}_{1t} = \frac{1.0198 \times 10^{17} C_R A \sigma}{m \|(\gamma - 1)\bar{D}\hat{\mathbf{x}} + \mathbf{r}_t\|^3} [(\gamma + 1)\bar{D}\hat{\mathbf{x}} + \mathbf{r}_t]. \quad (8)$$

The calculation of the luminosity reduction factor, σ , is presented in Appendix C.

Our solar model did not consider the 11-year solar cycle, or estimate daily variations of solar flux, or the geomagnetic tail.

2.5 Spacecraft Thruster Effects

This section presents the derivation used to incorporate the effects of body-mounted thrusters in our equations of motion.

First, we give the body-fixed acceleration components imparted by the thrusters. These terms are calculated as shown:

$$\ddot{x}_b = F_x/m, \quad \ddot{y}_b = F_y/m, \quad \ddot{z}_b = F_z/m.$$

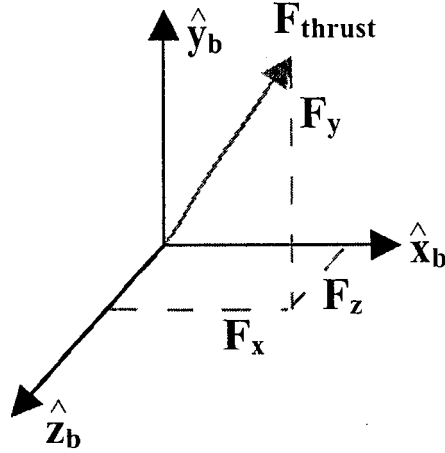


Figure 4: Vehicle Thrust in Body-Fixed Frame

where F_x , F_y , F_z are the components of the thrust \mathbf{F}_{thrust} in the body-fixed frame, as shown in Figure 4; m is the vehicle mass.

Consider an arbitrary alignment of a body-fixed coordinate frame with respect to the rotating x , y , z frame. The body-fixed x_b , y_b , z_b coordinate frame has its origin at the spacecraft's mass center.

The components of thrust expressed in the body frame must be transformed into the rotating reference frame in order to correctly incorporate these forces into the description of the motion. One way to express this transformation is as follows:

$$\begin{bmatrix} x \\ y \\ z \end{bmatrix} = T \begin{bmatrix} x_b \\ y_b \\ z_b \end{bmatrix},$$

where T is the transformation matrix formed as a combination of Euler rotations.

It is somewhat easier to visualize the individual rotations by considering the inverse rotation description, rotating instead from the rotating reference frame to that fixed in the spacecraft:

$$\begin{bmatrix} x_b \\ y_b \\ z_b \end{bmatrix} = T^{-1} \begin{bmatrix} x \\ y \\ z \end{bmatrix}.$$

Figure 5(a) shows the desired orientation of the body frame with respect to the rotating reference frame. However, by first assuming the coincident alignment of both the body frame and the rotating reference frame, we develop the inverse transformation matrix T^{-1} as a combination of Euler rotations through a set of Euler angles:

1. first rotate angle $(\psi + f)$ about the z_b axis as shown in Figure 5(b), where $f = \dot{f}(t - t_0)$
2. second rotate angle θ about the new orientation of the y_b axis, as shown in Figure 5(c)
3. third rotate angle ϕ about new orientation of the x_b axis, as shown in Figure 5(d)

Combine the sequence of rotations as follows with a right-to-left ordering of the rotation matrices:

$$\begin{aligned}
 T^{-1} &= \begin{bmatrix} 1 & 0 & 0 \\ 0 & c(\phi) & s(\phi) \\ 0 & -s(\phi) & c(\phi) \end{bmatrix} \begin{bmatrix} c(\theta) & 0 & -s(\theta) \\ 0 & 1 & 0 \\ s(\theta) & 0 & c(\theta) \end{bmatrix} \begin{bmatrix} c(\psi + f) & s(\psi + f) & 0 \\ -s(\psi + f) & c(\psi + f) & 0 \\ 0 & 0 & 1 \end{bmatrix} \\
 &= T_x^{-1}(\phi)T_y^{-1}(\theta)T_z^{-1}(\psi + f),
 \end{aligned}$$

where the functions c and s represent cosine and sine, respectively; the rotation matrix T_i^{-1} refers to the required Euler rotation matrix about the i_b -axis. Finally, the desired transformation matrix T (from the body-fixed frame to the rotating frame) is expressed as the inverse of T^{-1} :

$$T = (T^{-1})^{-1} = T_z(\psi + f)T_y(\theta)T_x(\phi).$$

These expressions premultiply the thrust force per unit mass acting upon the telescope spacecraft.

Consider the following example that demonstrates comparable thrust and solar forces: A 500 kg mass telescope spacecraft with a 1 mN thruster can produce an acceleration of 15 km/day². By choosing a solar flux reflectivity parameter C_{Rt} of 1.5 and placing various surface areas normal to the sun, the spacecraft's acceleration due to solar radiation pressure is shown in Table 1.

Contrast these low magnitudes to accelerations due to terrestrial and solar gravity (as given by Equation 5) of about 4,800 km/day². Of course, these magnitudes depend upon example. One point is that both the low thrust of

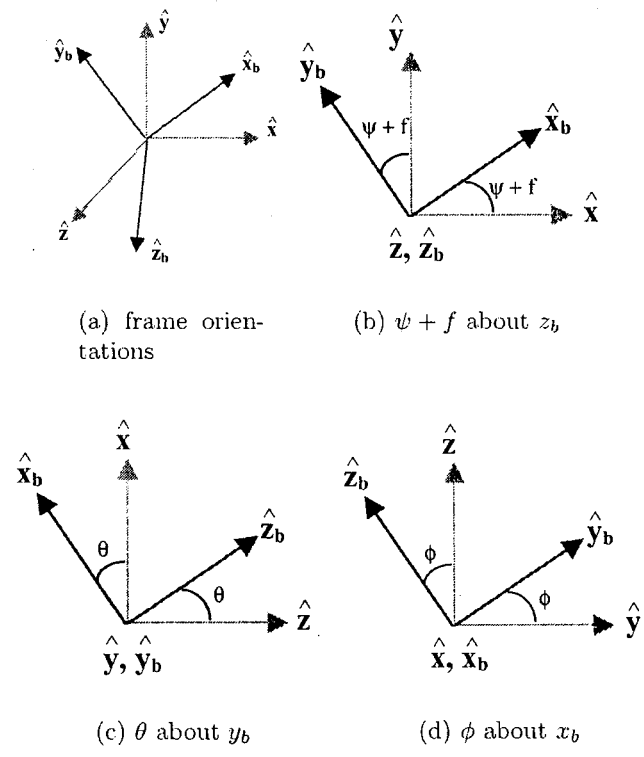


Figure 5: Frame Rotation from Body to Rotating Frames

electric propulsion and the low pressure of solar radiation produce accelerations very much lower than the gravitational effects. Another important point is that solar radiation pressure can be used for orbit control because the force from solar radiation pressure may be comparable to that from a thruster suite.

2.6 Summary

In this section, the force equations derived in Sections 2.1 through 2.5 are combined. The resulting equation models the elliptical restricted three-body problem, incorporating lunar, solar radiation, and thrust perturbations.

Combining the expressions of this section, given by Equations (4), (6),

Table 1: Acceleration due to Solar Radiation Pressure vs. Surface Area

Sun-Facing Surface Area (m ²)	Solar Radiation Pressure Acceleration (km/day ²)
1 ($\approx 3 \text{ ft} \times 3 \text{ ft}$)	1
100 ($\approx 33 \text{ ft} \times 33 \text{ ft}$)	10
150 ($\approx 40 \text{ ft} \times 40 \text{ ft}$)	15
1,000 ($\approx 100 \text{ ft} \times 100 \text{ ft}$)	100

and (8), along with the thrust expressions of Section 2.5, the differential equations of motion of the telescope are given by:

$$\begin{aligned}
 \ddot{\mathbf{R}}_t &= (\gamma + 1 - \rho)(-f^2 \dot{\mathbf{x}} + \ddot{f} \dot{\mathbf{y}}) \bar{D} - \ddot{\mathbf{r}}_t \\
 &= - \left(\frac{\mu_1}{\rho_{1t}^3} + \frac{\mu_2}{\rho_{2t}^3} \right) \mathbf{r}_t - \left[(\gamma + 1) \frac{\mu_1}{\rho_{1t}^3} + \gamma \frac{\mu_2}{\rho_{2t}^3} \right] \bar{D} \dot{\mathbf{x}} \quad \left. \vphantom{\frac{\mu_1}{\rho_{1t}^3}} \right\} \text{ER3B} \\
 &\quad - \mu_3 \frac{\rho_{3t}}{\rho_{3t}^3} \quad \left. \vphantom{\frac{\rho_{3t}}{\rho_{3t}^3}} \right\} \text{lunar} \\
 &\quad + \frac{1.0198 \times 10^{17} C_R A \sigma}{m \|(\gamma + 1) \bar{D} \dot{\mathbf{x}} + \mathbf{r}_t\|^3} [(\gamma + 1) \bar{D} \dot{\mathbf{x}} + \mathbf{r}_t] \quad \left. \vphantom{\frac{1.0198 \times 10^{17} C_R A \sigma}{m}} \right\} \text{SRP} \\
 &\quad + \begin{bmatrix} c(\psi') & -s(\psi') & 0 \\ s(\psi') & c(\psi') & 0 \\ 0 & 0 & 1 \end{bmatrix} \begin{bmatrix} c(\theta) & 0 & s(\theta) \\ 0 & 1 & 0 \\ -s(\theta) & 0 & c(\theta) \end{bmatrix} \begin{bmatrix} 1 & 0 & 0 \\ 0 & c(\phi) & -s(\phi) \\ 0 & s(\phi) & c(\phi) \end{bmatrix} \frac{\mathbf{F}_{\text{thrust}}}{m} \quad \left. \vphantom{\begin{bmatrix} c(\psi') \\ s(\psi') \\ 0 \end{bmatrix}} \right\} \text{thrust}
 \end{aligned}$$

where $\psi' = \psi + f$. The corresponding equations for the hub are

$$\begin{aligned}
 \ddot{\mathbf{R}}_h &= (\gamma + 1 - \rho)(-f^2 \dot{\mathbf{x}} + \ddot{f} \dot{\mathbf{y}}) \bar{D} + \ddot{\mathbf{r}}_h \\
 &= - \left(\frac{\mu_1}{\rho_{1h}^3} + \frac{\mu_2}{\rho_{2h}^3} \right) \mathbf{r}_h - \left[(\gamma + 1) \frac{\mu_1}{\rho_{1h}^3} + \gamma \frac{\mu_2}{\rho_{2h}^3} \right] \bar{D} \dot{\mathbf{x}} \quad \left. \vphantom{\frac{\mu_1}{\rho_{1h}^3}} \right\} \text{ER3B} \\
 &\quad - \mu_3 \frac{\rho_{3h}}{\rho_{3h}^3} \quad \left. \vphantom{\frac{\rho_{3h}}{\rho_{3h}^3}} \right\} \text{lunar} \\
 &\quad + \frac{1.0198 \times 10^{17} C_R A \sigma}{m \|(\gamma + 1) \bar{D} \dot{\mathbf{x}} + \mathbf{r}_h\|^3} [(\gamma + 1) \bar{D} \dot{\mathbf{x}} + \mathbf{r}_h]. \quad \left. \vphantom{\frac{1.0198 \times 10^{17} C_R A \sigma}{m}} \right\} \text{SRP}
 \end{aligned}$$

Combining the relative motion expressions of this section (Equations (5) and (7)), along with the solar radiation pressure of Equation (8) and the

thrust expressions of Section 2.5, the differential equations of relative motion for a telescope spacecraft are given by:

$$\begin{aligned}
\ddot{\mathbf{r}} = & -\mu_1 \left(\frac{\mathbf{r}_t}{\rho_{1t}^3} - \frac{\mathbf{r}_h}{\rho_{1h}^3} \right) - \mu_2 \left(\frac{\mathbf{r}_t}{\rho_{2t}^3} - \frac{\mathbf{r}_h}{\rho_{2h}^3} \right) & \left. \vphantom{\ddot{\mathbf{r}}} \right\} \text{ER3B} \\
& - \left[\mu_1(\gamma + 1) \left(\frac{1}{\rho_{1t}^3} - \frac{1}{\rho_{1h}^3} \right) + \mu_2\gamma \left(\frac{1}{\rho_{2t}^3} - \frac{1}{\rho_{2h}^3} \right) \right] \bar{D}\hat{\mathbf{x}} \\
& - \mu_3 \left(\frac{\boldsymbol{\rho}_{3t}}{\rho_{3t}^3} - \frac{\boldsymbol{\rho}_{3h}}{\rho_{3h}^3} \right) & \left. \vphantom{\ddot{\mathbf{r}}} \right\} \text{lunar} \\
& + \frac{1.0198 \times 10^{17} C_R A \sigma}{m \|(\gamma + 1)\bar{D}\hat{\mathbf{x}} + \mathbf{r}_t\|^3} [(\gamma + 1)\bar{D}\hat{\mathbf{x}} + \mathbf{r}_t] & \left. \vphantom{\ddot{\mathbf{r}}} \right\} \text{SRP}_t \\
& - \frac{1.0198 \times 10^{17} C_R A \sigma}{m \|(\gamma + 1)\bar{D}\hat{\mathbf{x}} + \mathbf{r}_h\|^3} [(\gamma + 1)\bar{D}\hat{\mathbf{x}} + \mathbf{r}_h] & \left. \vphantom{\ddot{\mathbf{r}}} \right\} \text{SRP}_h \\
& + \begin{bmatrix} c(\psi') & -s(\psi') & 0 \\ s(\psi') & c(\psi') & 0 \\ 0 & 0 & 1 \end{bmatrix} \begin{bmatrix} c(\theta) & 0 & s(\theta) \\ 0 & 1 & 0 \\ -s(\theta) & 0 & c(\theta) \end{bmatrix} \begin{bmatrix} 1 & 0 & 0 \\ 0 & c(\phi) & -s(\phi) \\ 0 & s(\phi) & c(\phi) \end{bmatrix} \frac{\mathbf{F}^{\text{thrust}}}{m} & \left. \vphantom{\ddot{\mathbf{r}}} \right\} \text{thrust}
\end{aligned}$$

We present the following example to permit comparison of the relative contribution of the terms to the telescope motion. The initial conditions are listed in Table 2; they were taken from the examples discussed in Part 2 of the research. As mentioned in that report, these values were selected so as to excite only the oscillatory linear modes.

Figure 6 presents the solution to numerical integration of four different force models selected from the summary equation above. The models were applied to both the hub and telescope, and the resulting state vectors were differenced in order to determine the position of the telescope relative to the hub. In each case, the same force model was applied to both the hub and telescope. Additionally, the same value of the reference distance \bar{D} was used for all force models.

The reference solution is represented in the figure by the x -axis. This refers to the circular restricted model case. The circular restricted model solution is obtained by including the elliptical restricted model (ER3B) terms, but with Earth's orbital eccentricity treated as being zero; this duplicates the model discussed in Part 2. The other models depicted in Figure 6 represent the addition of ellipticity (ER3B), lunar, and solar radiation (SRP) effects over 20 days. It is noted that the elliptical contribution provides the dominant perturbation to the circular restricted solution. In this example,

Table 2: Example Initial Conditions

	hub (state rel. to L_2)	telescope (state rel. to L_2)	telescope (state rel. to hub)
$x(0)$ (km)	-227,219.419	-227,219.483	-0.064780
$y(0)$ (km)	0.0	0.0	0.0
$z(0)$ (km)	-250,000.000	-249,999.974	0.026445
$\dot{x}(0)$ (km/day)	0.0	0.0	0.0
$\dot{y}(0)$ (km/day)	25,625.039	25,625.044	0.004421
$\dot{z}(0)$ (km/day)	0.0	0.0	0.0
mass m (kg)	500	500	
$\mathbf{F}_{\text{thrust}}$ (N)	$\mathbf{0}$	$\mathbf{0}$	
sun-facing area A (m ²)	150	150	

should the viewing of a scientific target be limited to no more than 10 days, the perturbation due to the elliptical contribution is less than 1 m.

In the MAXIM or similar missions, there may or may not be an actual hub spacecraft located at the aperture's center. Regardless, it is necessary to treat the hub as a central reference point for locating the positions of the individual telescope spacecraft. However, unlike the gravitational forces present, the solar radiation pressure effect upon a spacecraft with actual mass and area is substantial as compared to that upon a "phantom" hub. Therefore, for purposes of the simulation, the hub "spacecraft" is treated as having the same physical characteristics as the telescope. In this manner, the hub is maintained as an adequate reference for the position of the telescope.

The effects of thrusters were not simulated here, due to the vast uncertainties of force (both magnitude and direction) and duration. We considered trade studies involving thruster forces to be beyond the focus of this investigation.

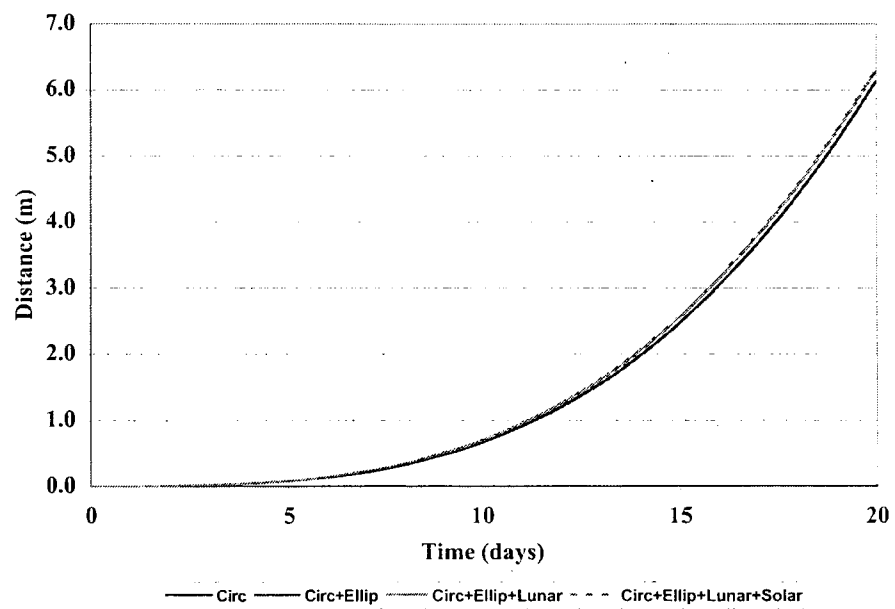


Figure 6: Effects of Perturbations on Relative Distance — Full Equations

3 Expanded Equations of Motion

3.1 Circular Restricted Three-Body Problem

In Part 2 [2], Equation (1) is expanded through terms which are linear in the coordinates of \mathbf{r} and no more than cubic in the coordinates of \mathbf{r}_h . This expansion takes the form

$$\begin{aligned} \ddot{\mathbf{r}} = & A_3 [-\mathbf{r} + 3x\hat{\mathbf{x}}] \\ & + A_4 [3x\mathbf{r}_h + 3x_h\mathbf{r} + (3\mathbf{r}_h \cdot \mathbf{r} - 15xx_h)\hat{\mathbf{x}}] \\ & + A_5 [(3\mathbf{r}_h \cdot \mathbf{r} - 15xx_h)\mathbf{r}_h + \frac{3}{2}(r_h^2 - 5x_h^2)\mathbf{r} \\ & - \frac{15}{2}(2x_h\mathbf{r}_h \cdot \mathbf{r} - 7xx_h^2 + xr_h^2)\hat{\mathbf{x}}], \end{aligned} \quad (9)$$

where the constants A_i are given by

$$A_i = \frac{\mu_1}{(x_e + D_1)^i} + \frac{\mu_2}{(x_e - D_2)^i}.$$

Terms involving A_i are considered to be of order i ; terms of order lower than 3 do not appear.

The acceleration vector $\ddot{\mathbf{r}}$ may be written relative to a rotating coordinate system which rotates at the constant angular rate n about the z -axis normal to the ecliptic, and with the x direction as previously defined. This gives

$$\ddot{\mathbf{r}} = \begin{bmatrix} \ddot{x} - 2n\dot{y} - n^2x \\ \ddot{y} + 2n\dot{x} - n^2y \\ \ddot{z} \end{bmatrix}.$$

where the column vector notation is used to indicate the xyz vector components.

3.2 Elliptical Restricted Three-Body Problem

Consider the elliptical restricted three-body equations of motion as given in Equation (5). The right side of this set of relative acceleration equations may be expanded as in Part 2 [2]. Consider the effects of various contributions to

the magnitude ordering scheme. For ordering purposes, take

$$\begin{aligned}\rho &= 3.04 \times 10^{-6} \\ \gamma &= 1.01 \times 10^{-2} \\ \frac{r_h}{D} &= 4.0 \times 10^{-3} \quad (r_h = 600,000 \text{ km}) \\ \frac{r}{D} &= 3.2 \times 10^{-9} \quad (r = 0.5 \text{ km}).\end{aligned}$$

A rough estimate may be obtained of the contributions that the various perturbations make to the circular restricted problem solution. Say that a perturbing term may be treated as modifying the linear frequencies associated with the circular restricted problem, and consider the square of the perturbing frequency to be roughly the magnitude of the coefficient of r in the perturbing acceleration. (Recall from Part 1 that the linear periods in and out of the xy -plane are approximately 177.566 days and 184.002 days, respectively.) Then, after 90 days, the effects of the terms containing various powers of r and r_h are given in Table 3, with effects included of roughly 20 m and larger.

Table 3: Along-Ellipsoid Effect of Sun-Earth Perturbation on Solution (90 days)

perturbing term	effect (m)
re	16.7
rr_h	289.3
rr_h^2	118.5
rr_h^3	47.4
rr_h^4	18.9

We recommend retaining terms which contribute down to approximately 20 m (can keep additional μ_1 terms if convenient). Retaining the rr_h^3 terms

results in the expanded/truncated differential equations

$$\begin{aligned}
\ddot{\mathbf{r}} = & A_3 [-\mathbf{r} + 3x\hat{\mathbf{x}}] \\
& + A_4 [3x\mathbf{r}_h + 3x_h\mathbf{r} + (3\mathbf{r}_h \cdot \mathbf{r} - 15xx_h)\hat{\mathbf{x}}] \\
& + A_5 [(3\mathbf{r}_h \cdot \mathbf{r} - 15xx_h)\mathbf{r}_h - \frac{3}{2}(r_h^2 - 5x_h^2)\mathbf{r} \\
& \quad - \frac{15}{2}(2x_h\mathbf{r}_h \cdot \mathbf{r} - 7xx_h^2 + xr_h^2)\hat{\mathbf{x}}] \\
& + A_6 [\frac{15}{2}\mathbf{r}_h(-xr_h^2 - 2x_h\mathbf{r} \cdot \mathbf{r}_h + 7xx_h^2) + \frac{5}{2}\mathbf{r}(7x_h^3 - 3x_hr_h^2) \\
& \quad + \frac{15}{2}(-r_h^2\mathbf{r}_h \cdot \mathbf{r} + 7xr_h^2x_h + 7x_h^2\mathbf{r} \cdot \mathbf{r}_h - 21xx_h^3)\hat{\mathbf{x}}].
\end{aligned}$$

Next consider the left side of the differential equation:

$$\begin{aligned}
\ddot{\mathbf{r}} = & \begin{bmatrix} \ddot{x} - \ddot{f}y - 2\dot{f}\dot{y} - f^2x \\ \ddot{y} + \ddot{f}x + 2\dot{f}\dot{x} - f^2y \\ \ddot{z} \end{bmatrix} \\
= & \begin{bmatrix} \ddot{x} - 2n_c\dot{y} - n_c^2x \\ \ddot{y} + 2n_c\dot{x} - n_c^2y \\ \ddot{z} \end{bmatrix} + \begin{bmatrix} -\ddot{f}y - 2(\dot{f} - n_c)\dot{y} - (f^2 - n_c^2)x \\ \dot{f}x + 2(f - n_c)\dot{x} - (f^2 - n_c^2)y \\ 0 \end{bmatrix}. \quad (10)
\end{aligned}$$

In this expanded form, the first vector term represents the acceleration which appears in the circular restricted problem (n_c refers to the mean motion of the circular restricted Earth orbit). The second vector term gives the perturbation which is added by including the elliptic restricted effects. The perturbation term is to be expanded in terms of the eccentricity e of Earth's orbit (≈ 0.017). In keeping with the earlier magnitude ordering, it is estimated that it is sufficient to retain only contributions which are linear in e , because er is approximately 8.5 m.

Say that the circular restricted problem takes D as being the reference value \bar{D} . Then, the corresponding mean motion is $n_c = \sqrt{\mu/\bar{D}^3}$. Now, in the elliptic restricted problem, the mean motion is

$$n = \sqrt{\frac{\mu}{a^3}} = \sqrt{\frac{\mu}{\bar{D}^3} \frac{\bar{D}^3}{a^3}} = \left(\frac{\bar{D}}{a}\right)^{3/2} n_c.$$

If \bar{D} is chosen to be the semi-major axis a , then $n = n_c$. If $\bar{D} = D_{\text{mean}} = a(1 + e^2/2)$, then

$$n = \left(1 + \frac{e^2}{2}\right)^{3/2} n_c \approx n_c.$$

Expressing \dot{f} and \ddot{f} in terms of time,

$$\dot{f} = \frac{h}{D^2} = \frac{\sqrt{\mu a(1-e^2)}}{D^2} = \frac{na^2\sqrt{1-e^2}}{D^2} \approx n_c \left(\frac{a}{D}\right)^2,$$

where $n = \sqrt{\mu/a^3}$, as given by Kepler's third law. Using the two-body relationship

$$D = \frac{a(1-e^2)}{1+e\cos f}.$$

$$\dot{f} \approx n_c \left(\frac{1+e\cos f}{1-e^2}\right)^2 \approx n_c(1+2e\cos f).$$

In terms of the mean anomaly ℓ ,

$$\dot{f} \approx n_c(1+2e\cos \ell).$$

Differentiating,

$$\ddot{f} \approx -2en_c^2 \sin \ell.$$

Using these results in the perturbing vector of Equation (10) gives

$$\begin{bmatrix} -\ddot{f}y - 2(\dot{f} - n_c)\dot{y} - (\dot{f}^2 - n_c^2)x \\ \ddot{f}x + 2(\dot{f} - n_c)\dot{x} - (\dot{f}^2 - n_c^2)y \\ 0 \end{bmatrix} = \begin{bmatrix} -2eyn_c^2 \sin \ell - 4eijn_c \cos \ell - 4exn_c^2 \cos \ell \\ 2exn_c^2 \sin \ell - 4e\dot{x}n_c \cos \ell - 4eyn_c^2 \cos \ell \\ 0 \end{bmatrix}.$$

3.3 Lunar Gravitational Effects

Consider the lunar force given above by Equation (7).

As in the previous work, it is desired that this contribution be expressed in terms of the position of the telescope relative to the hub. Let the vector \mathbf{r} again refer to the relative telescope position. Therefore,

$$\boldsymbol{\rho}_{3t} = \boldsymbol{\rho}_{3h} + \mathbf{r}. \quad (11)$$

As in the earlier analysis of the effects of Sun and Earth, the contribution of Equation (7) may be written as an expansion in terms of \mathbf{r} and its components. Accordingly, a similar binomial expansion development is followed as

that employed in Part 2 of the research. The square of the magnitude of ρ_{3t} is given by

$$\begin{aligned}\rho_{3t}^2 &= \rho_{3t} \cdot \rho_{3t} \\ &= \rho_{3h}^2 + r^2 + 2\rho_{3h} \cdot \mathbf{r} \\ &= \rho_{3h}^2 \left[1 + \left(\frac{r}{\rho_{3h}} \right)^2 + \frac{2\rho_{3h} \cdot \mathbf{r}}{\rho_{3h}^2} \right].\end{aligned}$$

Then,

$$\begin{aligned}\frac{1}{\rho_{3t}^3} &= \frac{1}{\rho_{3h}^3} \left[1 + \left(\frac{r}{\rho_{3h}} \right)^2 + \frac{2\rho_{3h} \cdot \mathbf{r}}{\rho_{3h}^2} \right]^{-3/2} \\ &= \rho_{3h}^{-3} (1 + \delta_3)^{-3/2},\end{aligned}$$

where

$$\delta_3 \triangleq \left(\frac{r}{\rho_{3h}} \right)^2 + \frac{2\rho_{3h} \cdot \mathbf{r}}{\rho_{3h}^2}$$

is assumed to be less than unity. Using a binomial expansion,

$$\begin{aligned}\frac{1}{\rho_{3t}^3} &= \frac{1}{\rho_{3h}^3} \sum_{k=0}^{\infty} \binom{-3/2}{k} \delta_3^k \\ &= \frac{1}{\rho_{3h}^3} \left[1 + \sum_{k=1}^{\infty} \binom{-3/2}{k} \delta_3^k \right].\end{aligned}$$

Using this expansion in Equation (7), and using Equation (11) to substitute for ρ_{3t} gives

$$\mathbf{F}_m = -\mu_3 \frac{\mathbf{r}}{\rho_{3h}^3} \left[1 + \sum_{k=1}^{\infty} \binom{-3/2}{k} \delta_3^k \right] - \mu_3 \frac{\rho_{3h}}{\rho_{3h}^3} \sum_{k=1}^{\infty} \binom{-3/2}{k} \delta_3^k.$$

Expanding through linear terms in r ,

$$\mathbf{F}_m \approx -\mu_3 \frac{\mathbf{r}}{\rho_{3h}^3} + 3\mu_3 \frac{\rho_{3h}}{\rho_{3h}^3} \frac{\mathbf{r} \cdot \rho_{3h}}{\rho_{3h}^2}. \quad (12)$$

It is preferable to treat these terms as an additive perturbation to the equations of the elliptical restricted three-body problem. Assume that the

baseline elliptical restricted problem contains an object with combined terrestrial and lunar mass, located at the mean Earth-Moon barycenter. Therefore, the expansion of Equation (7) should contain the lunar contribution to this combined mass along with terms representing the effect of the lunar motion about the barycenter. Accordingly, Equation (12) may be rewritten as

$$\begin{aligned} \mathbf{F}_m \approx & -\mu_3 \left(\frac{\mathbf{r}}{\rho_{2h}^3} - \frac{3\rho_{2h}}{\rho_{2h}^3} \frac{\mathbf{r} \cdot \rho_{2h}}{\rho_{2h}^2} \right) \\ & - \mu_3 \mathbf{r} \left(\frac{1}{\rho_{3h}^3} - \frac{1}{\rho_{2h}^3} \right) + 3\mu_3 \mathbf{r} \cdot \left(\frac{\rho_{3h}\rho_{3h}}{\rho_{3h}^5} - \frac{\rho_{2h}\rho_{2h}}{\rho_{2h}^5} \right). \end{aligned} \quad (13)$$

Because the vector ρ_{2h} was used in the earlier analysis, it is convenient to write ρ_{3h} as

$$\rho_{3h} = \rho_{2h} + \mathbf{r}_{em},$$

where \mathbf{r}_{em} refers to the lunar position relative to the mean barycenter. The square of the magnitude of ρ_{3h} is given by

$$\begin{aligned} \rho_{3h}^2 &= \rho_{3h} \cdot \rho_{3h} \\ &= \rho_{2h}^2 + r_{em}^2 + 2\rho_{2h} \cdot \mathbf{r}_{em} \\ &= \rho_{2h}^2 \left[1 + \left(\frac{r_{em}}{\rho_{2h}} \right)^2 + \frac{2\rho_{2h} \cdot \mathbf{r}_{em}}{\rho_{2h}^2} \right]. \end{aligned}$$

This gives

$$\frac{1}{\rho_{3h}} = \frac{1}{\rho_{2h}} \left[1 + \left(\frac{r_{em}}{\rho_{2h}} \right)^2 + \frac{2\rho_{2h} \cdot \mathbf{r}_{em}}{\rho_{2h}^2} \right]^{-1/2}$$

Using a Legendre polynomial expansion,

$$\frac{1}{\rho_{3h}} = \frac{1}{\rho_{2h}} \sum_{k=0}^{\infty} \left(\frac{r_{em}}{\rho_{2h}} \right)^k P_k(\cos S),$$

where

$$\cos S \triangleq \frac{\rho_{2h} \cdot \mathbf{r}_{em}}{\rho_{2h} r_{em}}.$$

Expanding through terms linear in r_{em} :

$$\frac{1}{\rho_{3h}} \approx \frac{1}{\rho_{2h}} \left(1 + \frac{r_{em}}{\rho_{2h}} \cos S \right),$$

giving

$$\frac{1}{\rho_{3h}^3} \approx \frac{1}{\rho_{2h}^3} \left(1 + 3 \frac{r_{em}}{\rho_{2h}} \cos S \right)$$

$$\frac{1}{\rho_{3h}^5} \approx \frac{1}{\rho_{2h}^5} \left(1 + 5 \frac{r_{em}}{\rho_{2h}} \cos S \right).$$

Using these representations in Equation (13),

$$\mathbf{F}_m \approx -\mu_3 \left(\frac{\mathbf{r}}{\rho_{2h}^3} - \frac{3\rho_{2h}\mathbf{r} \cdot \rho_{2h}}{\rho_{2h}^5} \right) \quad (14)$$

$$- 3\mu_3 \left[\mathbf{r}\rho_{2h} \cdot \mathbf{r}_{em} + \mathbf{r} \cdot \rho_{2h}\mathbf{r}_{em} + \mathbf{r} \cdot \mathbf{r}_{em}\rho_{2h} \right. \\ \left. - 5\mathbf{r} \cdot \rho_{2h}\rho_{2h}\rho_{2h} \cdot \mathbf{r}_{em} / \rho_{2h}^2 \right] / \rho_{2h}^5.$$

Examining Equation (14), the form of the first term in \mathbf{F}_m is identical to the corresponding terrestrial term derived in the earlier work. The only difference is that, here, the mass coefficient is μ_3 rather than μ_2 . This term represents the effect of a lunar mass collocated with the terrestrial mass; the remainder of \mathbf{F}_m represents the effect of the lunar motion *about* Earth. The first term may be added to the earlier work simply by replacing μ_2 with $\mu_2 + \mu_3$ in the relative equations of motion for the elliptical restricted three-body problem.

For the second term of Equation (14), the Earth-hub position vector ρ_{2h} is expanded in a fashion similar to that of the earlier work. In the context of the elliptical restricted problem using a reference location of L_2 ,

$$\rho_{2h} = \gamma \bar{D} \hat{\mathbf{x}} + \mathbf{r}_h$$

where γ and \bar{D} are constants as previously defined. The square of the magnitude of ρ_{2h} is given by

$$\rho_{2h}^2 = \rho_{2h} \cdot \rho_{2h}$$

$$= (\gamma \bar{D})^2 + r_h^2 + 2\gamma \bar{D} x_h$$

$$= \gamma \bar{D}^2 \left[1 + \left(\frac{r_h}{\gamma \bar{D}} \right)^2 + \frac{2x_h}{\gamma \bar{D}} \right],$$

where x_h is the x -component of \mathbf{r}_h . This gives

$$1/\rho_{2h} = (1 + c_h)^{1/2} / (\gamma \bar{D}).$$

where

$$\epsilon_h \triangleq \left(\frac{r_h}{\gamma \bar{D}} \right)^2 + \frac{2x_h}{\gamma \bar{D}}.$$

Once again, powers of this fraction are formed using binomial expansions, giving

$$\frac{1}{\rho_{2h}^\ell} = \frac{1}{(\gamma \bar{D})^\ell} \left[1 + \sum_{k=1}^{\infty} \binom{-\ell/2}{k} \epsilon_h^k \right].$$

The negative powers of ρ_{2h} that appear in the second term of Equation (14) are then formed using the appropriate values of ℓ in this binomial expansion. Expanding through linear terms in r_h and substituting, \mathbf{F}_m becomes

$$\begin{aligned} \mathbf{F}_m \approx & -\mu_3 \left(\frac{\mathbf{r}}{\rho_{2h}^3} - \frac{3\rho_{2h}\mathbf{r} \cdot \boldsymbol{\rho}_{2h}}{\rho_{2h}^5} \right) \\ & - 3\mu_3 [(-2xx_{em} + yy_{em} - zz_{em})\hat{\mathbf{x}} + (yx_{em} + xy_{em})\hat{\mathbf{y}} \\ & \quad + (zx_{em} + xz_{em})\hat{\mathbf{z}}] / (\gamma \bar{D})^4 \\ & - \mu_3 [-15x_{em}x_h\mathbf{r} + 3\mathbf{r}_h \cdot \mathbf{r}_{em}\mathbf{r} - 15x\mathbf{r}_{em}x_h \\ & \quad + 3\mathbf{r} \cdot \mathbf{r}_h\mathbf{r}_{em} + 3(\mathbf{r} \cdot \mathbf{r}_{em})(-5x_h\hat{\mathbf{x}} + \mathbf{r}_h) + 105x_{em}x_h\hat{\mathbf{x}} \\ & \quad - 15x_{em}\mathbf{r}_h - 15x\mathbf{r}_h \cdot \mathbf{r}_{em}\hat{\mathbf{x}} - 15x_{em}\mathbf{r} \cdot \mathbf{r}_h\hat{\mathbf{x}}] / (\gamma \bar{D})^5. \end{aligned} \tag{15}$$

Again, a rough estimate of the contributions that the various perturbations make to the solution are presented. As for the inclusion of the ellipticity in Section 3.2, the perturbing terms are treated as modifying the linear frequencies. After 90 days, the effects of the lunar terms containing various powers of the relevant variables are given in Table 4, including contributions greater than roughly 0.9 m.

Table 4: Along-Ellipsoid Effect of Lunar Perturbation on Solution (90 days)

perturbing term	effect (m)
rr_{em}	2.3
rr_{em}^2	0.6
$rr_h r_{em}$	0.9

3.4 Summary

In this section, the force equations derived in Sections 3.1 through 3.3 are combined. The models for solar radiation pressure and thrust are repeated here from the equation of Section 2.6 for completeness. The resulting equation models the expanded elliptical restricted three-body problem, incorporating lunar, solar radiation, and thrust perturbations.

Combining the expressions of this section, the expanded differential equations of relative motion for a telescope spacecraft are given by:

$$\begin{aligned}
 \ddot{\mathbf{r}} = & A_3[-\mathbf{r} + 3x\hat{\mathbf{x}}] + A_4[3x\mathbf{r}_h + 3x_h\mathbf{r} + (3\mathbf{r}_h \cdot \mathbf{r} - 15xx_h)\hat{\mathbf{x}}] \\
 & + A_5[(3\mathbf{r}_h \cdot \mathbf{r} - 15xx_h)\mathbf{r}_h + \frac{3}{2}(r_h^2 - 5x_h^2)\mathbf{r} \\
 & \quad - \frac{15}{2}(2x_h\mathbf{r}_h \cdot \mathbf{r} - 7xx_h^2 + xr_h^2)\hat{\mathbf{x}}] \\
 & + A_6[\frac{15}{2}\mathbf{r}_h(-xr_h^2 - 2x_h\mathbf{r} \cdot \mathbf{r}_h + 7xx_h^2) + \frac{5}{2}\mathbf{r}(7x_h^3 - 3x_hr_h^2) \\
 & \quad + \frac{15}{2}(-r_h^2\mathbf{r}_h \cdot \mathbf{r} + 7xr_h^2x_h + 7x_h^2\mathbf{r} \cdot \mathbf{r}_h - 21xx_h^3)\hat{\mathbf{x}}] \\
 & - 3\mu_3[(-2xx_{em} + yy_{em} + zz_{em})\hat{\mathbf{x}} + (yx_{em} + xy_{em})\hat{\mathbf{y}} \\
 & \quad + (zx_{em} + xz_{em})\hat{\mathbf{z}}]/(\gamma\bar{D})^4 \\
 & - \mu_3[-15x_{em}x_h\mathbf{r} + 3\mathbf{r}_h \cdot \mathbf{r}_{em}\mathbf{r} - 15x\mathbf{r}_{em}x_h \\
 & \quad + 3\mathbf{r} \cdot \mathbf{r}_h\mathbf{r}_{em} + 3(\mathbf{r} \cdot \mathbf{r}_{em})(-5x_h\hat{\mathbf{x}} + \mathbf{r}_h) + 105xx_{em}x_h\hat{\mathbf{x}} \\
 & \quad - 15xx_{em}\mathbf{r}_h - 15x\mathbf{r}_h \cdot \mathbf{r}_{em}\hat{\mathbf{x}} - 15x_{em}\mathbf{r} \cdot \mathbf{r}_h\hat{\mathbf{x}}]/(\gamma\bar{D})^5 \\
 & + \frac{1.0198 \times 10^{17}C_R A\sigma}{m\|(\gamma + 1)\bar{D}\hat{\mathbf{x}} + \mathbf{r}_h + \mathbf{r}\|^3} [(\gamma + 1)\bar{D}\hat{\mathbf{x}} + \mathbf{r}_h + \mathbf{r}] \\
 & - \frac{1.0198 \times 10^{17}C_R A\sigma}{m\|(\gamma + 1)\bar{D}\hat{\mathbf{x}} + \mathbf{r}_h\|^3} [(\gamma + 1)\bar{D}\hat{\mathbf{x}} + \mathbf{r}_h] \\
 & + \begin{bmatrix} c(\psi') & -s(\psi') & 0 \\ s(\psi') & c(\psi') & 0 \\ 0 & 0 & 1 \end{bmatrix} \begin{bmatrix} c(\theta) & 0 & s(\theta) \\ 0 & 1 & 0 \\ -s(\theta) & 0 & c(\theta) \end{bmatrix} \begin{bmatrix} 1 & 0 & 0 \\ 0 & c(\phi) & -s(\phi) \\ 0 & s(\phi) & c(\phi) \end{bmatrix} \frac{\mathbf{F}_{\text{thrust}}}{m},
 \end{aligned}$$

}

ER3B

}

lunar

}

SRP_t

}

SRP_h

}

thrust

where $\psi' = \psi + f$.

We present the following example to permit comparison of the relative contribution of the terms to the telescope motion. The initial conditions are the same as those presented earlier in Table 2.

As in Figure 6, Figure 7 presents the solution to four different force models selected from the relative motion summary equation above. Where hub position was required, it was obtained from separate integration of the full,

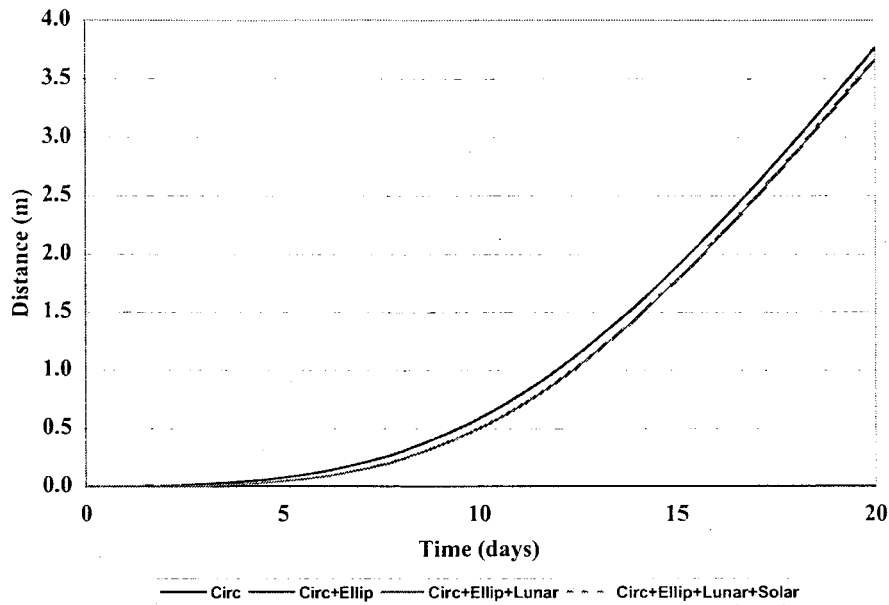


Figure 7: Effects of Perturbations on Relative Distance — Expanded Equations

unexpanded hub equations from Section 2.6, using the same force model as for the relative motion.

Once again, the reference solution is represented in the figure by the x -axis. This refers to the circular restricted model case. The other models depicted in Figure 6 represent the addition of ellipticity (ER3B), lunar, and solar radiation (SRP) effects over 20 days. Solar radiation is again treated as being applied to both the telescope and to either a real or phantom spacecraft at the hub, with the same physical characteristics as the telescope.

4 Modeling Uncertainties

4.1 Elliptical Restricted Three-Body Problem

Very Similar Values for Different Definitions. In computing the value of \bar{D} , the reference distance between the centers of the sun and earth, we need to determine the mean distance between Earth's center and the Earth–Moon barycenter.

The astronomical unit (AU) is defined in Seidelmann [4] as the radius of a circular orbit in which a body of negligible mass, and free of perturbations, would revolve around the sun in $2\pi/k$ days, where k is the Gaussian gravitational constant. This is slightly less than the semi-major axis of Earth's orbit. Begin with the distance of the AU:

$$\begin{aligned}\text{AU} &= 149,597,870.000 \text{ km [4, page 700, IAU System]} \\ &= 149,597,870.660 \text{ km [4, page 700, Best Estimate]}\end{aligned}$$

Yet compare these values with that from Dunham and Muhonen [5, page 200]:

$$\text{AU} = 149,597,870.691 \text{ km}$$

The mean distance from Earth to the sun also has different values:

$$\begin{aligned}1.0000010178 \text{ AU [4, page 700, IAU System]} \\ 1.00000105726665 \text{ AU [4, page 700, Best Estimate]}\end{aligned}$$

The calculation of the actual mean distance yields the following:

$$\begin{aligned}149,598,022.261 \text{ km, using the values from the IAU System} \\ 149,598,028.825 \text{ km, using the values from the Best Estimate}\end{aligned}$$

Again, compare these values with that from Dunham and Muhonen [5, page 200]:

$$\begin{aligned}\text{Earth+Moon semi-major axis} &= 1.000001018 \text{ AU} \\ &= 149,598,023.0 \text{ km}\end{aligned}$$

Dunham and Muhonen define their value as the mean distance of the Earth+Moon barycenter from the sun. Contrast this value to that of Seidelmann, who specifies this value as the mean distance of only Earth from the sun; however, the values are very close to one another.

We continue using these prominent resources for the eccentricity, e .

On page 700, Seidelmann gives the value of 0.016708617 for the mean eccentricity of Earth's orbit about the sun. On page 200, Dunham and Muhonen give the value of 0.01670862 as the Earth+Moon's eccentricity about the sun.

Sensitivity of \bar{D} . From the above, the derived constant \bar{D} depends on two constants with different values:

$$\begin{aligned}\bar{D} &= a(1 + e^2/2) \\ &= 149,618,904.49 \text{ km,} \quad \text{using IAU System for } a \text{ and Seidelmann for } e \\ &= 149,618,911.06 \text{ km,} \quad \text{using Best Estimate for } a \text{ and Seidelmann for } e \\ &= 149,618,905.22 \text{ km,} \quad \text{using Dunham and Muhonen for both } a \text{ and } e\end{aligned}$$

These different values were applied in separate simulations and do not substantially affect the analysis results.

4.2 Lunar Gravitational Effects

Description of the Lunar Motion Around Earth. The moon's motion around Earth is not specified by an analytical model. The motion is specified by the software and ephemerides files provided by the JPL. For the needs of this report, the JPL ephemerides provide the positions of Sun, Earth, and Moon to very high precision. The JPL ephemerides are given as blocks of Chebyshev coefficients, which, when interpolated, reproduce the original JPL numerical integrations to within 1.5 cm.

The instructions for using the JPLEPH.200 ephemeris files state that one calls the JPL model with the moon as the target and Earth+Moon barycenter as reference point. Yet a comment was found within the FORTRAN code that the lunar state is always geocentric.

5 Sensitivity Summary

It is recognized that the hub position knowledge is likely to be much less precise than that of the relative motion, perhaps on the order of 1 km. Therefore, it is useful to consider the effect of this imprecision upon the telescope's position relative to the hub.

Appendix A presents a detailed derivation of the variational equations used to address the sensitivity of telescope motion to errors in knowledge of the hub position.

The results of the analysis clearly show that the errors in telescope position relative to the hub, based on knowledge of hub position to 1.7 km are sufficiently small that they may be ignored.

Several sample tests of this behavior were conducted. For one test case, the initial conditions of Table 2 were used here as a nominal set of initial conditions for the hub and telescope.

The integration was then performed with the hub offset from its nominal initial state by 1 km in each directional component. This was to simulate an initial error in hub position. As seen in Figure 8, the telescope position relative to the hub differs from the nominal case by millimeters over 40 days.

The simulation was also repeated with the initial hub position offset from the nominal state by 17.3 km (10 km in each direction). Figure 9 demonstrates the roughly ten-fold increase in error over the previous example.

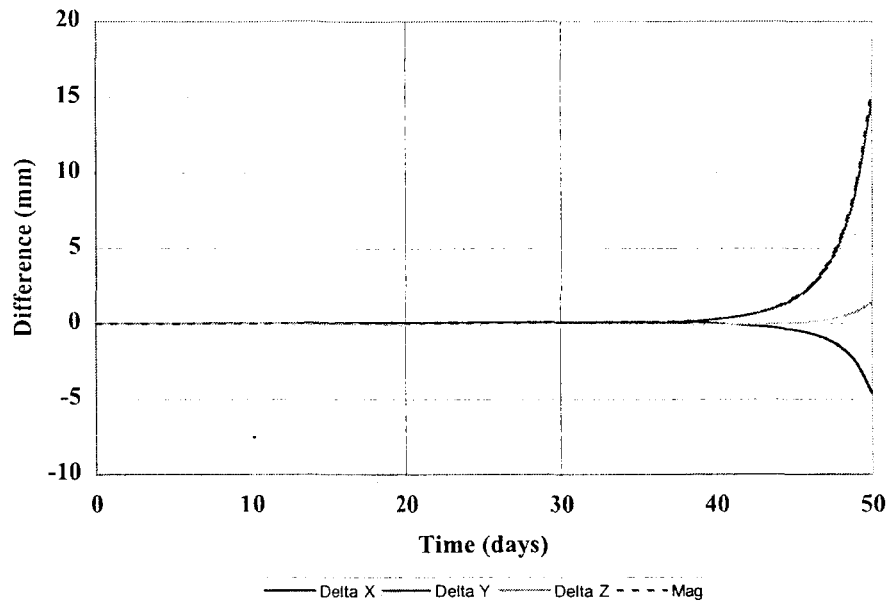


Figure 8: Relative Motion Error Caused by 1.7 km Initial Hub Position Error

6 Summary and Conclusion

This report details our further work describing the formation flying between spacecraft near the Sun-Earth L_2 libration point, beginning with the circular restricted three-body problem for the hub motion about L_2 .

Continuing from our previous works, these analyses develop the elliptical restricted three-body problem from previous work with circular problem. We built on our familiarity with the circular problem to address the following as perturbations upon the circular problem:

- elliptical orbit of Earth-Moon about Sun
- lunar gravitational effects
- solar radiation pressure effects
- thrusters on vehicle

These were incorporated as additive perturbations to the circular restricted three-body problem with expansions of varying levels of fidelity. We

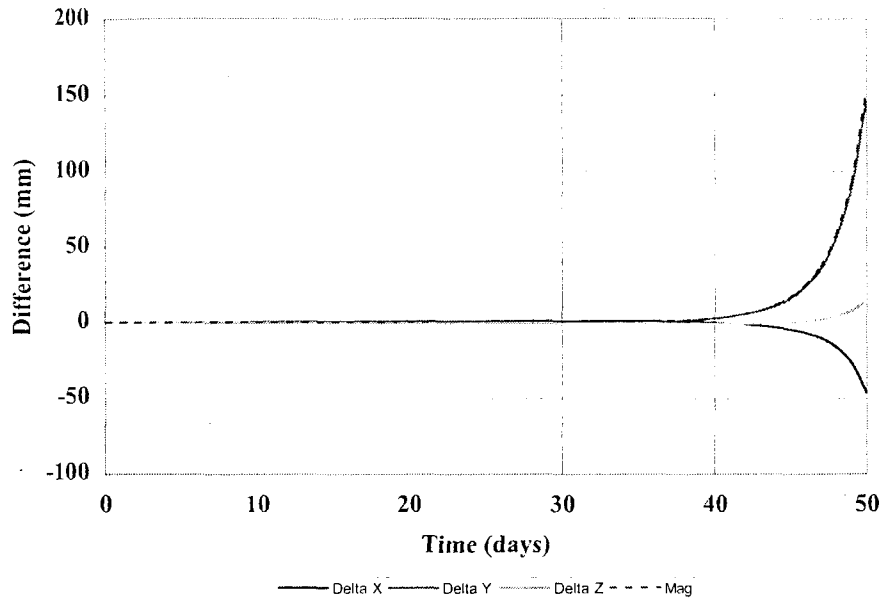


Figure 9: Relative Motion Error Caused by 17.3 km Initial Hub Position Error

develop two forms of models of the full derivation:

- full nonlinear baseline
- expanded form of full nonlinear baseline to appropriate order

Section 2 presented the derivation of the full nonlinear baseline with the perturbations. The equations were implemented through their coding in a MATLAB simulation. One example was presented using the discovery from Part 2 of valid initial conditions that excite only oscillatory motion in the linear modes. The results shown in Figure 6 demonstrate the dominant perturbation due to the elliptical motion of Earth about the sun. In this example, the perturbations due to lunar and solar radiation pressure are negligible. Overall, the figure indicates that during the typical 5-day science observation of this example, these perturbations contribute less than 1 m of relative position difference. The proposed electric propulsion should have little trouble maintaining position.

Section 3 presented the expanded circular and elliptical portions of the full model through terms which are linear in the coordinates of the telescope position relative to the hub and no more than cubic in the coordinates of the hub position relative to L_2 . The derivation describes the magnitude of the various terms and why some were truncated. Additionally, the lunar gravity model was expanded and some terms truncated due to very small perturbations upon the motion. As before, the perturbations due to the elliptical motion of the Earth about the Sun are dominant. Again, lunar and solar radiation pressure effects are negligible.

Modeling uncertainties were discussed in Section 4. One type of uncertainty is that the same listed number can be found to have different definitions between two popular references. Calculations, of course, give slightly different results; however, they do not substantially affect the results.

Section 5 explains the results of a longer derivation given in Appendix A. During the 18-months of part-time work on this report, our sponsor requested that we investigate the sensitivity of telescope motion to errors in hub position. The analysis and simulation show that errors in the knowledge of hub position of 1 km and 10 km (in each of the three position components) yield millimeters of error in telescope position.

Appendix B presents a back-of-the-envelope look at the relative motion between a hub and telescope at the Earth-Moon L_2 point. Our sponsor made a comment that future work may be redirected to this vicinity. Our work addressed the effects of the largest contributions to the elliptical restricted problem. The perturbation caused by solar gravitation was found to be negligible.

Appendix C presents a derivation of the luminosity reduction factor in the context of the solar radiation pressure model. The luminosity reduction factor accounts for shadowing effects due to a partial eclipse.

In conclusion, based on earlier literature searches, we believe this new work is unique because it describes the primary perturbations to the description of relative motion between nearby spacecraft. We verified that the effects of the elliptical motion of the Earth about the Sun is the dominant perturbation to the circular restricted three body problem. Contributions due to lunar gravity and solar radiation pressure are nearly negligible in the chosen examples.

Appendices

A Sensitivity of Telescope Motion to Errors in Hub Position

This appendix demonstrates the low sensitivity to errors in hub position, of the telescope motion relative to the hub. The effects of 1 km hub position errors upon the relative telescope motion are presented. The model used is the elliptical restricted model as presented in Section 3.2.

A.1 Derivation of Variational Equations

Consider the second-order differential equation of motion of a telescope relative to the hub, assumed to take the form of the earlier expanded and truncated form:

$$\begin{aligned}\ddot{\mathbf{r}} = & A_3 [-\mathbf{r} + 3x\dot{\mathbf{x}}] \\ & + A_4 [3x\mathbf{r}_h + 3x_h\mathbf{r} + (3\mathbf{r}_h \cdot \mathbf{r} - 15xx_h)\dot{\mathbf{x}}] \\ & + A_5 [(3\mathbf{r}_h \cdot \mathbf{r} - 15xx_h)\mathbf{r}_h + \frac{3}{2}(r_h^2 - 5x_h^2)\mathbf{r} \\ & \quad - \frac{15}{2}(2x_h\mathbf{r}_h \cdot \mathbf{r} - 7xx_h^2 + xr_h^2)\dot{\mathbf{x}}] \\ & + A_6 [\frac{15}{2}\mathbf{r}_h(-xr_h^2 - 2x_h\mathbf{r} \cdot \mathbf{r}_h + 7xx_h^2) + \frac{5}{2}\mathbf{r}(7x_h^3 - 3x_hr_h^2) \\ & \quad + \frac{15}{2}(-r_h^2\mathbf{r}_h \cdot \mathbf{r} + 7xr_h^2x_h + 7x_h^2\mathbf{r} \cdot \mathbf{r}_h - 21xx_h^3)\dot{\mathbf{x}}],\end{aligned}$$

where

$$\begin{aligned}\mathbf{r} &= [x \quad y \quad z]^T \\ \ddot{\mathbf{r}} &= \begin{bmatrix} \ddot{x} - 2n_c\dot{y} - n_c^2x \\ \ddot{y} + 2n_c\dot{x} - n_c^2y \\ \ddot{z} \end{bmatrix} + \begin{bmatrix} 2eyn_c^2 \sin \ell - 4e\dot{y}n_c \cos \ell - 4exn_c^2 \cos \ell \\ -2exn_c^2 \sin \ell + 4e\dot{x}n_c \cos \ell - 4eyn_c^2 \cos \ell \\ 0 \end{bmatrix}, \\ A_n &= \frac{\mu_1}{(1+\gamma)^n \bar{D}^n} + \frac{\mu_2}{\gamma^n \bar{D}^n},\end{aligned}$$

and

- \mathbf{r} = telescope position relative to the hub
- \mathbf{r}_h = hub position relative to L_2
- x, y, z = Cartesian components of \mathbf{r}
- μ_1 = solar Keplerian constant
- μ_2 = terrestrial Keplerian constant (Earth + Moon)
- \bar{D} = reference Sun-Earth distance
- x_e = distance from system barycenter to L_2
- D_1 = distance from system barycenter to Sun
- D_2 = distance from system barycenter to Earth-Moon barycenter
- $\gamma = (x_e - D_2)/D$
- n_c = circular restricted terrestrial mean motion
- ℓ = mean anomaly of Earth orbit.

The rotating coordinate system is defined to have x -axis along the Sun-Earth line of syzygy and z -axis normal to Earth's orbit about the sun.

The vector differential equation may be written in the form

$$\begin{bmatrix} \ddot{x} \\ \ddot{y} \\ \ddot{z} \end{bmatrix} = \mathbf{f} = \begin{bmatrix} f_x \\ f_y \\ f_z \end{bmatrix}.$$

The vector function \mathbf{f} represents the acceleration relative to the rotating frame. This function is linear in x, y, z , and their derivatives.

Say that there is a nominal solution \mathbf{r}_n associated with a nominal hub position \mathbf{r}_{hn} . It is desired to estimate the sensitivity of the relative telescope motion to errors in \mathbf{r}_h , which are on the order of 1 km.

Define the state vector \mathbf{x} as

$$\mathbf{x} = [x \ y \ z \ \dot{x} \ \dot{y} \ \dot{z}]^T.$$

The time derivative of this state is then

$$\dot{\mathbf{x}} = [\dot{x} \ \dot{y} \ \dot{z} \ f_x \ f_y \ f_z]^T.$$

Referring to this vector as the function $\mathbf{F}(\mathbf{x}, \mathbf{r}_h)$, the differential equation now takes the first-order form

$$\dot{\mathbf{x}} = \mathbf{F}, \tag{16}$$

where the nominal solution satisfies

$$\dot{\mathbf{x}}_n = \mathbf{F}_n. \quad (17)$$

The solution \mathbf{x} is now considered to be \mathbf{x}_n as perturbed by an error in \mathbf{r}_h . It is desired to examine the effect of this error upon \mathbf{x} . Writing \mathbf{x} as a linearized Maclaurin series in this error (or, equivalently, a Taylor series about the nominal hub trajectory) gives

$$\mathbf{x} = \mathbf{x}_n + \left. \frac{\partial \mathbf{x}}{\partial \mathbf{r}_h} \right|_n \cdot (\mathbf{r}_h - \mathbf{r}_{hn}), \quad (18)$$

where

$$\left. \frac{\partial \mathbf{x}}{\partial \mathbf{r}_h} \right|_n = \begin{bmatrix} \frac{\partial x}{\partial x_h} & \frac{\partial x}{\partial y_h} & \frac{\partial x}{\partial z_h} \\ \frac{\partial y}{\partial x_h} & \frac{\partial y}{\partial y_h} & \frac{\partial y}{\partial z_h} \\ \frac{\partial z}{\partial x_h} & \frac{\partial z}{\partial y_h} & \frac{\partial z}{\partial z_h} \\ \frac{\partial \dot{x}}{\partial x_h} & \frac{\partial \dot{x}}{\partial y_h} & \frac{\partial \dot{x}}{\partial z_h} \\ \frac{\partial \dot{y}}{\partial x_h} & \frac{\partial \dot{y}}{\partial y_h} & \frac{\partial \dot{y}}{\partial z_h} \\ \frac{\partial \dot{z}}{\partial x_h} & \frac{\partial \dot{z}}{\partial y_h} & \frac{\partial \dot{z}}{\partial z_h} \end{bmatrix}_n \triangleq U.$$

The subscript n refers to evaluation using the nominal trajectories; x_h , y_h , and z_h are the Cartesian components of the hub motion relative to L_2 .

It is the quantities of the elements of this matrix U that are of interest, in particular, the partial derivatives of the position components. Once these elements are determined, the effect of the hub position error upon the relative telescope motion may be approximated by

$$\begin{bmatrix} x - x_n \\ y - y_n \\ z - z_n \end{bmatrix} = \begin{bmatrix} \frac{\partial x}{\partial x_h} & \frac{\partial x}{\partial y_h} & \frac{\partial x}{\partial z_h} \\ \frac{\partial y}{\partial x_h} & \frac{\partial y}{\partial y_h} & \frac{\partial y}{\partial z_h} \\ \frac{\partial z}{\partial x_h} & \frac{\partial z}{\partial y_h} & \frac{\partial z}{\partial z_h} \end{bmatrix}_n \begin{bmatrix} x_h - x_{hn} \\ y_h - y_{hn} \\ z_h - z_{hn} \end{bmatrix}$$

Because the components of the hub position error are presumed to be no greater than 1 km, it is sufficient to examine the position partials within U ; they are treated as being scaled by unity to form the relative position variations.

A Maclaurin series may be formed as well for the derivative of the state, as

$$\dot{\mathbf{x}} = \dot{\mathbf{x}}_n + \left. \frac{\partial \dot{\mathbf{x}}}{\partial \mathbf{r}_h} \right|_n \cdot (\mathbf{r}_h - \mathbf{r}_{hn}).$$

This derivative may instead be formed by differentiation of Equation (18), giving

$$\dot{\mathbf{x}} = \dot{\mathbf{x}}_n + \frac{d}{dt} \left(\left. \frac{\partial \mathbf{x}}{\partial \mathbf{r}_h} \right|_n \right) \cdot (\mathbf{r}_h - \mathbf{r}_{hn}) + \left. \frac{\partial \mathbf{x}}{\partial \mathbf{r}_h} \right|_n \cdot \frac{d}{dt} (\mathbf{r}_h - \mathbf{r}_{hn}). \quad (19)$$

It is assumed that the change in hub position error is of higher order than the error itself. Therefore, these two equations indicate that

$$\left. \frac{\partial \dot{\mathbf{x}}}{\partial \mathbf{r}_h} \right|_n \approx \frac{d}{dt} \left(\left. \frac{\partial \mathbf{x}}{\partial \mathbf{r}_h} \right|_n \right). \quad (20)$$

The function \mathbf{F} may also be written as a linearized series, giving

$$\mathbf{F} = \mathbf{F}_n + \left. \frac{\partial \mathbf{F}}{\partial \mathbf{r}_h} \right|_n \cdot (\mathbf{r}_h - \mathbf{r}_{hn}) + \left. \frac{\partial \mathbf{F}}{\partial \mathbf{x}} \right|_n \cdot \left. \frac{\partial \mathbf{x}}{\partial \mathbf{r}_h} \right|_n \cdot (\mathbf{r}_h - \mathbf{r}_{hn}), \quad (21)$$

recognizing the dependence of \mathbf{F} upon \mathbf{r}_h both directly as well as indirectly through \mathbf{x} . Substituting Equations (19) and (21) into Equation (16), and taking into account the nominal solution of Equation (17) as well as the approximation of Equation (20),

$$\frac{d}{dt} \left(\left. \frac{\partial \mathbf{x}}{\partial \mathbf{r}_h} \right|_n \right) = \left. \frac{\partial \mathbf{F}}{\partial \mathbf{x}} \right|_n \cdot \left. \frac{\partial \mathbf{x}}{\partial \mathbf{r}_h} \right|_n + \left. \frac{\partial \mathbf{F}}{\partial \mathbf{r}_h} \right|_n$$

or

$$\dot{U} = \left. \frac{\partial \mathbf{F}}{\partial \mathbf{x}} \right|_n \cdot U + \left. \frac{\partial \mathbf{F}}{\partial \mathbf{r}_h} \right|_n \quad (22)$$

Recall that the vector function \mathbf{F} is linear in \mathbf{x} , with no additive constant. Therefore,

$$\mathbf{F} = \left. \frac{\partial \mathbf{F}}{\partial \mathbf{x}} \right|_n \cdot \mathbf{x}.$$

Substituting into Equation (17),

$$\dot{\mathbf{x}}_n = \left. \frac{\partial \mathbf{F}}{\partial \mathbf{x}} \right|_n \cdot \mathbf{x}_n.$$

Note the similarity of this equation to the homogeneous part of Equation (22). This indicates that any column of the homogeneous solution of Equation (22) takes the form of the general solution of Equation (17).

A.2 Linear Equations

It may be seen that, for the purpose of determining the gross effects of hub position error on the relative telescope motion, it is sufficient to consider only the first-order contributions to the differential equations. Say that the nominal solution for \mathbf{x} is known in the form of a Taylor series. Therefore, the homogeneous solution to Equation (22) is also known in the form of a Taylor series, given as

$$U_h = U_{h0} + \epsilon U_{h1} + \frac{\epsilon^2}{2} U_{h2} + \dots$$

Similarly, let the nominal system matrix also be written as a Taylor series:

$$\left. \frac{\partial \mathbf{F}}{\partial \mathbf{x}} \right|_n = \left. \frac{\partial \mathbf{F}}{\partial \mathbf{x}} \right|_{n0} + \epsilon \left. \frac{\partial \mathbf{F}}{\partial \mathbf{x}} \right|_{n1} + \frac{\epsilon^2}{2} \left. \frac{\partial \mathbf{F}}{\partial \mathbf{x}} \right|_{n2} + \dots$$

Because the dominant terms of \mathbf{F} are void of the components of \mathbf{r}_h , the nonhomogeneous part of Equation (22) is of higher order, with Taylor series

$$\left. \frac{\partial \mathbf{F}}{\partial \mathbf{r}_h} \right|_n = \epsilon \left. \frac{\partial \mathbf{F}}{\partial \mathbf{r}_h} \right|_{n1} + \frac{\epsilon^2}{2} \left. \frac{\partial \mathbf{F}}{\partial \mathbf{r}_h} \right|_{n2} + \dots$$

Now, consider the particular solution to Equation (22) as taking the form of a Taylor series as well. Because the nonhomogeneous part of the equation begins at order 1, so does the particular solution:

$$U_p = \epsilon U_{p1} + \frac{\epsilon^2}{2} U_{p2} + \dots$$

Substituting these series expansions into Equation (22) gives, at order zero,

$$\dot{U}_{h0} = \left. \frac{\partial \mathbf{F}}{\partial \mathbf{x}} \right|_{n0} \cdot U_{h0}. \quad (23)$$

As previously mentioned, this solution is assumed to be known from the knowledge of the nominal motion. At order one,

$$\dot{U}_{h1} = \left. \frac{\partial \mathbf{F}}{\partial \mathbf{x}} \right|_{n_0} \cdot U_{h1} + \left. \frac{\partial \mathbf{F}}{\partial \mathbf{x}} \right|_{n_1} \cdot U_{h0},$$

the solution to which is again assumed to be known, and

$$\dot{U}_{p1} = \left. \frac{\partial \mathbf{F}}{\partial \mathbf{x}} \right|_{n_0} \cdot U_{p1} + \left. \frac{\partial \mathbf{F}}{\partial \mathbf{r}_h} \right|_{n_1} \cdot \quad (24)$$

For Equation (24), only the particular solution is required. The system matrix here is the same as that of Equation (23); terms of the homogeneous solution to Equation (24) are already provided in the solution to Equation (23). It is assumed that the solutions are convergent for any given time; therefore, the gross contribution to the particular solution may be found from this equation alone. Accordingly, henceforth, the matrix U is assumed to refer to those terms through U_{h1} and U_{p1} .

For purposes of this analysis, the order 0 terms are considered to be those with the numerical coefficient A_3 ; order 1 terms are those with the coefficient A_4 . Other terms, including those involving the eccentricity e are treated as higher order. For that reason, the mean motion n of Earth's orbit may be approximated by n_c .

A.3 Solution Development

The solution for each vector of the linear system is constructed in the standard fashion. Let \mathbf{u} represent a column vector of U , and \mathbf{v} represent the corresponding column of the nonhomogeneous part of Equation (22), through the prescribed order. Then, the linear system takes the form

$$\dot{\mathbf{u}} = A\mathbf{u} + \mathbf{v},$$

where the matrix A refers to the matrix of partial derivatives seen in Equation (23). The homogeneous solution may be constructed using standard methods, as will be seen below; therefore, it is necessary to develop the particular solution to the system of differential equations given by Equation (24).

In these differential equations, the nonhomogeneous part contains trigonometric terms, which may be written as exponential terms with exponential

multipliers equal to the characteristic multipliers of the homogeneous system. Accordingly, the particular solution is developed for the case of a single such exponential term at a time; the solution for a number of such terms may be constructed by superposition of the individual solutions. It is assumed that the characteristic multipliers are distinct, as is the case for the hub-telescope system.

A.3.1 Non-secular Solution

First, examine the case where the nonhomogeneous vector \mathbf{v} contains periodic (or, equivalently, exponential) contributions with frequencies not equal to one of the eigenvectors of the system matrix A .

Consider a general first-order nonhomogeneous linear system of differential equations given by

$$\dot{\mathbf{x}} = A\mathbf{x} + e^{i\Omega t}\hat{\mathbf{e}}_j,$$

where $\hat{\mathbf{e}}_j$ is the j^{th} system unit vector, and $i\Omega$ is not one of the system eigenvalues. The particular solution of such a system may be found using the method of undetermined coefficients. Say that the particular solution is of the form

$$\mathbf{x}_p = \mathbf{b}e^{i\Omega t},$$

where the vector \mathbf{b} is a constant vector which is to be determined. Substituting \mathbf{x}_p into the differential equation,

$$i\Omega\mathbf{b}e^{i\Omega t} = A\mathbf{b}e^{i\Omega t} + e^{i\Omega t}\hat{\mathbf{e}}_j.$$

Equating coefficients of the exponential,

$$(i\Omega I - A)\mathbf{b} = \hat{\mathbf{e}}_j. \quad (25)$$

As $i\Omega$ is not an eigenvalue of A , the solution may be formed as

$$\mathbf{b} = (i\Omega I - A)^{-1}\hat{\mathbf{e}}_j.$$

For the problem of interest, the non-secular particular solution is a linear combination of particular solutions of this type, each scaled by the appropriate constant coefficient found in the differential equation. In the system

$$\dot{\mathbf{u}} = A\mathbf{u} + \mathbf{v},$$

say that the individual contributions to the particular solution are now written as

$$\mathbf{u}_{pi} = c_i \mathbf{b}_i e^{i\Omega_i t}.$$

where each c_i is the appropriate scaling constant. Then, the full particular solution is the sum of these solutions,

$$\mathbf{u}_p = \sum_i \mathbf{u}_{pi}.$$

Combining with the homogeneous solution, the complete solution for \mathbf{u} is

$$\mathbf{u} = \sum_i (e^{i\Omega_i t} - e^{At}) c_i \mathbf{b}_i.$$

Note that this solution satisfies the requirement of zero initial conditions for the variational equations.

A.3.2 Secular Solution

Next, examine the case where the nonhomogeneous vector \mathbf{v} contains periodic (or exponential) contributions with frequencies equal to one of the eigenvalues of A . In this case, a secular solution will result.

Consider a general first-order nonhomogeneous linear system of differential equations given by

$$\dot{\mathbf{x}} = A\mathbf{x} + e^{\lambda_i t} \hat{\mathbf{e}}_j,$$

where λ_i is the i^{th} eigenvalue of the matrix A .

The particular solution of such a system may again be found using the method of undetermined coefficients. Say that the particular solution is of the form

$$\mathbf{x}_p = (\mathbf{a}t + \mathbf{b})e^{\lambda_i t},$$

where the vectors \mathbf{a} and \mathbf{b} are constant vectors which are to be determined. Substituting \mathbf{x}_p into the differential equation,

$$(\mathbf{a} + \lambda_i \mathbf{a}t + \lambda_i \mathbf{b})e^{\lambda_i t} = A(\mathbf{a}t + \mathbf{b})e^{\lambda_i t} + e^{\lambda_i t} \hat{\mathbf{e}}_j.$$

Equating coefficients of t and unity,

$$(\lambda_i I - A)\mathbf{a} = \mathbf{0} \tag{26}$$

and

$$(\lambda_i I - A)\mathbf{b} = -\mathbf{a} + \hat{\mathbf{e}}_j. \quad (27)$$

Equation (26) may be solved to give

$$\mathbf{a} = \alpha \mathbf{x}_i,$$

where \mathbf{x}_i is the i^{th} eigenvector of A and α is yet to be determined. Substituting into Equation (27),

$$(\lambda_i I - A)\mathbf{b} = -\alpha \mathbf{x}_i + \hat{\mathbf{e}}_j. \quad (28)$$

Next, let \mathbf{y}_i denote the i^{th} left eigenvector of A , satisfying

$$\mathbf{y}_i^T (\lambda_i I - A) = \mathbf{0}^T.$$

The elements of \mathbf{y}_i describe the linear dependence of the rows of $\lambda_i I - A$. Therefore, a summation of the weighted rows of Equation (28) allows the elimination of \mathbf{b} . This is performed by writing

$$\begin{aligned} \mathbf{0}^T &= \mathbf{y}_i^T (\lambda_i I - A)\mathbf{b} = -\mathbf{y}_i^T \alpha \mathbf{x}_i + \mathbf{y}_i^T \hat{\mathbf{e}}_j \\ &= -\mathbf{y}_i^T \alpha \mathbf{x}_i + y_{ij}, \end{aligned}$$

where y_{ij} is the j^{th} element of \mathbf{y}_i . Solving for α ,

$$\alpha = \frac{y_{ij}}{\mathbf{y}_i^T \mathbf{x}_i}. \quad (29)$$

Let the columns of $\lambda_i I - A$ be given by the column vectors \mathbf{c}_i . Therefore, an n -dimensional Equation (28) may be represented as

$$\begin{bmatrix} \mathbf{c}_1 & \mathbf{c}_2 & \cdots & \mathbf{c}_n \end{bmatrix} \mathbf{b} = -\alpha \mathbf{x}_i + \hat{\mathbf{e}}_j.$$

Now, examine all but the j^{th} row of this equation:

$$\begin{aligned} \begin{bmatrix} \underline{\mathbf{c}}_1 & \underline{\mathbf{c}}_2 & \cdots & \underline{\mathbf{c}}_n \end{bmatrix} \mathbf{b} &\triangleq M\mathbf{b} \\ &= -\alpha \underline{\mathbf{x}}_i, \end{aligned}$$

where an underbar denotes the removal of row j .

The eigenvalue λ_i is assumed to be distinct. Therefore, it is possible to arbitrarily set the j^{th} element of \mathbf{b} , b_j , to unity, and solve for the remainder

of the vector. By setting b_j to unity, the contributions associated with the j^{th} column of $\lambda_i I - A$ may be separated from the remainder of the equation as

$$\overline{M}\underline{\mathbf{b}} = -\alpha\underline{\mathbf{x}}_i - \underline{\mathbf{c}}_j,$$

where an overbar denotes the removal of column j . Because the eigenvalue is distinct, there is no zero eigenvalue, and a single row and column have been removed from $\lambda_i I - A$, the remaining matrix, \overline{M} , is nonsingular. Therefore, solving for $\underline{\mathbf{b}}$,

$$\underline{\mathbf{b}} = -\overline{M}^{-1} (\alpha\underline{\mathbf{x}}_i + \underline{\mathbf{c}}_j). \quad (30)$$

The vector \mathbf{b} is then formed by augmenting $\underline{\mathbf{b}}$ with the inclusion of unity as the j^{th} element.

To illustrate this procedure, consider the following example:

$$\dot{\mathbf{x}} = \begin{bmatrix} 2 & -1 \\ 3 & -2 \end{bmatrix} \mathbf{x} + \begin{bmatrix} e^t \\ 0 \end{bmatrix}.$$

Here, the exponential multiplier associated with the nonhomogeneous part of the equation is 1, which is also an eigenvalue of the system matrix. The corresponding eigenvector is

$$\mathbf{x}_1 = \begin{bmatrix} 1 \\ 1 \end{bmatrix}$$

and the associated left eigenvector is

$$\mathbf{y}_1 = [3 \quad -1]^T.$$

Equation (29) gives α as

$$\alpha = \frac{3}{(3)(1) + (-1)(1)} = \frac{3}{2};$$

Equation (30) gives the single element vector $\underline{\mathbf{b}}$ as

$$\underline{\mathbf{b}} = -(1/3) \left[\frac{3}{2}(1) + (-3) \right] = \frac{1}{2}.$$

Therefore, the particular solution is

$$\mathbf{x}_p = \left(\frac{3}{2} \begin{bmatrix} 1 \\ 1 \end{bmatrix} t + \begin{bmatrix} 1 \\ 1/2 \end{bmatrix} \right) e^t.$$

For the problem of interest, the particular solution is a linear combination of particular solutions of this type, each scaled by the appropriate constant coefficient found in the differential equation. In the system

$$\dot{\mathbf{u}} = \mathbf{A}\mathbf{u} + \mathbf{v},$$

say that the individual contributions to the particular solution are now written as

$$\mathbf{u}_{pi} = c_i (\alpha_i t \mathbf{x}_i + \mathbf{b}_i) e^{\lambda_i t},$$

where c_i is the appropriate scaling constant. Then, the full particular solution is the sum of these solutions,

$$\mathbf{u}_p = \sum_i \mathbf{u}_{pi}.$$

Combining with the homogeneous solution, the complete solution for \mathbf{u} is

$$\mathbf{u} = -e^{\mathbf{A}t} \sum_i c_i \mathbf{b}_i + \mathbf{u}_p.$$

Note that this solution satisfies the requirement of zero initial conditions for the variational equations.

A.3.3 State Transition Matrix

In both the secular and non-secular cases, the exponential state transition matrix is constructed in the usual fashion. Letting P denote the matrix of eigenvectors of the matrix A , and Λ the diagonal matrix of eigenvalues, the exponential matrix is given by

$$e^{\mathbf{A}t} = P \Lambda P^{-1}.$$

A.4 Out-of-Plane Solution

This approach is now applied to the z and \dot{z} -components of Equation (22), which are not coupled with the in-plane components. These out-of-plane components are

$$\dot{U}_z = \begin{bmatrix} 0 & 1 \\ -A_3 & 0 \end{bmatrix} U_z + 3A_4 \begin{bmatrix} 0 & 0 & 0 \\ z & 0 & x \end{bmatrix}, \quad (31)$$

where

$$U_z = \begin{bmatrix} \frac{\partial z}{\partial x_h} & \frac{\partial z}{\partial y_h} & \frac{\partial z}{\partial z_h} \\ \frac{\partial \dot{z}}{\partial x_h} & \frac{\partial \dot{z}}{\partial y_h} & \frac{\partial \dot{z}}{\partial z_h} \end{bmatrix}_n$$

For a single vector \mathbf{u} of U_z ,

$$\dot{\mathbf{u}} = \begin{bmatrix} 0 & 1 \\ -A_3 & 0 \end{bmatrix} \mathbf{u} + \mathbf{v}, \quad (32)$$

where \mathbf{v} is the appropriate nonhomogeneous column of Equation (31).

For each non-zero column \mathbf{v} , the periodic forcing function is of frequency which is the same or approximately the same as the natural frequency of the system. (If higher-order frequency compensation is employed, the low-order frequencies of the two non-zero columns will, in fact, be identical.) Therefore, the secular response associated with each non-zero forcing column is examined. Additionally, the non-secular response is examined for the case where the third-column forcing function possesses the nearly resonant frequency of the linear solution.

A.4.1 Secular

First consider the secular case, where \mathbf{v} is of the form

$$\mathbf{v} = \begin{bmatrix} 0 \\ \mathcal{A} \sin(\sqrt{A_3}t + \psi) \end{bmatrix}.$$

This corresponds to the first nonhomogeneous column of Equation (31). (If the third column is treated as secular, it differs only by a 90° shift in phase.) Using exponential representation,

$$\mathbf{v} = \mathcal{A}_1 \begin{bmatrix} 0 \\ e^{i\sqrt{A_3}t} \end{bmatrix} + \mathcal{A}_2 \begin{bmatrix} 0 \\ e^{-i\sqrt{A_3}t} \end{bmatrix},$$

where

$$\mathcal{A}_1 = \frac{\mathcal{A}}{2}(\sin \psi - i \cos \psi)$$

and

$$\mathcal{A}_2 = \frac{\mathcal{A}}{2}(\sin \psi + i \cos \psi).$$

The particular solution may now be determined using the method of Section A.3.2, treating each of the two exponential vectors of \mathbf{v} individually.

Using the earlier notation, let $\lambda_1 = i\sqrt{A_3}$ and $\lambda_2 = -i\sqrt{A_3}$. The eigenvectors are

$$\mathbf{x}_1 = \begin{bmatrix} 1 \\ i\sqrt{A_3} \end{bmatrix} \quad \text{and} \quad \mathbf{x}_2 = \begin{bmatrix} 1 \\ -i\sqrt{A_3} \end{bmatrix};$$

the left eigenvectors are

$$\mathbf{y}_1 = [i\sqrt{A_3} \ 1]^T \quad \text{and} \quad \mathbf{y}_2 = [-i\sqrt{A_3} \ 1]^T.$$

For the nonhomogeneous contribution given by $e^{i\sqrt{A_3}t}\hat{\mathbf{e}}_2$, the method of undetermined coefficients gives

$$\alpha = \frac{1}{i2\sqrt{A_3}},$$

$$\bar{M} = i\sqrt{A_3},$$

and

$$\mathbf{b} = \begin{bmatrix} \frac{1}{2A_3} - \frac{i}{\sqrt{A_3}} \\ 1 \end{bmatrix}.$$

Therefore, this part of the particular solution is

$$\mathbf{u}_{p1} = \mathcal{A}_1 \left(\frac{1}{2} \begin{bmatrix} -\frac{i}{\sqrt{A_3}} \\ 1 \end{bmatrix} t + \begin{bmatrix} \frac{1}{2A_3} - \frac{i}{\sqrt{A_3}} \\ 1 \end{bmatrix} \right) e^{i\sqrt{A_3}t}.$$

In similar fashion, the part of the particular solution corresponding to $e^{-i\sqrt{A_3}t}\hat{\mathbf{e}}_2$, is formed. Combining gives the full particular solution as

$$\begin{aligned} \mathbf{u}_p = & \mathcal{A}_1 \left(\frac{1}{2} \begin{bmatrix} -\frac{i}{\sqrt{A_3}} \\ 1 \end{bmatrix} t + \begin{bmatrix} \frac{1}{2A_3} - \frac{i}{\sqrt{A_3}} \\ 1 \end{bmatrix} \right) e^{i\sqrt{A_3}t} \\ & + \mathcal{A}_2 \left(\frac{1}{2} \begin{bmatrix} \frac{i}{\sqrt{A_3}} \\ 1 \end{bmatrix} t + \begin{bmatrix} \frac{1}{2A_3} + \frac{i}{\sqrt{A_3}} \\ 1 \end{bmatrix} \right) e^{-i\sqrt{A_3}t}. \end{aligned}$$

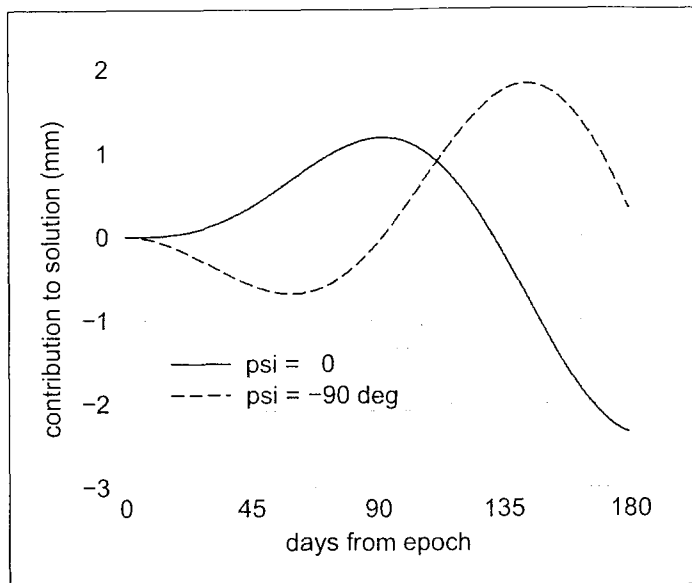


Figure 10: $\frac{\partial z}{\partial x_h}$ and $\frac{\partial z}{\partial z_h}$ with resonance

Referring to Section A.3.2, the behavior of the position partial derivative over 180 days is presented in Figure 10, for a pair of fundamental values of the phase angle. As previously mentioned, the hub position error components are taken to be 1 km; therefore, in this and all other figures, the contributions to the telescope motion variation is the same as the position partial derivatives themselves.

A.4.2 Non-Secular

Next, consider the response associated with Equation (32), where the vector \mathbf{v} is a nearly-resonant vector of the form

$$A \cos(\omega t + \phi) \hat{\mathbf{e}}_2.$$

From the earlier analysis, the phase angle ϕ is taken as $\psi + 90^\circ$. The frequency ω is taken as the natural linear frequency of the in-plane motion. As shown in the earlier analysis, this frequency is given by

$$\omega = \sqrt{n^2 - A_3/2 + \sqrt{(n^2 - A_3/2)^2 - (n^2 + 2A_3)(n^2 - A_3)}}.$$

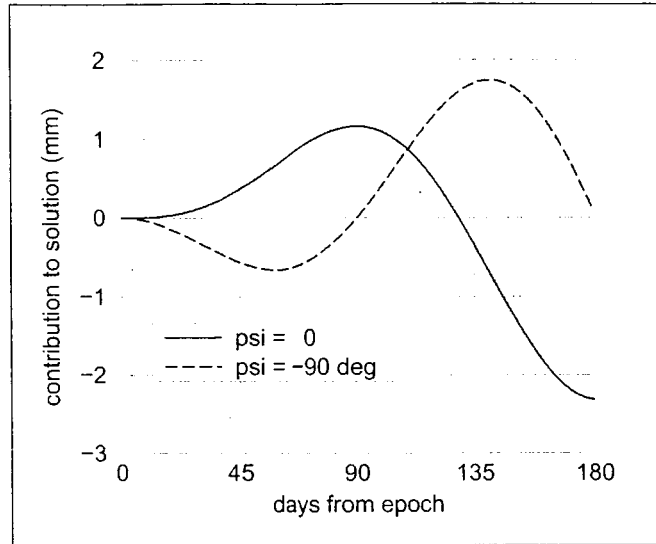


Figure 11: $\frac{\partial z}{\partial z_h}$ without resonance

For comparison, ω is approximately 0.035385 rad/day, while $\sqrt{A_3}$ is approximately 0.034148 rad/day.

Following the method of Section A.3.1, the vector \mathbf{b} is constructed as

$$(\omega I - A)^{-1} \hat{\mathbf{e}}_2.$$

The resulting position partials in the solution vector \mathbf{u} are presented in Figure 11.

A.5 In-Plane Particular Solution

The in-plane (x and y) components of Equation (22) are now treated. These differential equations are of the form

$$\dot{U}_{xy} = \begin{bmatrix} 0 & 0 & 1 & 0 \\ 0 & 0 & 0 & 1 \\ n^2 + 2A_3 & 0 & 0 & 2n \\ 0 & n^2 - A_3 & -2n & 0 \end{bmatrix} U_{xy} + 3A_4 \begin{bmatrix} 0 & 0 & 0 \\ 0 & 0 & 0 \\ -2x & y & z \\ y & x & 0 \end{bmatrix}, \quad (33)$$

where

$$U_{xy} = \begin{bmatrix} \frac{\partial x}{\partial x_h} & \frac{\partial x}{\partial y_h} & \frac{\partial x}{\partial z_h} \\ \frac{\partial y}{\partial x_h} & \frac{\partial y}{\partial y_h} & \frac{\partial y}{\partial z_h} \\ \frac{\partial \dot{x}}{\partial x_h} & \frac{\partial \dot{x}}{\partial y_h} & \frac{\partial \dot{x}}{\partial z_h} \\ \frac{\partial \dot{y}}{\partial x_h} & \frac{\partial \dot{y}}{\partial y_h} & \frac{\partial \dot{y}}{\partial z_h} \end{bmatrix}_n$$

For a single vector \mathbf{u} of U_{xy} ,

$$\dot{\mathbf{u}} = \begin{bmatrix} 0 & 0 & 1 & 0 \\ 0 & 0 & 0 & 1 \\ n^2 + 2A_3 & 0 & 0 & 2n \\ 0 & n^2 - A_3 & -2n & 0 \end{bmatrix} \mathbf{u} + \mathbf{v}, \quad (34)$$

where \mathbf{v} is the appropriate column of the above matrix.

From the earlier analysis of the linearized circular restricted three-body problem, the system matrix of Equation (34) has one eigenvalue corresponding to a convergent solution, one corresponding to a divergent solution, and a complex conjugate pair which corresponds to a periodic solution. In that analysis, it was specified that the initial conditions would be selected in such a manner as to excite only the periodic modes. Therefore, as in the previous section, it is assumed here that x and y in Equation (34) exhibit that behavior; z has already been seen to be periodic.

A.5.1 Secular

First, examine the secular solutions associated with resonant forcing vectors \mathbf{v} .

Again using the notation of Section A.3.2, consider the eigenvalues given by $\lambda_1 = i\omega$ and $\lambda_2 = -i\omega$. The corresponding eigenvectors are

$$\mathbf{x}_1 = \begin{bmatrix} i2n\omega \\ -\chi \\ -2n\omega^2 \\ -i\omega\chi \end{bmatrix} \quad \text{and} \quad \mathbf{x}_2 = \begin{bmatrix} -i2n\omega \\ -\chi \\ -2n\omega^2 \\ i\omega\chi \end{bmatrix},$$

where

$$\chi = \omega^2 + n^2 + 2A_3;$$

the left eigenvectors are

$$\mathbf{y}_1 = \begin{bmatrix} i2n\omega(n^2 + 2A_3) \\ (n^2 - A_3)\chi \\ -2n\omega^2 \\ i\omega\chi \end{bmatrix}$$

and

$$\mathbf{y}_2 = \begin{bmatrix} -i2n\omega(n^2 + 2A_3) \\ (n^2 - A_3)\chi \\ -2n\omega^2 \\ -i\omega\chi \end{bmatrix}$$

Consider the contribution associated with the second column of Equation (33) as the vector \mathbf{v} of Equation (34). The order 1 solutions for x and y are of the form

$$3A_4x = -\mathcal{A} \cos(\omega t + \phi) \quad \text{and} \quad 3A_4y = k\mathcal{A} \sin(\omega t + \phi),$$

where

$$k = \frac{\chi}{2\omega n}.$$

These functions may then again be written as combinations of complex exponentials.

For the nonhomogeneous contribution to \mathbf{v} of $e^{i\omega t} \hat{\mathbf{e}}_3$, the scalar α is given by

$$\alpha = -\frac{2n\omega^2}{d},$$

where

$$d = \omega^6 + 5(n^2 + A_3)\omega^4 - (5n^2 - 4A_3)(n^2 + 2A_3)\omega^2 - (n^2 - A_3)(n^2 + 2A_3)^2.$$

The associated vector \mathbf{b} is

$$\mathbf{b} = \begin{bmatrix} 4n^2\omega^2/d - i/\omega \\ 2n/\zeta + i4n\chi\omega^3/(d\zeta) \\ 1 \\ -2n\omega^2\chi(\omega^2 - n^2 + A_3)/(d\zeta) + i2n\omega/\zeta \end{bmatrix},$$

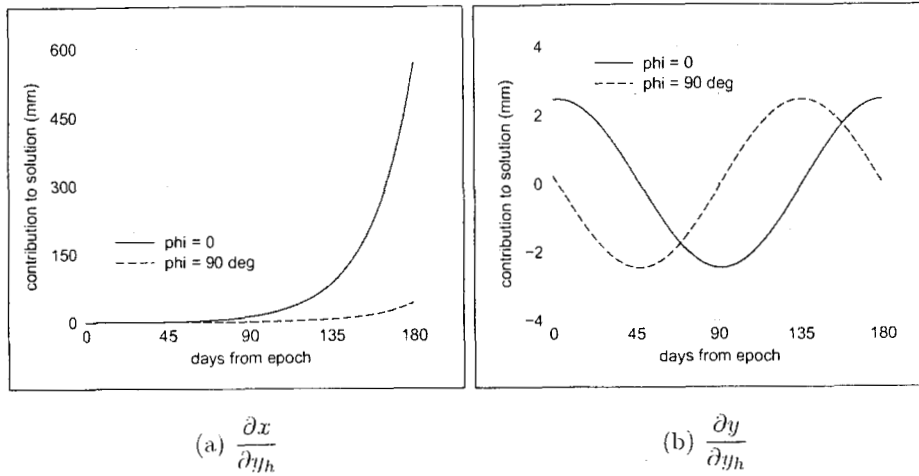


Figure 12: $\frac{\partial x}{\partial y_h}$ and $\frac{\partial y}{\partial y_h}$ with resonance

where

$$\zeta = \omega^2 + n^2 - A_3.$$

For the contribution of $e^{-i\omega t} \hat{e}_3$, the scalar α is the same, and the associated vector \mathbf{b} is the complex conjugate.

For the contribution of $e^{i\omega t} \hat{e}_4$,

$$\alpha = i \frac{\omega \chi}{d}$$

and

$$\mathbf{b} = \begin{bmatrix} -2n/\chi - i4n\omega^3/d \\ \chi^2/d - i/\omega \\ 2n\omega^2(\omega^2 - n^2 - 2A_3)/d - i2n\omega/\chi \\ 1 \end{bmatrix}$$

For the contribution of $e^{i\omega t} \hat{e}_4$, the resulting α and \mathbf{b} are the complex conjugates of these.

Combining into the solution vector \mathbf{u} , the resulting position partial derivatives, in the second column of matrix U_{xy} , are presented in Figures 12(a) (x -component) and 12(b) (y -component).

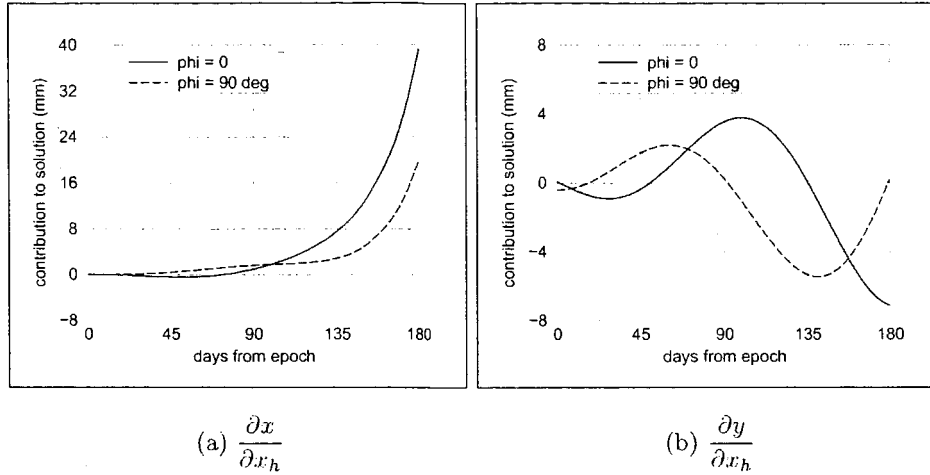


Figure 13: $\frac{\partial x}{\partial x_h}$ and $\frac{\partial y}{\partial x_h}$ with resonance

Next, the same procedure is followed for the first column. The solution is constructed using the same α scalars and \mathbf{b} vectors as above. The resulting position partial derivatives are presented in Figures 13(a) (x -component) and 13(b) (y -component).

Finally, the procedure is followed for the third column. If the low-order solution for z is taken as being resonant with the system matrix, the solution associated with the forcing function $3A_4z\hat{\mathbf{e}}_3$ may be constructed using the same α and \mathbf{b} expressions as above. The resulting position partial derivatives are presented in Figures 14(a) (x -component) and 14(b) (y -component).

A.5.2 Non-Secular

Finally, the case is treated where the uncompensated low-order solution for z is considered to be non-resonant with the in-plane system. The third-column forcing vector is taken to be of the form

$$A \sin(\sqrt{A_3}t + \phi)\hat{\mathbf{e}}_3.$$

Again following the method of Section A.3.1, the vector \mathbf{b} is constructed as

$$(\omega I - A)^{-1}\hat{\mathbf{e}}_3.$$

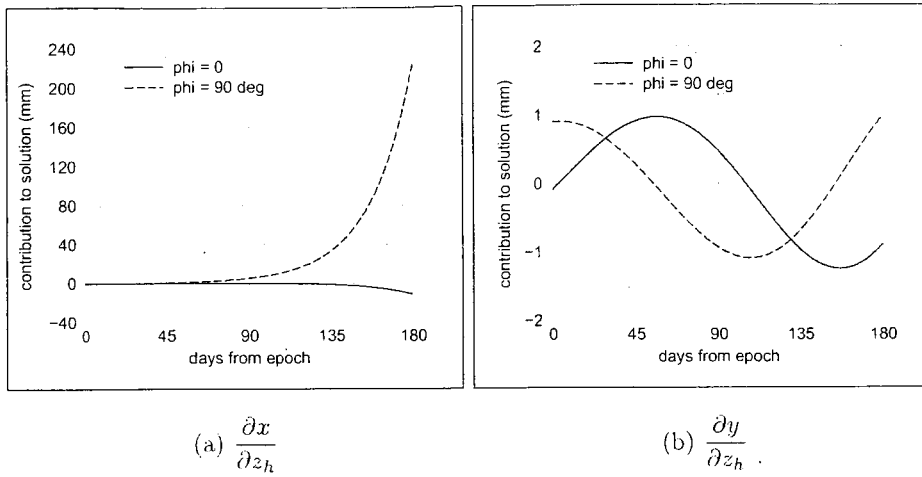


Figure 14: $\frac{\partial x}{\partial z_h}$ and $\frac{\partial y}{\partial z_h}$ with resonance

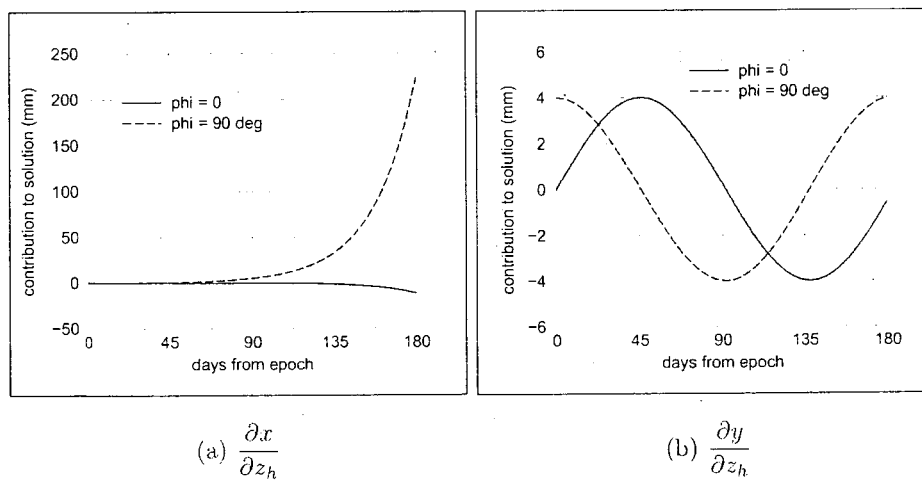


Figure 15: $\frac{\partial x}{\partial z_h}$ and $\frac{\partial y}{\partial z_h}$ without resonance

The resulting solution vector \mathbf{u} is presented in Figures 15(a) (x -component) and 15(b) (y -component).

A.6 Summary

From the plots of this appendix, it is recognized that all of the small-magnitude contributions to the solution of the variational equations are in the millimeter range. Over 180 days, the large-magnitude contributions reach hundreds of millimeters. However, even these contributions remain extremely small over the first 90 days from epoch. Therefore, it is concluded that the errors which are induced by 1 km errors in hub position are sufficiently small that they may be ignored.

B Relative Motion Near Earth-Moon L_2 Libration Point

At the sponsor's request, a rudimentary analysis was performed into the approach which would be taken in an investigation of relative motion near the Earth-Moon L_2 point. In this system, Earth and Moon are the primary bodies; here, the fundamental periods in and out of the xy -plane are approximately 14.650 days and 15.275 days, respectively.

Consider the case of a hub orbiting the L_2 point at roughly a distance of 30,000 km, with a telescope located 100 m from the hub. The effects of various terms of the elliptical restricted expansion over 15 days are given in Table 5.

Table 5: Along-Ellipsoid Effect of Earth-Moon Perturbation on Solution (15 days)

perturbing term	effect (m)
re	21.5
rr_h	114.1
$rr_h e$	8.4
rr_h^2	64.4
rr_h^3	31.5
rr_h^4	14.9

The effects are shown for terms which contribute to as low as approximately 10 m over the 15 days. It is noted that the largest contributions from perturbations by Sun during this time period are on the order of less than 1 m. Perturbing forces from solar radiation pressure and spacecraft thruster firing are on the same order as for the Sun-Earth system.

C Calculation of Luminosity Reduction Due to Partial Eclipse

The calculation of the luminosity reduction factor, σ , is shown here. This symbol is a variable within Equation (8), which is used to compute the force per unit mass due to solar radiation pressure.

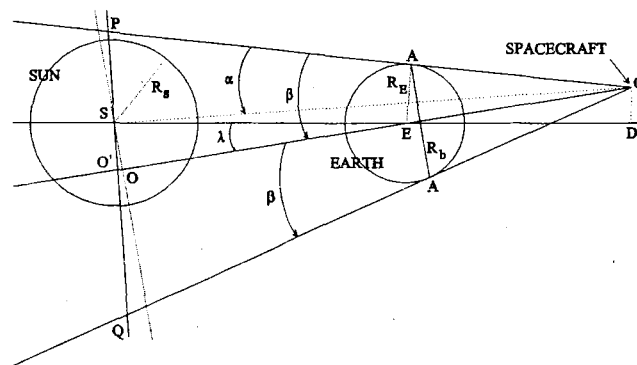


Figure 16: Solar Radiation Shadowing Geometry

Figure 16 shows the shadowing geometry. In the figure, line CS is normal to line PQ; line CD is normal to the Sun-Earth line, SE; line SO is normal to line CO. The distance R_b is the Earth's effective obscuration radius. Distances R_E and R_S are the mean radii of Earth and Sun, respectively. Solar shadowing is based on projecting $2R_b$ onto line PQ.

The calculation of σ is a matter of the geometry of two intersecting circles. Figure 17 shows the additional geometry and the notation used in the calculation. The projection of the obscuration disk on the plane normal to the spacecraft-Sun line (CS) is an ellipse of negligible eccentricity. This ellipse is very closely approximated as a circle. The comment lines in the accompanying FORTRAN code describes the notations used in Figures 16 and 17. The routine calculates the solar radiation force per unit mass at any distance greater than the Sun-Earth distance. The code also calculates the diminished radiation force for all spacecraft trajectories that pass through any portion of the Earth's shadow. It is assumed that the radiation force falls off linearly in proportion to the percentage of solar area lost to obscuration.

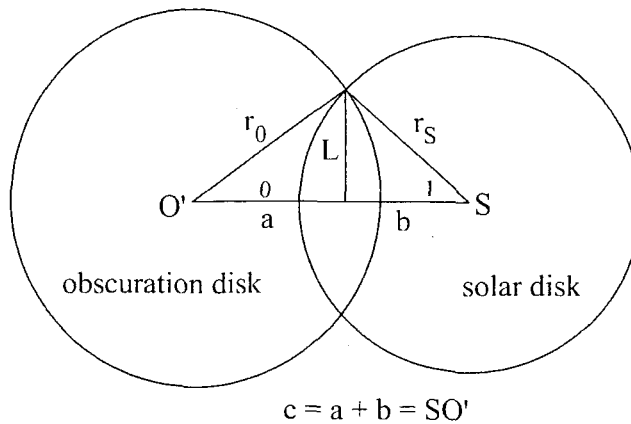


Figure 17: Earth Obscuration and Solar Disk Geometry

```

PROGRAM SOLRAD
C
  IMPLICIT REAL*8(A-H,O-Z)
  REAL*8 LRF,MASS
  COMMON/INPUTS/CR,AREA,MASS
C
C   EXAMPLE DRIVER FOR SOLAR RADIATION FORCE
C
  CR=1.5D0
  AREA=10.D0
  MASS=2000.D0
  SE=149597870.D0
C   SEE FIG 16:
  WRITE(*,*) ' INPUT CE AND CD = '
  READ(*,*) CE,CD
C
  CALL LRFACTOR(SE,CE,CD,LRF)
  WRITE(*,*) ' LRF = ',LRF
C
  CS=DSQRT(SE**2+CE**2)
  CALL RFORCE(LRF,CS,F)
  WRITE(*,101) F
101 FORMAT(' SOLAR RADIATION FORCE/MASS (M/S^2) = ',1PD11.4)

```

```

STOP
END
C
SUBROUTINE LRFACTOR(SE,CE,CD, LRF)
IMPLICIT REAL*8(A-H,O-Z)
REAL*8 LRF,L
DATA RS/696000.DO/
DATA RE/6378.14D0/
DATA PI/3.141592653589793D0/
C
C   LRF = LUMINOSITY REDUCTION FACTOR (OUTPUT)
C
C FIG 16 CALCULATIONS:
C
C   RS = SOLAR RADIUS (KM)
C   RE = EARTH RADIUS (KM)
C
C   SE = SUN EARTH DISTANCE (KM) (INPUT)
C   CE = SATELLITE TO EARTH DISTANCE (KM) (INPUT)
C       CE IS A PORTION OF CO.
C   CD = NORMAL DISTANCE OF SATELLITE TO SUN-EARTH
C       LINE (KM) (INPUT) (GE ZERO)
C
C   CS = SATELLITE TO SUN DISTANCE (KM)
C   CO = SATELLITE TO SUN (THRU E) OFFSET DISTANCE (KM)
C   OS = PERPENDICULAR DISTANCE OF SUN FROM CO (KM)
C       CO + OS + CS FORMS A RIGHT TRIANGLE WITH
C       HYPOTENUSE CS.
C   PS = NORTHERN LIMIT OF SOLAR OSBSCURATION ALONG LINE PQ
C       NORMAL TO CS. PS MEASURED FROM SOLAR CENTER S.
C
C FIG 17 CALCULATIONS:
C
C   RO = RADIUS OF OSBSCURATION DISK (KM)
C   C = SEPARATION BETWEEN GEOMETRIC CENTER OF SOLAR DISK
C       AND GEOMETRIC CENTER OF OSBSCURATION DISK (KM)
C       = SMALLA + SMALLB
C       = SO'

```

```

C      L = DISTANCE FROM LINE SEGMENT C TO EITHER POINT OF
C      INTERSECTION OF THE 2 DISK PERIMETERS (KM)
C      L**2 = R0**2 - SMALLA**2 = R1**2 - SMALLB**2 (RIGHT
C      TRIANGLES)
C      THETA0 = DATAN(L/SMALLA)
C      THETA1 = DATAN(L/SMALLB)
C      S0 = SECTOR AREA SUBTENDED BY 2*THETA0 (KM**2)
C      S1 = SECTOR AREA SUBTENDED BY 2*THETA1 (KM**2)
C      ASHADOW = AREA OF INTERSECTION OF OBSCURATION DISK AND
C      SOLAR DISK (KM**2)
C      SUNAREA = AREA OF SOLAR DISK (KM**2)
C
C      SEE FIG 16 FOR THE FOLLOWING:
C
C      ED=DSQRT(CE**2-CD**2)
C      COSINE(LAMBDA)
C      COSL=ED/CE
C      CO=SE*COSL+CE
C      SINE(LAMBDA)
C      SINL=CD/CE
C      OS=SE*SINL
C      CA=DSQRT(CE**2-RE**2)
C      CS=DSQRT((SE+ED)**2+CD**2)
C      OBSCURATION OCCURS WHEN DABS(PS).LE.RS
C      PS=CS*(RE*CO-OS*CA)/(CA*CO+OS*RE)
C      IF(PS.LT.-RS) THEN
C          NO ECLIPSE
C          LRF=1.000
C          RETURN
C          ENDIF
C      IF(PS.GT.RS) THEN
C          TOTAL ECLIPSE
C          LRF=0.000
C          RETURN
C          ENDIF
C
C      PARTIAL ECLIPSE (DABS(PS).LE.RS)
C

```

```

C      COSINE(BETA - ALPHA)
COSBA=CO/CS
C      "NORTHERN" RADIUS OF OBSCURATION MEASURED FROM O'
C      "NORTH" TO P ALONG LINE PQ:
SOP=OS/COSBA
RADIUSN=PS+SOP
RO=RADIUSN

C
C      SEE FIG 17 FOR THE FOLLOWING:
C
C      C=SOP
SMALLB=(RS**2-RO**2+C**2)/(2.DO*C)
SMALLA=C-SMALLB
L=DSQRT(RS**2-SMALLB**2)
THETA0=DATAN(L/SMALLA)
THETA1=DATAN(L/SMALLB)
SO=RO**2*THETA0
S1=RS**2*THETA1
ASHADOW=SO+S1-C*L
SUNAREA=PI*RS**2
LRF=1.DO-ASHADOW/SUNAREA
RETURN
END

C
SUBROUTINE RFORCE(LRF,CS,F)
IMPLICIT REAL*8(A-H,O-Z)
REAL*8 LRF,MASS
COMMON/INPUTS/CR,AREA,MASS

C
C      LRF = LUMINOSITY REDUCTION FACTOR (INPUT)
C      CS = HELIOCENTRIC DISTANCE TO NGST (KM) (INPUT)
C      F = SOLAR RADIATION FORCE PER UNIT MASS
C          (NEWTONS/KG = M/S^2) (OUTPUT)
C
C      CR = SOLAR FLUX REFLECTION PARAMETER 0 <= CR <= 2
C          (INPUT THRU COMMON)
C      AREA = NGST AREA PROJECTED NORMAL TO SUN LINE CE
C          (METERS**2)

```

```
C          (INPUT THRU COMMON)
C      MASS = NGST MASS (KG) (INPUT THRU COMMON)
C
F=1.0198D17*CR*AREA*LRF/(1000.DO*CS)**2/MASS
RETURN
END
```

D Constant Parameters

Table 6: Physical Constants [5]

gravitational parameter, Sun alone	μ_1	132,712,440,017.987 km ³ /s ²
gravitational parameter, Earth alone	μ_2	398,600.4415 km ³ /s ²
gravitational parameter, Earth-Moon	μ_2	403,503.236 km ³ /s ²
gravitational parameter, Moon alone	μ_3	4,902.8003 km ³ /s ²
astronomical unit	AU	149,597,870.691 km
mean Earth-Moon barycen- ter distance from Sun		1.000001018 AU
eccentricity of Earth-Moon barycenter orbit about Sun	e	0.01670862
mean motion of Earth-Moon barycenter orbit about Sun	n	$0.199106385 \times 10^{-6}$ rad/s
L_2 distance ratio	γ	0.01007824

Table 7: Computed Values and Coefficients

reference Sun- Earth distance	\bar{D}	149,618,905.218739 km
gravitational coefficients (see page 126)	A_3	$1.16556055765939 \times 10^{-3}$ 1/day ²
	A_1	$5.84525170441422 \times 10^{-10}$ 1/(km-day ²)
	A_5	$3.86396147244215 \times 10^{-16}$ 1/(km ² -day ²)
	A_6	$2.56240418152728 \times 10^{-22}$ 1/(km ³ -day ²)

References

- [1] Segerman, Alan M. and Zedd, Michael F., "Investigations of Spacecraft Orbits Around the L_2 Sun-Earth Libration Point—Part 1," April, 2002.
- [2] Segerman, Alan M. and Zedd, Michael F., "Investigations of Spacecraft Orbits Around the L_2 Sun-Earth Libration Point—Part 2," November, 2002.
- [3] Richardson, David L., "Subcontractor Report for L_2 Formation Flight Support and Analysis," September, 2004 (revised).
- [4] *Explanatory Supplement to the Astronomical Almanac*, ed. by Seidelmann, P. Kenneth, University Science Books, Mill Valley, California, 1992.
- [5] Dunham, David W., and Muhonen, Daniel P. "Tables of Libration-Point Parameters for Selected Solar System Objects." *The Journal of the Astronautical Sciences* (January–March 2001): 197-217.